



**Universidade Federal do Rio de Janeiro
Centro de Ciências da Saúde
Faculdade de Medicina
Hospital Universitário Clementino Fraga Filho
Instituto do Coração Edson Saad
Programa de Pós-Graduação em Medicina Cardiologia**

Estratégias para redução de radiação na Cintilografia Miocárdica de Perfusão: Estabelecimento do valor prognóstico de um protocolo rápido com baixa dose de radiação em gamacâmara CZT e avaliação de seu valor incremental em pacientes com DAC conhecida e alta capacidade de exercício.

Thaís Ribeiro Peclat Monteiro

Rio de Janeiro

Novembro/2019

Estratégias para redução de radiação na Cintilografia Miocárdica de Perusão: Estabelecimento do valor prognóstico de um protocolo rápido com baixa dose de radiação em gamacâmara CZT e avaliação de seu valor incremental em pacientes com DAC conhecida e alta capacidade de exercício.

Thaís Ribeiro Peclat Monteiro

Tese de doutorado apresentada ao Programa de Pós-Graduação em Medicina (Cardiologia) do Departamento de Clínica Médica da Faculdade de Medicina e do Instituto do Coração Edson Saad da Universidade Federal do Rio de Janeiro, como requisito final para obtenção de grau de Doutora em Cardiologia.

Orientador: Ronaldo de Souza Leão Lima

Rio de Janeiro

Novembro/2019

FICHA CATALOGRÁFICA

Monteiro, Thaís Ribeiro Peclat

Estratégias para redução de radiação na cintilografia miocárdica de perfusão: Estabelecimento do valor prognóstico de um protocolo rápido com baixa dose de radiação em gamacâmara CZT e avaliação de seu valor incremental em pacientes com DAC conhecida e alta capacidade de exercício / Thaís Ribeiro Peclat Monteiro. Rio de Janeiro: UFRJ / Faculdade de Medicina, 2019.

132 f.; 31 cm.

Orientador: Ronaldo de Souza Leão Lima

Tese (Doutorado em Clínica Médica - Cardiologia) – Universidade Federal do Rio de Janeiro, Faculdade de Medicina, Pós-Graduação em Medicina (Cardiologia), 2019.

Referências bibliográficas: f. 36 – 40; 58 – 59; 75 – 76; 97 – 99; 103.

1. Imagem de Perfusão do Miocárdio. 2. Cintilografia. 3. Doses de Radiação. 4. Prognóstico. 5. Câmaras gama. 6. Doença da Artéria Coronariana. I. Lima, Ronaldo de Souza Leão. II. Universidade Federal do Rio de Janeiro, Faculdade de Medicina, Pós-Graduação em Medicina (Cardiologia), III. Título.

**Estratégias para redução de radiação na Cintilografia Miocárdica de Perfusão:
Estabelecimento do valor prognóstico de um protocolo rápido com baixa dose de
radiação em gamacâmara CZT e avaliação de seu valor incremental em pacientes com
DAC conhecida e alta capacidade de exercício.**

Thaís Ribeiro Peclat Monteiro

ORIENTADOR: Prof. Ronaldo de Souza Leão Lima

Tese de Doutorado apresentada ao Programa de Pós-Graduação em Medicina (Cardiologia) do Departamento de Clínica Médica da Faculdade de Medicina e do Instituto do Coração Edson Saad da Universidade Federal do Rio de Janeiro, como requisito final para obtenção de grau de Doutora em Cardiologia.

Aprovada por:

Presidente, Prof. Dr. Paolo Blanco Villela

Prof. Dr. Paulo Henrique Rosado de Castro

Prof. Dr. Gustavo Luiz Gouvêa de Almeida Jr

Prof. Dr. Roberto Muniz Ferreira

Prof^a Dr^a Maria Carolina Pinheiro Pessoa Landersmann

Rio de Janeiro

Novembro/2019

DEDICATÓRIA

À **Deus**, autor e consumidor da minha fé, meu melhor amigo e Senhor da minha vida. Àquele a quem dou toda a honra e glória por este trabalho e a quem reconheço como possibilitador de todos os milagres que vivi para finalizá-la. Porque dEle e por Ele, e para Ele são todas as coisas (Rm 11:36).

Aos meus pais **Paulo Peclat** e **Ida Cléa Ribeiro Peclat** por serem meus maiores exemplos de amor, dedicação, retidão, garra e fé. Àqueles a quem devo tudo o que sou e a quem dedico hoje e para sempre tudo o que eu conquistar. Eu os amo acima de tudo!

Ao meu irmão **Thiago Russell Ribeiro Peclat**, por desde sempre ser meu maior incentivador em cada desafio e entusiasta em cada conquista. Meu exemplo de responsabilidade, humildade e sabedoria.

Ao meu marido **João Ricardo Monteiro**, pelo amor, apoio e compreensão ao longo dos 10 anos de dedicação intensa para tornar a formação em MDPHD uma realidade. O caminho não teria sido tão valioso sem você ao meu lado.

À minha cunhada **Amanda Meneguetti** por toda ajuda, incentivo e carinho e por ter me dado, junto ao meu irmão, o maior presente ao longo destes anos, minha amada sobrinha **Sophia Peclat**, a quem também, carinhosamente, dedico esta conquista.

Aos meus sogros **Sidney Monteiro** e **Elizabeth Monteiro**, por terem sido parte fundamental da minha vida em todos estes anos, me amando como a uma filha e fazendo absolutamente tudo pela minha felicidade.

Ao meu cunhado **Pedro Henrique Monteiro**, por ser incansável em me ajudar, sempre tão prestativo, adicionando tanto a este trabalho. Obrigada por tanto carinho e dedicação e por escolher ser como um irmão para mim.

AGRADECIMENTOS

À tia **Lucinha Peclat**, por me ensinar a sempre florescer onde eu fosse plantada.

À tia **Norma Peclat**, por sua oração que jamais cessou e por sua fé inabalável que me deu sustento.

À tia **Rosa Peclat**, por seu imenso carinho e dedicação, priorizando meus sonhos e bem-estar.

À tia **Luciane Peclat**, por ter sempre me amado como uma segunda mãe.

À prima **Patrícia Peclat**, por me ensinar a ser forte como ela e a encarar sempre os desafios da vida com bom humor.

Aos primos **Késya Nogueira** e **William Nogueira**, por terem me ensinado a ver milagres a cada manhã em um momento fundamental para a finalização desta etapa, constantemente me lembrando que eu tudo posso naquEle que me fortalece.

Às primas **Natasha Peclat**, **Bruna Peclat**, **Michelli Peclat** e **Beatri Peclat**, por sempre torcerem por mim e se alegrarem com minhas conquistas.

À amiga **Ana Carolina Souza**, por ter compartilhado comigo todas as flores e espinhos desta longa caminhada. Por sua participação científica ativa neste projeto e por sempre me incentivar a ser melhor em tudo através de seu próprio exemplo de pessoa e profissional.

À amiga **Mariane Nalbones**, por me amar como uma irmã, por sempre priorizar minha felicidade, por sonhar meus sonhos como se fossem dela e por acreditar tanto em mim.

Aos amigos **Daniel Berredo** e **Evelyn Alvares**, por terem sido minha força, fôlego e inspiração quando eu não mais os tive. Por serem incansáveis em amar, me possibilitando fazer o meu melhor para a conclusão deste trabalho.

À amiga **Renée Sarmento**, por sempre me mostrar o melhor de cada situação e por ser uma inspiração para mim.

À amiga **Larissa Franco**, pela amizade e carinho, por sempre me incentivar e por ter sido parte essencial destes anos.

Aos amigos **Caroline Rosa**, **Joyce Lessa**, **Juliana Pestana**, **Peter França**, **Ricardo Fernandes**, **Sérgio Ferreira**, **Thalita Belato**, **Thiago Brillhante**, por me amarem como família, por dividirem o sonho da medicina comigo, por terem sido minha base de apoio durante os anos de faculdade e por ressignificarem para mim o valor de uma amizade.

Aos amigos **Catarina Aragon**, **Danilo Clemente**, **Duncan Ross**, **Ludmila Abdon**, **Marcus Pinto**, **Mariana Laporta** e **Stella Victorelli**, pelo carinho incessante, por acreditarem em mim e por sempre torcerem pelo meu sucesso.

To my Mayo friends and co-workers **Karina Kanamori, Katie Nenn, Kelly Hogan, Julianna Zeidler, Gina Warner, Sonu Kashyap, Lilian Gomez and Mariana Tarragó** for giving me so much support and love, and for always making me believe in me.

Aos queridos **Eduardo Chini** e **Cláudia Chini**, por confiarem em mim, acreditarem no meu potencial e por me darem a chance de crescer tanto como cientista e profissional.

Aos colegas **Victor Freitas, Aline Nakamoto, Felipe Neves, Letícia Glerian, Izabella da Silva, Thalita Soares** e **Caio Ferreira** pela participação, dedicação e responsabilidade na coleta dos dados, possibilitando a concretização deste projeto.

Aos **Dr. Gabriel Camargo** e **Dr. Ilan Gottlieb**, pela importante contribuição científica adicionada por eles neste trabalho.

Aos membros das **bancas de qualificação e defesa** pelas inestimáveis contribuições a este trabalho.

Ao professor e Dr. **Paulo Mourão**, por ser incansável em manter vivo o Programa de Formação em Pesquisa Médica (MDPhD) através do qual tive a oportunidade de realizar este Doutorado em concomitância com minha formação médica. A ele minha gratidão por ter esta visão diferenciada, dando aos alunos da UFRJ esta incrível oportunidade, tão valorizada internacionalmente. Além disso, minha gratidão por ele ter sido um exemplo de mestre e líder, escolhendo ouvir minha história e acreditar no meu real desejo de percorrer este caminho, particularizando minha situação e com tanto discernimento e generosidade me concedendo a oportunidade de um processo seletivo extraordinário. A sua escolha mudou completamente minha formação e vida.

Ao orientador prof. Dr. **Ronaldo Leão**, por escolher me orientar, me concedendo a oportunidade de me tornar a primeira aluna de MDPhD do curso de Doutorado em Medicina-Cardiologia do Instituto do Coração Edson Saad, nesta Universidade que aprendi a amar e respeitar; onde me graduei Médica e agora me formo Doutora.

RESUMO

**Estratégias para redução de radiação na Cintilografia Miocárdica de Perfusão:
Estabelecimento do valor prognóstico de um protocolo rápido com baixa dose de
radiação em gamacâmara CZT e avaliação de seu valor incremental em pacientes com
DAC conhecida e alta capacidade de exercício.**

Thaís Ribeiro Peclat Monteiro

ORIENTADOR: Prof. Ronaldo de Souza Leão Lima

Resumo da Tese de Doutorado submetida ao Programa de Pós-Graduação em Medicina (Cardiologia) do Departamento de Clínica Médica da Faculdade de Medicina e do Instituto do Coração Edson Saad da Universidade Federal do Rio de Janeiro, como requisito final para obtenção de grau de Doutora em Cardiologia.

Introdução: O aumento da exposição à radiação de origem médica tem se destacado de forma relevante na atualidade. A Cintilografia de Perfusão Miocárdica (CPM) é um dos principais métodos diagnósticos e prognósticos utilizados na doença arterial coronariana (DAC). Apesar de sua ampla adoção, este método apresenta a desvantagem de depender do uso de radiofármacos. A fim de garantir a adequação deste método de imagem ao princípio de exposição mínima à radiação determinado pelos órgãos competentes, foi estabelecido um conjunto de estratégias. Entre outros, elas objetivam a utilização de protocolos com redução da dose e o refinamento dos critérios de apropriação da CPM nos diferentes cenários clínicos. **Objetivos:** 1) Estabelecer o valor prognóstico de um novo protocolo realizado em menos tempo e com menor dose de radiação em GC CZT. 2) Comparar o valor prognóstico desse novo protocolo de Cintilografia de perfusão miocárdica realizado de forma mais rápida e com menor dose de radiação em GC CZT com aquele realizado em GCs tradicionais. 3) Avaliar o valor prognóstico incremental da Cintilografia Miocárdica de Perfusão em relação à realização do TE apenas, em pacientes com DAC conhecida que atingiram alta performance aeróbica (>10 METs). **Métodos:** Cada objetivo resultou em um artigo original independente e seus métodos, resultados e conclusões são mostrados separadamente nas seções seguintes deste resumo. 1) Para avaliação do valor prognóstico de um protocolo mais rápido e com uso de menor dose em GC CZT, foi analisada uma coorte de 2930 pacientes submetidos à CPM nesta GC, entre 2011 e 2012. 2) Com a finalidade de comparar o valor prognóstico desta GC com as tradicionais, foram selecionados 3554 pacientes de um total de 6128 que foram submetidos ao exame, entre 2008 e 2012. Foi utilizado um escore de propensão baseado no sexo, idade, índice de massa corporal (IMC), sintomas, fatores de risco cardiovasculares, história de eventos coronarianos e tipo de estresse empregado durante o teste. Uma correspondência 1 a 1 sem substituição, foi realizado para produzir dois grupos com 1777 indivíduos em cada um, divididos de acordo com o tipo de gamacâmara

utilizada. 3) Para avaliação do valor incremental da CPM em pacientes com DAC conhecida e alta capacidade de exercício, foram analisados 926 pacientes submetidos à CPM com estresse por exercício pelo protocolo de Bruce entre 2008 e 2012. Em todos os estudos, os pacientes que realizaram o exame na GC CZT foram submetidos ao protocolo de 1 dia, com uso de 99mTc-sestamibi, começando com repouso (5 mCi) seguido pelo estresse (15 mCi). Os tempos de aquisição foram, respectivamente, de 6 e 3 min. Na GC Anger, foi utilizado protocolo de dois dias, com dose de 10-12 mCi 99mTc-sestamibi em ambas as fases e tempo de aquisição das imagens de 6 minutos. A CPM foi classificada em normal e anormal e a soma dos escores de estresse, repouso e diferença (SSS, SRS, SDS) calculados. Eventos duros foram considerados morte por todas as causas e infarto agudo do miocárdio (IAM) não-fatal. Revascularização tardia foi considerada aquela ocorrida ≥ 60 dias após a data do exame. **Resultados:** A dosimetria média utilizada nos exames em GC CZT foi de 6 mSv e o tempo médio total de exame foi de 48 ± 13 min. A dosimetria média na GC tradicional foi de 9,5 mSv. 1) Ao analisar os exames realizados em GC CZT, a taxa anual de evento duro e revascularização tardia foram maiores em pacientes com maior extensão de defeito e isquemia. SSS foi maior em pacientes com eventos duros comparados com aqueles sem eventos ($5,0 \pm 6,3$ vs. $2,6 \pm 4,9$, $p < 0.001$), assim como o SDS ($1,9 \pm 0,7$ vs $3,4 \pm 1,7$, $p < 0.001$). O mesmo ocorreu para os pacientes com ou sem revascularização tardia (SSS: $4,7 \pm 2,5$ vs. $7,1 \pm 6,6$; SDS: $1,7 \pm 0,6$ vs. $3,8 \pm 2,9$, $p < 0.01$). 2) Na comparação entre GC Ventri e GC CZT, ao acessar os dados de pacientes com exames normais, foi visto que a taxa anualizada de eventos duros foi maior em pacientes que realizaram exame na GC Ventri (1,0%/ano vs 0,5%/ano; $p < 0.01$). No entanto, pacientes com exames anormais não apresentaram diferença significativa na taxa anualizada de eventos duros entre as duas GC's (3,3%/ano vs 3,2%/ano; $p = \text{NS}$). 3) No estudo que analisou pacientes com DAC conhecida e alta capacidade de exercício, foi visto que pacientes que atingiram ≥ 10 METs eram mais novos, predominantemente do sexo masculino e tiveram menor prevalência de fatores de risco cardiovascular quando comparados aos que atingiram < 10 METs. Além disso, pacientes com maior capacidade de exercício tiveram menor taxa anualizada de eventos duros em relação aos que atingiram < 10 METs (1,13 %/ano vs 3,95 %/ano, $p < 0.001$). Em considerando apenas pacientes com ≥ 10 METs, aqueles com exames anormais tiveram maior taxa anualizada de eventos duros em comparação com aqueles com exames normais (3,37 %/ano vs 0,57 %/ano, $p = 0.023$). Capacidade de exercício < 10 METs e exame anormal foram preditores de eventos duros. **Conclusão:** Um protocolo mais rápido e com menor dose de radiação em GC CZT manteve a habilidade de estratificar pacientes com maior risco de eventos, mostrando prognóstico confiável, e não-inferior ao obtido em GC Anger. Além disso, a CPM foi capaz de estratificar pacientes com DAC conhecida que atingiram ≥ 10 METs para a ocorrência de morte por todas as causas e IAM não-fatal, suportando a realização da imagem perfusional neste grupo de pacientes.

ABSTRACT

Strategies for reducing radiation in Myocardial Perfusion Imaging: Establishing the prognostic value of a fast, low-radiation protocol in a CZT camera and the assessment of its incremental value in patients with known CAD and high exercise capacity

Thaís Ribeiro Peclat Monteiro

ORIENTADOR: Prof. Ronaldo de Souza Leão Lima

Abstract da Tese de Doutorado submetida ao Programa de Pós-Graduação em Medicina (Cardiologia) do Departamento de Clínica Médica da Faculdade de Medicina e do Instituto do Coração Edson Saad da Universidade Federal do Rio de Janeiro, como requisito final para obtenção de grau de Doutora em Cardiologia.

Introduction: Increased exposure to radiation of medical origin has been prominently highlighted nowadays. Myocardial perfusion imaging (MPI) is one of the main diagnostic and prognostic methods used in coronary artery disease (CAD). Despite its wide adoption, this method has the disadvantage of relying on the use of radiopharmaceuticals. In order to ensure the adequacy of this imaging method to the principle of minimum radiation exposure determined by the competent agencies, a set of strategies was created. Among other goals, they recommend the use of lower dose protocols and the improvement of MPI indication criteria for patients with known CAD who achieved ≥ 10 METs. **Objective:** 1) To establish the prognostic value of a new protocol performed in less time and with lower radiation dose in a CZT GC. 2) To compare the prognostic value of this new myocardial perfusion scintigraphy protocol performed faster and with lower radiation dose in a CZT GC with that performed in traditional GCs. 3) To evaluate the incremental prognostic value of myocardial perfusion scintigraphy in relation to performing ET only in patients with known CAD who achieved high aerobic performance (> 10 METs). **Methods:** Each objective resulted in an independent original article and its methods, results and conclusions are shown separately in the following sections of this summary. 1) In order to assess the prognostic value of the protocol using a CZT GC, a cohort of 2930 patients who underwent MPI in this GC between 2011 and 2012 was analyzed. 2) For the purpose of comparing the prognostic value of this GC with the standard GC's, a cohort of 3554 patients was selected out of a 6128 group who underwent MPI between 2008 and 2012. Patient selection made use of a propensity score based on sex, age, body mass index (BMI), symptoms, cardiovascular risk factors, coronary event history and the type of stress test used during the exam. A 1 to 1 nearest neighbor matching with no replacement was performed to produce two groups with 1777 individuals in each, divided according to the type of gamma camera used. 3) Finally, to assess the incremental value of MPI in patients with known CAD and high exercise capacity, we analyzed 926 patients who

underwent MPI with the Bruce protocol stress test between 2008 and 2012. Patients who underwent CZT GC were subjected to a one-day protocol using ^{99m}Tc -sestamibi, starting with the rest phase (5 mCi) followed by stress (15 mCi). Acquisition times were respectively 6 and 3 minutes. For the Anger GC, a two-day protocol was used, with a 10-12 mCi ^{99m}Tc -sestamibi dose in both exam phases and a 6 minutes image acquisition time. MPI was classified as normal or abnormal and the summed stress, rest and difference scores (SSS, SRS, SDS) were calculated. Hard events considered were all-cause death and non-fatal myocardial infarction (MI). Late revascularizations were the ones that occurred ≥ 60 days after the exam.

Results: The mean dose used in the GC CZT camera exams was 6 mSv and the mean total exam time was 48 ± 13 min. The mean dose used in the Ventri GC was 9.5 mSv. 1) When analyzing the exams performed using the CZT GC, the annual rate of hard events and late revascularization was greater in patients with more total defect and ischemia. SSS was greater in patients with hard events when compared to those without it (5.0 ± 6.3 vs. 2.6 ± 4.9 , $p < 0.001$), as well as the SDS (1.9 ± 0.7 vs 3.4 ± 1.7 , $p < 0.001$). The same was observed with or without late revascularization (SSS: 4.7 ± 2.5 vs. 7.1 ± 6.6 ; SDS: 1.7 ± 0.6 vs. 3.8 ± 2.9 , $p < 0.01$).

2) When comparing the Ventri GC and the CZT GC it was observed that the annualized rate of hard events was greater in patients examined using the Ventri GC (1.0%/year vs 0.5%/year; $p < 0.01$) when considering patients with normal exam results. However, when assessing patients with abnormal scan results there was no significant difference in the annualized rate of hard events when comparing both GC types (3.3%/year vs 3.2%/year; $p = \text{NS}$).

3) While analyzing patients with known CAD and high exercise capacity, it was observed that patients who achieved ≥ 10 METs were younger, predominantly male and had a lower prevalence of cardiovascular risk factors when compared to their counterparts who achieved < 10 METs. Moreover, patients with high exercise capacity had a lower rate of hard events when compared to those who achieved < 10 METs (1.13 %/year vs 3.95 %/year, $p < 0.001$). When considering only patients who achieved ≥ 10 METs, those with abnormal scan results had a higher annualized rate of hard events when compared to those with normal scan results (3.37 %/year vs 0.57 %/year, $p = 0.023$). An exercise capacity < 10 METs and abnormal scan results were independent predictors of hard events.

Conclusion: A faster, low-radiation, MPS protocol in a CZT camera was able to maintain the ability to stratify patients with increased risk of events, presenting a non-inferior prognostic value when compared to Anger GC's. Besides, MPI was able to stratify patients with known CAD achieved ≥ 10 METs for the occurrence of all-cause death and non-fatal MI, supporting its use in this group of patients.

LISTA DE FIGURAS

Introdução e revisão de literatura:

Figura 1 Curva Temporal de volume de exames de imagem não-invasivos	24
Figura 2 Aumento da participação da cardiologia nuclear como fonte de radiação.....	27
Figura 3 Comparação da sensibilidade entre a GC CZT e GCs tradicionais	29
Figura 4 Relação entre a dose e o tempo de captura de imagens e possíveis novos protocolos investigativos utilizando as novas tecnologias da cintilografia miocárdica de perfusão	30
Figura 5 Efeito de diferentes protocolos na dose efetiva.....	33

Artigo 1: Prognostic value of a faster, low-radiation myocardial perfusion SPECT protocol in a CZT camera

Figure 1 Example of six post-stress short-axis, vertical long axis and longitudinal long axis images processed using a 6, 5, 4, 3, 2 and 1 min acquisition, with a progressive reduction on image quality from to 6 to 1 min.	48
Figure 2 Kaplan-Meier curves of hard events (a) or late revascularization (b) according to SSS categories. Blue line SSS 0-2, green line SSS 3-5; yellow line SSS 6-11; purple line SSS ≥ 12	53
Figure 3 Kaplan-Meier curves of hard events (a) or late revascularization (b) according to SDS categories. Blue line SDS 0, green line SDS 1-2; yellow line SDS 3-5; purple line SDS ≥ 6	55

Artigo 2: Comparison of the prognostic value of myocardial perfusion imaging using a CZT-SPECT camera with a conventional anger camera

Figure 1 Flow diagram of the study..... 62

Figure 2 Kaplan-Meier curves for hard events. (1) Blue: Ventri normal scans; (2) Green: Ventri-abnormal scans; (3) Yellow: CZT normal scans; and (4) Purple: CZT abnormal scans. 70

Figure 3 Kaplan-Meier curves for late revascularization. (1) Blue: Ventri normal scans; (2) Green: Ventri-abnormal scans; (3) Yellow: CZT normal scans; and (4) Purple: CZT abnormal scans. 71

Artigo 3: The additional Prognostic Value of Myocardial Perfusion SPECT in Patients with Known Coronary Artery Disease with high exercise capacity

Figure 1 Study cohort derivation flowchart..... 80

Figure 2 Survival free of hard events stratified by cardiac workload. Blue line Patients reaching < 10 METs; Red line Patients reaching ≥ 10 METs. 88

Figure 3 Survival free of hard events stratified by patients achieving < 10 METs, ≥ 10 METs with abnormal scans and ≥ 10 METs with normal scans. Green line Patients reaching < 10 METs; Red line Patients reaching ≥ 10 METs with abnormal scans; Blue line Patients reaching ≥ 10 METs with normal scans. For the pairwise comparisons, 1 - ≥ 10 METs Normal, 2- ≥ 10 METs Abnormal and 3 - < 10 METs..... 90

Figure 4 Annualized rate of hard events (%/year [95% CI]) per group of cardiac workload and scan results in % person-years..... 91

Figure 5 Survival free of hard events in patients achieving ≥ 10 METs according to the presence of ischemia in MPI. Blue line Patients achieving ≥ 10 METs with no ischemia; Red line Patients achieving ≥ 10 METs with ischemia. 92

Figure 6 Multivariable-Adjusted models showing the incremental prognostic value of exercise capacity and MPI results in Patients with Known CAD. 93

LISTA DE TABELAS

Introdução e revisão de literatura:

Tabela 1 Protocolos atuais em Cintilografia Miocárdica de Perfusão: Radiofármacos recomendados e suas respectivas doses efetivas.	32
--	----

Artigo 1: Prognostic value of a faster, low-radiation myocardial perfusion SPECT protocol in a CZT camera

Table 1 Baseline data.....	46
Table 2 Intra- and interobserver agreement rates of MPS readings using 1 to 6 min time frames	48
Table 3 Characteristics of patients with or without hard events.....	50
Table 4 Characteristics of patients with or without late revascularization.....	50
Table 5 Annualized hard events and late revascularization rates for	54
Table 6 Annualized hard events and late revascularization rates for individual SDS groups..	56

Artigo 2: Comparison of the prognostic value of myocardial perfusion imaging using a CZT-SPECT camera with a conventional angler camera

Table 1 Baseline characteristics	66
Table 2 Scans results, perfusion scores, and gated SPECT measurements.....	66
Table 3 Annualized event rate (%/year)	69

Artigo 3: The additional Prognostic Value of Myocardial Perfusion SPECT in Patients with Known Coronary Artery Disease with high exercise capacity

Table 1 Baseline Characteristics relative to cardiac workload.....	84
Table 2 Exercise test and SPECT parameters relative to cardiac workload.....	86
Table 3 Prevalence of outcomes relative to cardiac workload during the entire follow up time	87
Table 4 Univariable and Multivariate Indicators of Hard Events	94

LISTA DE ABREVIATURAS E SIGLAS

Termos em lingua portuguesa:

CPM Cintilografia miocárdica de perfusão

DAC Doença arterial coronariana

DCV Doenças cardiovasculares

GC Gamacâmara

Gy Gray

IAM Infarto agudo do miocárdio

SCA Síndrome coronariana aguda

SCC Síndrome coronariana crônica

SI Sistema internacional

SUS Sistema Único de Saúde

Sv Sievert

TE Teste ergométrico

Termos em língua inglesa

ALARA As low as reasonable achievable

ASNC American Society of Nuclear Cardiology

BMI Body mass index

CABG Coronary artery bypass graft

CAD Coronary artery Disease

CZT Cadmium Zinc Telluride

ECG electrocardiography

EF Ejection Fraction

ESC European Society of Cardiology

LNT Linear no-threshold model

LVEF Left ventricle Ejection Fraction

MAPHR Maximum age-predicted heart rate

METs Metabolic Equivalentents

MI Myocardial Infarction

MPI Myocardial perfusion imaging

MPS Myocardial perfusion SPECT

PCI Percutaneous coronary intervention

SDS Summed difference scores

SPECT single photon emission computed tomography

SRS Summed rest scores

SSS Summed stress scores

TPD Total Perfusion Defect

UNSCEAR United Nations Scientific Committee on the Effects of Atomic Radiation

SUMÁRIO

1	Introdução e revisão da literatura	19
1.1	Doença Arterial Coronariana	19
1.1.1	Epidemiologia e relevância.....	19
1.1.2	Fisiopatologia e classificação	20
1.1.3	Abordagem diagnóstica e estratificação de risco na DAC crônica.....	20
1.2	Cintilografia Miocárdica de perfusão.....	22
1.2.1	Origem da Cardiologia Nuclear	22
1.2.2	Estabelecimento do valor diagnóstico e prognóstico da CPM	23
1.3	Radiação e Cintilografia Miocárdica de Perfusão	24
1.3.1	Radiação Absorvida, Equivalente e Efetiva	24
1.3.2	Riscos associados à radiação	25
1.3.3	Riscos associados à radiação na medicina e na cardiologia nuclear.....	26
1.3.4	As novas tecnologias na CPM e a busca por estratégias de redução de radiação.....	27
1.3.5	A apropriação da CPM como estratégia de redução de exposição à radiação.....	33
2	Motivação e Justificativa.....	34
3	Objetivos	35
4	Artigos.....	35
5	Referências bibliográficas	36
6	Artigo 1	41
6.1	Abstract	41
6.2	Introduction	42
6.3	Materials and methods	42
6.4	Study protocol	43
6.4.1	Image analysis.....	43
6.4.2	Follow-up.....	45

6.4.3	Statistical analyses	45
6.5	Results	45
6.6	Discussion	56
6.7	Conclusion.....	58
6.8	References	58
7	Artigo 2	60
7.1	Abstract	60
7.2	Introduction	60
7.3	Methods.....	61
7.3.1	Population and Study Design.....	61
7.3.2	Cardiac Imaging and Stress Protocol.....	63
7.3.3	Follow-Up.....	64
7.3.4	Statistical Analysis.....	65
7.4	Results	65
7.5	Discussion	72
7.6	New Knowledge Gained	74
7.7	Conclusion.....	74
7.8	Acknowledgments.....	74
7.9	Compliance with Ethical Standards	74
7.9.1	Disclosure	74
7.9.2	Ethical standards	74
7.9.3	Informed consent	74
7.10	References	75
8	Artigo 3	77
8.1	Abstract	77
8.2	Introduction	77
8.3	Methods.....	79

8.3.1	Study Cohort	79
8.3.2	Study Protocol.....	81
8.3.2.1	Exercise Testing	81
8.3.2.2	SPECT Imaging.....	81
8.3.3	Imaging Interpretation	81
8.3.4	Follow-up.....	82
8.3.5	Statistical analyses	83
8.4	Results	83
8.4.1	Cohort baseline Characteristics	83
8.4.2	Stress-ECG Test and SPECT Findings	85
8.4.3	Outcomes	87
8.5	Discussion	95
8.6	Limitations	96
8.7	New Knowledge Gained	97
8.8	Conclusion.....	97
8.9	References	97
9	Considerações finais.....	100
9.1	Referências bibliográficas	103
10	Conclusão	104
11	Anexos.....	105
	ANEXO A - Produção Científica	105
	ANEXO B – Artigo 1	107
	ANEXO C – Artigo 2.....	115
	ANEXO D – Artigo 3.....	122



The additional prognostic value of myocardial perfusion SPECT in patients with known coronary artery disease with high exercise capacity

Thais R. Peclat, MD,^a Ana Carolina do A. H. de Souza, MD,^a Victor F. Souza, MD,^a Aline M. K. Nakamoto, MD,^a Felipe M. Neves, MD,^a Izabella C. R. Silva,^a and Ronaldo S. L. Lima, MD^{a,b,c}

^a Cardiology, Clementino Fraga Filho University Hospital, Federal University of Rio de Janeiro, Rio de Janeiro, Brazil

^b Fonte Imagem, Rio de Janeiro, Brazil

^c Clínica de Diagnóstico por Imagem, Rio de Janeiro, Brazil

Received Sep 12, 2019; Revised Nov 2, 2019; accepted Nov 4, 2019
doi:10.1007/s12350-019-01960-0

Background. The prognostic value of myocardial perfusion imaging (MPI) in patients with known coronary artery disease (CAD) and high exercise capacity is still unknown. We sought to determine the MPI additional prognostic value over electrocardiography (ECG) stress testing alone in patients with known CAD who achieved ≥ 10 metabolic equivalents (METs).

Methods and Results. We evaluated 926 patients with known CAD referred for MPI with exercise stress. Patients were followed for a mean of 32.4 ± 9.7 months for the occurrence of all-cause death or nonfatal myocardial infarction (MI). Those achieving ≥ 10 METs were younger, predominantly male, and had lower prevalence of cardiovascular risk factors. Patients reaching ≥ 10 METs had a lower annualized rate of hard events compared to their counterparts achieving < 10 METs (1.13%/year vs 3.95%/year, $P < .001$). Patients who achieved ≥ 10 METs with abnormal scans had a higher rate of hard events compared to those with normal scans (3.37%/year vs 0.57%/year, $P = .023$). Cardiac workload < 10 METs and an abnormal MPI scan were independent predictors of hard events.

Conclusions. MPI is able to stratify patients with known CAD achieving ≥ 10 METs for the occurrence of all-cause death and nonfatal MI, with incremental prognostic value over ECG stress test alone. (J Nucl Cardiol 2019)

Key Words: CAD • MPI • SPECT • ECG stress • METs • prognostic • outcomes • exercise capacity

Electronic supplementary material The online version of this article (<https://doi.org/10.1007/s12350-019-01960-0>) contains supplementary material, which is available to authorized users.

The authors of this article have provided a PowerPoint file, available for download at SpringerLink, which summarizes the contents of the paper and is free for reuse at meetings and presentations. Search for the article DOI on SpringerLink.com.

The authors have also provided an audio summary of the article, which is available to download as ESM, or to listen to via the JNC/ASNC Podcast.

Reprint requests: Thais R. Peclat, MD, Cardiology, Clementino Fraga Filho University Hospital, Federal University of Rio de Janeiro, Rio de Janeiro, Brazil; thais_peclat@hotmail.com

J Nucl Cardiol 2019

1071-3581/\$34.00

Copyright © 2019 American Society of Nuclear Cardiology.

Published online: 02 December 2019

Abbreviations

MPI	Myocardial perfusion imaging
CAD	Coronary artery disease
METs	Metabolic equivalents
SPECT	Single photon emission computed tomography
MI	Myocardial infarction
CABG	Coronary artery bypass graft
PCI	Percutaneous coronary intervention
SSS	Summed stress score
SDS	Summed difference score
SRS	Summed rest score

INTRODUCTION

Coronary artery disease (CAD) remains as the leading cause of death in adults in the USA, accounting for about one-third of all deaths in subjects over age 35.¹ In patients with known or suspected CAD, accurate risk stratification and management guidance is of great value to improve outcomes.

Exercise electrocardiography (ECG) stress test and myocardial perfusion imaging with single photon emission computed tomography (MPI SPECT) are both robust, widely used tools for risk stratification in stable CAD.^{2,3} It is known that MPI has higher sensitivity over exercise ECG stress test for detection of ischemia in patients with an intermediate pretest likelihood of CAD.⁴ Moreover, MPI may provide additional clinical information on ventricular function and regional perfusion.

Exercise capacity is an established predictor of mortality⁵⁻¹⁰ and along the past two decades several authors have brought to discussion whether this parameter would be sufficient to support clinical decision. Patients achieving ≥ 10 metabolic equivalents (METs) were shown to have excellent prognosis with low rates of cardiovascular events and low prevalence of $\geq 10\%$ LV ischemia regardless of peak exercise heart rate. That led to questioning on the usefulness of MPI-derived information^{11,12} and later, on the use of exercise capacity as criteria to skip imaging protocols. In that context, provisional protocols were created to better address the groups of patients who could have been selected for this approach, preserving them from unnecessary radiation exposure.^{13,14} However, these provisional protocols typically excluded patients with known CAD.¹⁴

Patients with known CAD are an important segment of the population commonly referred to MPI due to its well-established prognostic value, worthy to be used in

the management of those patients. An association between exercise capacity and overall mortality in patients with known cardiovascular disease has been previously demonstrated.¹⁵ However, no further investigation was done to better understand how workload relates to MPI results regarding the ability to predict outcomes in this particular group.

The aim of this study is to determine the additional MPI prognostic value over ECG stress testing alone in patients with known CAD who achieved high exercise capacity (≥ 10 METs).

METHODS**Study Cohort**

We evaluated 4,187 consecutive patients with known or suspected CAD referred for clinically indicated MPI with exercise stress in an outpatient clinic in Rio de Janeiro, Brazil, between March 2008 and October 2012. The following were considered as exclusion criteria: suspected CAD, early revascularization (coronary angioplasty or coronary artery bypass grafting surgery occurring < 60 days after MPI), and a history of significant cardiac valve disease, severe nonischemic cardiomyopathy, or any condition which might affect short-term prognosis.

Patients were classified as having known CAD based on reported medical history of myocardial infarction (MI), coronary artery bypass graft (CABG), or percutaneous coronary intervention (PCI). From 948 patients meeting all criteria, follow-up was completed in 926 (97.6% of the total). Study cohort flowchart is shown on Figure 1.

Prior to the scan, patients' medical history and physical examination data were collected in a standard questionnaire by a team of experienced cardiologists. Cardiac risk factors including hypertension, diabetes, hypercholesterolemia, smoking, obesity, and family history of CAD were collected. Cardiac symptoms were based on Diamond and Forrester criteria¹⁶ and classified as asymptomatic, noncardiac pain, atypical angina, typical angina, and shortness of breath.

All study procedures were in accordance with the Ethical Standards of the Institutional Research Committee. Informed consent was obtained from all individual participants included in the study.

Study Protocol

Exercise testing Stress-ECG test was performed based on a symptom-limited Bruce treadmill protocol. Exercise workload was defined by the total METs achieved. Ischemic ST segment depression was defined

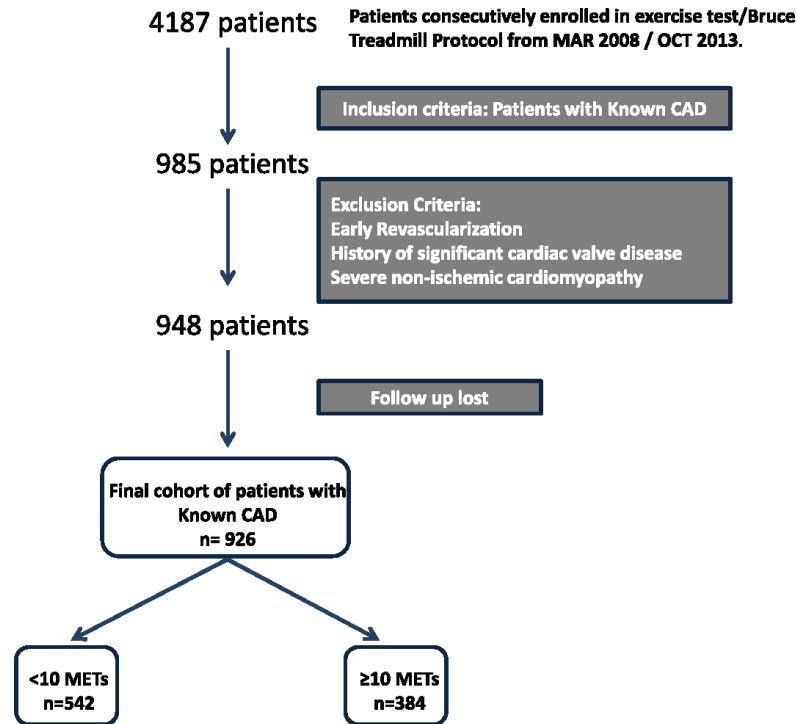


Figure 1. Flowchart of the study cohort.

as a horizontal or down-sloping depression of the ST segment by ≥ 1 mm present ≥ 80 ms after the J-point for three consecutive beats.

SPECT imaging SPECT imaging protocols have been previously described and validated,^{17–19} and will be summarized here. Patients underwent either a 2-day or 1-day Tc-99m-sestamibi-gated MPI protocol based on the scan date, since the camera used for most patients in our laboratory changed during the observation period. For the 2-day protocol a dose of 10–12 mCi ^{99m}Tc-sestamibi was injected with a scan time of 6 minutes. For the rest phase, images were acquired after 15 to 40 minutes. In the stress phase, ^{99m}Tc-sestamibi was injected near maximal exercise, which was continued at maximal workload for at least 1 minute and image acquisition was performed after 15 to 30 minutes. MPI images were acquired through the gated SPECT technique using a two-headed gamma camera (Venti, GE Healthcare, Waukesha, WI, USA).

The 1-day ^{99m}Tc-sestamibi rest/stress protocol was also used, starting with rest study (injection of 5 mCi) followed by stress (15 mCi), in a CZT camera. CZT-SPECT was performed using a camera with multipinhole collimator (Discovery 530, GE Healthcare, Milwaukee, USA). Images were acquired in 6, 3, and 1 minute, respectively, for rest, supine stress, and prone stress.

Imaging Interpretation

All images were jointly interpreted by two experienced cardiologists. Image processing was performed with the software Evolution for Cardiac[®] using 12 iterations. Images were reconstructed without scatter or attenuation correction. Poststress-gated short axis, and vertical and horizontal long-axis tomograms as well as polar maps were generated and analyzed.

Semi quantitative 17-segment visual interpretation of the gated myocardial perfusion images was

performed.^{20,21} Each segment was scored by consensus using a standard five-point scoring system²² (0 = normal, 1 = equivocal, 2 = moderate, 3 = severe reduction of uptake, and 4 = absence of detectable tracer uptake) and each reader chose a score based on both quantitative perfusion data and qualitative visual assessment. Summed stress scores (SSS) were obtained by adding the scores of the 17 segments of the stress images. Summed rest scores (SRS) were obtained by adding scores of the 17 segments of the rest images and a summed difference score (SDS) was calculated by segmental subtraction (SSS – SRS).

For evaluating the correlation of SSS and the SDS with outcomes, we performed separate analyses with different cut points for each perfusion variable. With the purpose of evaluating the prognostic value and the stratification power based on the extent of defect and ischemia, we segmented our study population based on SSS and SDS values, as it is a widely established type of classification^{17,23} to achieve the result.

We converted SSS into percentage of total myocardial defect extension by calculating the ratio between SSS and its maximum possible score (68). An abnormal scan was considered as having an SSS ≥ 4 or percentage of total defect $\geq 5\%$.

Left ventricular ejection fraction (LVEF) and end-systolic and end-diastolic volumes (ESV and EDV, respectively) were automatically calculated (Cedars-Sinai Medical Center, Los Angeles, California).

Follow-Up

Follow-up was performed by telephone interview every 6 months after MPI. All-cause death and nonfatal MI were registered. Events were confirmed through review of hospital charts, physician's records, and national death certification. Nonfatal MI was defined based on the criteria of typical chest pain, elevated cardiac enzyme levels, and typical alterations of the electrocardiogram.²⁴ All-cause death and nonfatal MI were classified as hard events and time to first event was considered.

Statistical Analysis

Categorical variables are presented as frequencies and were calculated using the Pearson χ^2 or Fisher's exact test. Continuous variables are expressed as mean \pm SD or median and interquartile range (IQR) and were compared using Student *T* test or Mann-Whitney test, accordingly. Poisson regression was performed to calculate annualized rate of hard events. Kaplan-Meier curves were generated to visually assess survival in different clinical groups. For pairwise

comparisons between these groups, the log-rank test was used. A Cox regression model was used for testing predictors of hard events. Variables with a *P* value < 0.05 in the univariable analysis or clinical significance were considered in the model. Proportional hazard assumption was tested by using Martingale residuals and we tested for an interaction between exercise capacity and MPI results. Incremental prognostic value of MPI was evaluated by sequential multivariable models, built by the addition of exercise capacity and MPI results to demographic and clinical characteristics. Final model fit was assessed with the goodness-of-fit χ^2 test. A *P*-value $< .05$ was considered statistically significant. All analyses were performed with IBM SPSS statistics version 22.0 Armonk, NY: IBM Corp.

RESULTS

Cohort Baseline Characteristics

A total of 926 patients were followed for a mean 32.4 ± 9.7 months. The clinical characteristics of this study cohort are summarized in Table 1. Patients were divided into two groups: those who achieved ≥ 10 METs (41.5%), named Group 1; and < 10 METs (58.5%), named Group 2. Patients achieving higher workloads were younger, more often male, and had lower rates of hypertension, diabetes mellitus, and obesity. There was no significant difference between groups concerning the presence of angina.

Stress-ECG Test and SPECT Findings

Table 2 shows findings on the stress-ECG test and SPECT imaging stratified by groups of workload achievement. Maximum heart rate during the test was higher in the group of patients who achieved ≥ 10 METs (148 vs 137, *P* $< .001$), as well the prevalence of patients achieving $\geq 85\%$ of their maximum age-predicted heart rate (MAPHR, 82.8% vs 74.1%, *P* = .002). The prevalence of chest pain during the ECG stress was lower in Group 1 for both typical (2.3% vs 7.4%, *P* = .003) and atypical angina (1.8% vs 2.4%, *P* = .003) compared to Group 2. There was no significant difference in the prevalence of exercise ST depression between groups.

When comparing exercise capacity to SPECT imaging results, there was no significant difference between Groups 1 and 2, respectively, on mean SSS (2.69 vs 2.97, *P* = .824), SDS (0.69 vs 0.87, *P* = .424), or percentage of total defect (3.9 vs 4.3, *P* = .824). The prevalence of patients with significant left ventricular

Table 1. Baseline characteristics relative to cardiac workload

Baseline characteristics	Group 1 ≥ 10 METs 384 (41.5%)	Group 2 < 10 METs 542 (58.5%)	Entire cohort n = 926	P value*
Age	59.6 (9)	66.7 (9.2)		< .001
Male	363 (94.5%)	379 (69.9%)	742 (80.1%)	< .001
Symptoms				
Asymptomatic	286 (74.5%)	396 (73.1%)	682 (73.6%)	.63
Typical angina	16 (4.2%)	24 (4.4%)	40 (4.3%)	.847
Atypical angina	64 (16.7%)	93 (17.2%)	157 (16.9%)	.844
Shortness of breath	5 (1.3%)	12 (2.2%)	17 (1.8%)	.308
Non-cardiac chest pain	13 (3.3%)	17 (3.1%)	30 (3.4%)	.331
Hypertension	216 (56.3%)	345 (63.7%)	561 (60.5%)	.023
Diabetes mellitus	67 (17.4%)	162 (29.9%)	229 (24.7%)	< .001
Hyperlipidemia	220 (57.3%)	327 (60.3%)	547 (59%)	.354
BMI ≥ 30	65 (17.6%)	123 (24%)	188 (20.3%)	.023
History of tobacco use	140 (36.4%)	202 (37.3%)	342 (36.9%)	.968
Previous MI	158 (41.1%)	240 (44.3%)	398 (42.9%)	.342
Previous CABG	174 (32.1%)	107 (27.9%)	281 (30.3%)	.095
Previous PCI	356 (65.7%)	253 (65.9%)	609 (65.7%)	.503
Family history of CAD	177 (46.1%)	225 (41.5%)	402 (43.4%)	.166

BMI, body mass index; MI, myocardial infarction; CABG, coronary artery bypass graft; PCI, percutaneous coronary intervention; CAD, coronary artery disease

*Values < .05 are considered statistically significant

Table 2. Exercise test and SPECT parameters relative to cardiac workload

Tests parameters	Group 1 ≥ 10 METs n = 384	Group 2 < 10 METs n = 542	P value*
Stress-ECG test			
Exercise ST depression [n (%)]	35 (9.1)	47 (8.7)	.815
Maximum HR (bpm) (median (25th, 75th))	148 (138, 162)	137 (126, 149)	< .001
> 85% MAPHR [n (%)]	303 (82.8)	380 (74.1)	.002
Chest pain during stress [n (%)]	16 (4.1)	53 (9.7)	.003
SPECT imaging			
Abnormal scans [n (%)]	74 (19.3)	119 (22)	.322
Mean of SSS (± SD)	2.69 (4.5)	2.97 (5)	.824
Mean of SDS (± SD)	0.69 (1.8)	0.87 (2.2)	.424
Mean % of LV defect (± SD)	3.9 (0.33)	4.3 (0.31)	.824
Percentage of LV defect n (%)			
< 5%	310 (80.7)	423 (78)	
5-7%	18 (4.7)	29 (5.4)	
8-9%	10 (2.6)	12 (2.2)	.678
> 10%	46 (12)	78 (14.4)	
EF < 40% [n (%)]	24 (6.3)	63 (11.7)	.006

HR, heart rate; MAPHR, maximum age-predicted heart rate; SSS, summed stress score; SDS, summed difference score; LV, left ventricle; EF, ejection fraction

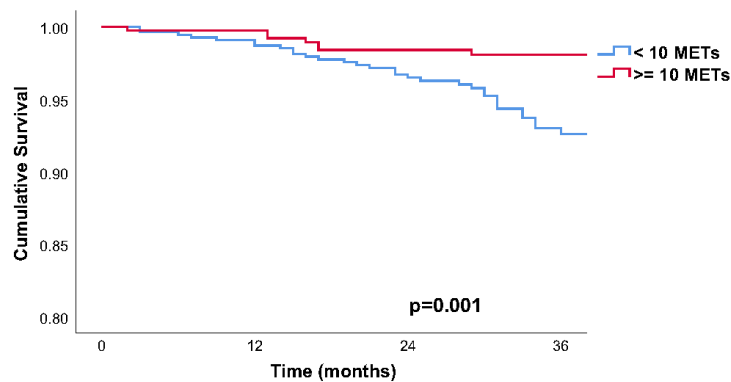
*Values < .05 are considered statistically significant

Table 3. Prevalence of outcomes relative to cardiac workload

Event	Group 1 ≥ 10 METs 384 (41.5%)	Group 2 < 10 METs 542 (58.5%)	Entire cohort n = 926	P value*
Hard events [n (%)]	10 (2.6)	48 (8.9)	58 (6.3)	< .001
All-cause mortality [n (%)]	6 (1.6)	36 (6.6)	42 (4.5)	< .001
Nonfatal MI [n (%)]	4 (1)	16 (3)	20 (2.1)	.04

MI, myocardial infarction

*Values < .05 are considered statistically significant



Number at risk

Time(months)	0	12	24	36
< 10 METs	542	524	436	233
≥10 METs	384	376	311	166

Figure 2. Survival that is free of hard events stratified by cardiac workload. *Blue line* patients reaching < 10 METs; *red line* patients reaching ≥ 10 METs.

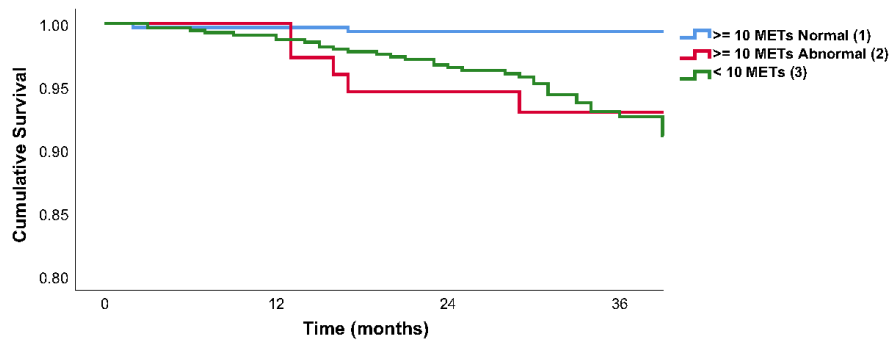
dysfunction (EF < 40%) was lower in those reaching higher cardiac workloads (6.3% vs 11.7% $P = .006$).

Outcomes

A total of 42 deaths (4.5%) and 20 nonfatal MIs (2.1%) (58 hard events) occurred during the follow-up period, as shown on Table 3. The group of patients who achieved ≥ 10 METs had a lower annualized rate of hard events when compared to Group 2 (1.13%/year vs 3.95%/year, $P < .001$). The difference in the cumulative

survival that is free of hard events according to cardiac workload achievement is shown in the Kaplan-Meier survival curve ($P = .001$, Figure 2).

In order to evaluate MPI prognostic contribution for patients with high exercise capacity, we analyzed survival only in patients achieving ≥ 10 METs, stratified for scan results, SSS, and SDS groups. Kaplan-Meier curves show the comparison of cumulative survival among patients achieving < 10 METs, ≥ 10 METs with abnormal scans, and ≥ 10 METs with normal scans, showing increased survival rate in the



Number at risk					Pairwise comparisons	p value
	0	12	24	36		
Time(months)	0	12	24	36	1 vs 2	0.023
≥10 METs Normal	310	302	257	137	1 vs 3	<0.001
≥10 METs Abnormal	74	74	62	39	2 vs 3	0.394
< 10 METs	542	524	436	233		

Figure 3. Survival that is free of hard events stratified by patients achieving < 10 METs, ≥ 10 METs with abnormal scans, and ≥ 10 METs with normal scans. *Green line* patients reaching < 10 METs; *red line* patients reaching ≥ 10 METs with abnormal scans; *blue line* patients reaching ≥ 10 METs with normal scans. For the pairwise comparisons, 1: ≥ 10 METs normal, 2: ≥ 10 METs abnormal, and 3: < 10 METs.

latter (Figure 3). Consistently, patients who reached ≥ 10 METs with a normal scan had a significant lower annualized rate of hard events compared to those who reached ≥ 10 METs with abnormal scans and those who reached < 10 METs (0.57%/year, 3.37%/year, and 3.95%/year, respectively, $P = .001$, Figure 4). There was also a stepwise increment in the annualized rate of events according to the increase in total defect severity, based on SSS groups. There was no difference in the prevalence of these events when stratifying patients with ≥ 10 METs according to the presence of ischemia (Figure 5).

Finally, in the Cox proportional hazards model, cardiac workload achievement < 10 METs (2.72 [1.28-5.77], $P = .009$) and an abnormal MPI result (1.9 [1.15-3.39], $P = .01$) were independently associated with hard events. The variables considered in the univariable and multivariable models are shown in Table 4. In order to assess the incremental prognostic value of MPI results, we constructed multivariable models by sequentially adding exercise capacity and MPI results to demographic and clinical characteristics. Figure 6 shows improvement in the model statistics when these two variables were added. The final model global is

$\chi^2 = 22.5$, $P = .001$. No interaction between exercise capacity and MPI results was observed.

DISCUSSION

Clinical application of exercise testing as a gatekeeper for nuclear imaging has been a matter of debate along the last decade. MPI cost-effectiveness, procedure costs, and related benefits are mounting challenges in an era of advanced cardiac imaging technologies.³ In this context, it is crucial to reassess the risk stratification ability of each method in specific populations.

It is established that patients achieving ≥ 10 METs have low rates of cardiovascular events and low prevalence of ≥ 10% LV ischemia on MPI regardless of peak exercise heart rate.^{11,12} Duvall et al attempted to create a provisional injection protocol by applying the ≥ 10 METs cutoff as criterion to abstain from radiotracer injection. However, groups such as older adults and patients with known CAD were excluded.¹⁴ More recently, Smith et al described that exercise capacity also influences outcomes in patients who are ≥ 65 years old and is associated with a low occurrence of significant ischemia in MPI.¹³ Nonetheless, it is still

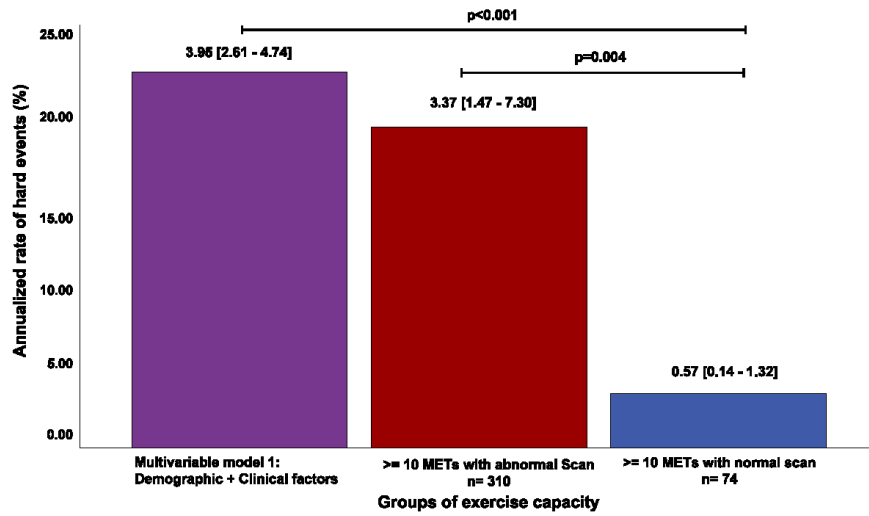


Figure 4. Annualized rate of hard events (%/year [95% CI]) per group of cardiac workload and scan results in % person-years.

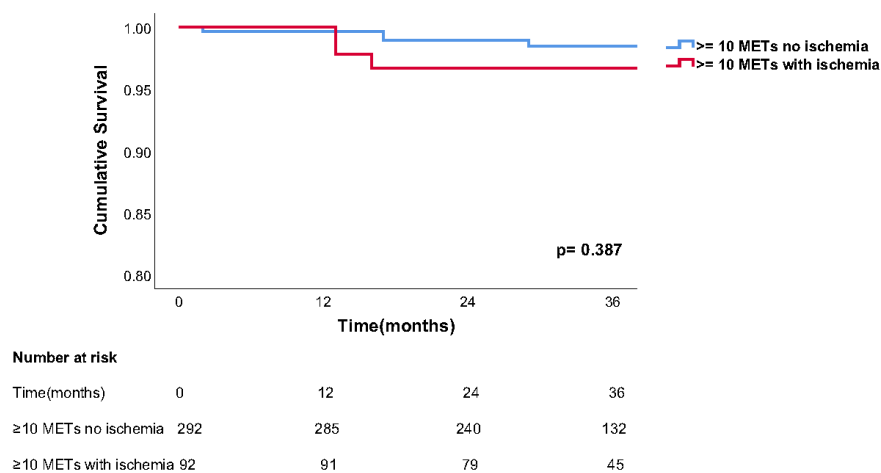


Figure 5. Survival that is free of hard events in patients achieving ≥ 10 METs according to presence of ischemia in MPI. Blue line patients achieving ≥ 10 METs with no ischemia; red line patients achieving ≥ 10 METs with ischemia.

not clear if patients with known CAD would show similar results.

In this study, we addressed the association of high exercise capacity (≥ 10 METs) with mortality and

cardiovascular events in a population comprised of patients with known CAD referred for exercise ECG-stress MPI. Of most importance, we tried to determine the additional contribution of MPI prognostic value in

Table 4. Univariable and multivariate indicators of hard events

Predictors	Univariable		Multivariable	
	Hazard ratio (95% CI)	P value*	Hazard ratio (95% CI)	P value*
Age	1.03 (1.00-1.07)	.014	1.02 (0.98-1.05)	.254
Male gender	1.16 (0.54-2.47)	.697	0.64 (0.30-1.4)	.268
Diabetes mellitus	1.66 (0.96-2.87)	.068	0.64 (0.36-1.14)	.133
< 10 METs	3.1 (1.55-6.16)	.001	2.72 (1.28-5.77)	.009
Abnormal scan	1.74 (1.03-2.95)	.037	1.98 (1.15-3.39)	.013
LVEF	0.99 (0.98-1.01)	.818	1 (0.99-1)	.876
< 10 METs * abnormal scan	-	-	0.51 (0.11-2.29)	.386
Hypertension	0.85 (0.5-1.46)	.57		
Dyslipidemia	1.01 (0.59-1.74)	.958		
Previous MI	0.89 (0.52-1.53)	.688		
Family history of CAD	0.83 (0.48-1.42)	.5		
ST segment depression	0.32 (0.07-1.31)	.114		
SSS	0.98 (0.93-1.03)	.588		
SDS	1.00 (0.99-1.01)	.096		

No significant interaction was observed between exercise capacity and MPI results in the multivariable analysis
CI, confidence interval; METs, metabolic equivalents; LVEF, left ventricle ejection fraction; MI, myocardial infarction; CAD, coronary artery disease; SSS, summed stress score; SDS, summed difference score
*Values < .05 are considered statistically significant

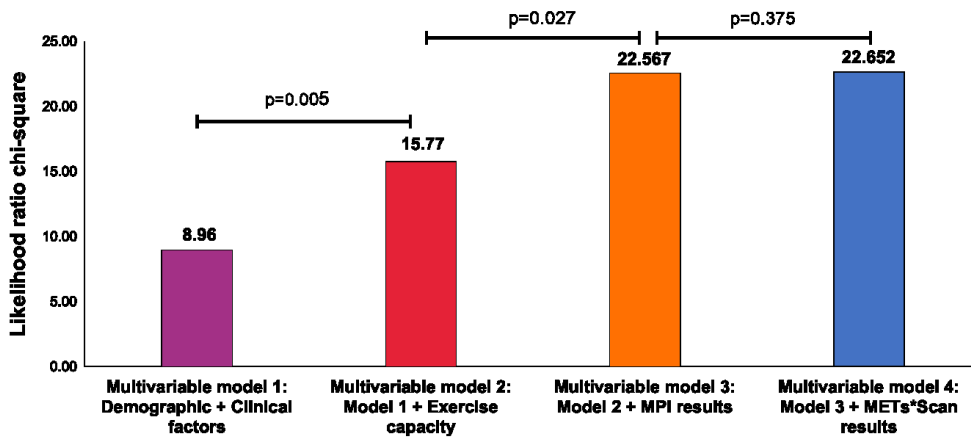


Figure 6. Multivariable-adjusted models showing incremental prognostic value of exercise capacity and MPI results in patients with known CAD.

that specific population. We showed that patients attaining higher workloads were younger, predominantly male, and had significant lower rates of cardiac risk factors. Approximately 70% of the population was asymptomatic before the test, with no significant

difference on the prevalence of pretest symptoms among Groups 1 and 2 in this study. This fact is suggestive of CAD follow-up as the main reason for scan referral. There was no significant difference in the prevalence of ST depression between Groups 1 and 2. Also, there was

no difference in the prevalence of abnormal scans or extent of ischemia in patients with ST depression compared to those without ST depression.

Survival analyses showed that patients with known CAD achieving ≥ 10 METs had a significantly better prognosis compared to those attaining < 10 METs for all-cause mortality and nonfatal MI, with a lower annualized rate of hard events. This finding is similar to what has been previously described.¹¹ To further understand how scan results predicted hard events in the study population, we performed survival analyses only in patients attaining ≥ 10 METs and found out that those with abnormal scans had a significant higher rate of events. Furthermore, the increase in the annualized rate of hard event is proportional to the extent of defect, as determined by SSS values. The results suggest that although a higher exercise capacity is associated with a lower prevalence of all-cause mortality and nonfatal MI, MPI can still provide valuable prognostic information. These findings were corroborated by Cox regression analyses which showed that both exercise capacity and scan results were independently associated with hard events.

Regarding ischemic burden, we did not find significant difference in the survival that is free of hard event in this cohort with established CAD achieving ≥ 10 METs. Although it is worth mentioning that the survival analysis stratified by SDS groups was potentially limited by the number of events in this subgroup (10 events), we also believe that our study cohort's peculiarities may explain the lack of prognostic value of SDS. In a previous study, Gimelli et al.²⁵ aimed to evaluate the incremental prognostic value of MPI over other imaging methods. The group described that when focusing only in a population of ascertained known CAD, without early revascularized patients and a small number of events, SDS was also not a predictor of cardiac events.

Based on what was mentioned above and the fact that under the same constraints the percentage of total defect kept its prognostic value, we believe that for our cohort, the greater contribution of MPI is determined not by quantification of new ischemia, but by the sum of ischemia and previous myocardial scar. Nevertheless, we agree that new studies focusing exclusively on the MPI prognostic value for similar cohorts are necessary to further support this assumption. Thus, our study's results may contribute to better determine the appropriate referral criteria to MPI in patients with known CAD who achieved high exercise capacity in the stress-ECG test.

Limitations

Our study has some limitations, including its retrospective, observational, and single-institution

nature. It is worth noticing that despite having a large sample size, the prevalence of events in the group with higher exercise capacity is low and it might have limited further subgroup analyses.

Additionally, the cardiologists who interpreted the scans were not blinded to clinical data, as the protocol was part of the clinical routine. Hence, it could have been a source of bias.

NEW KNOWLEDGE GAINED

MPI is able to stratify patients with known CAD and high exercise capacity for the occurrence of all-cause death and nonfatal MI, with an incremental prognostic value over ECG stress test alone.

CONCLUSION

MPI was able to stratify the risk for the occurrence of all-cause death and nonfatal MI in patients with known CAD achieving ≥ 10 METs, with an incremental prognostic value compared to ECG stress test alone. These results support the performance of perfusion imaging in this subset of patients, as opposed to what had been proposed with provisional protocols that aimed to reduce patients' exposure to radiation.

Disclosure

The authors Thais R. Peclat, Ana Carolina do A. H. de Souza, Victor F. Souza, Aline M. K. Nakamoto, Felipe M. Neves, Izabella C. R. Silva, and Ronaldo S. L. Lima have nothing to disclose.

References

1. Sanchis-Gomar F, Perez-Quilis C, Leischik R, Lucia A. Epidemiology of coronary heart disease and acute coronary syndrome. *Ann Transl Med* 2016;4:256.
2. Hansen CL, Goldstein RA, Akinboboye OO, Berman DS, Botvinick EH, Churchwell KB, et al. Myocardial perfusion and function: Single photon emission computed tomography. *J Nucl Cardiol* 2007;14:e39-60.
3. Bourque JM, Beller GA. Value of exercise ECG for risk stratification in suspected or known CAD in the era of advanced imaging technologies. *JACC Cardiovasc Imaging* 2015;8:1309-21.
4. Klocke FJ, Baird MG, Lorell BH, Bateman TM, Messer JV, Berman DS, et al. ACC/AHA/ASNC guidelines for the clinical use of cardiac radionuclide imaging—Executive summary: A report of the American College of Cardiology/American Heart Association Task Force on Practice Guidelines (ACC/AHA/ASNC Committee to Revise the 1995 Guidelines for the Clinical Use of Cardiac Radionuclide Imaging). *J Am Coll Cardiol* 2003;42:1318-33.
5. Peterson PN, Magid DJ, Ross C, Ho PM, Rumsfeld JS, Lauer MS, et al. Association of exercise capacity on treadmill with future cardiac events in patients referred for exercise testing. *Arch Intern Med* 2008;168:174-9.

6. Morise AP, Jalisi F. Evaluation of pretest and exercise test scores to assess all-cause mortality in unselected patients presenting for exercise testing with symptoms of suspected coronary artery disease. *J Am Coll Cardiol* 2003;42:842-50.
7. Goraya TY, Jacobsen SJ, Pellikka PA, Miller TD, Khan A, Weston SA, et al. Prognostic value of treadmill exercise testing in elderly persons. *Ann Intern Med* 2000;132:862-70.
8. Kodama S, Saito K, Tanaka S, Maki M, Yachi Y, Asumi M, et al. Cardiorespiratory fitness as a quantitative predictor of all-cause mortality and cardiovascular events in healthy men and women: A meta-analysis. *JAMA* 2009;301:2024-35.
9. Lee DS, Verocai F, Husain M, Al Khdair D, Wang X, Freeman M, et al. Cardiovascular outcomes are predicted by exercise-stress myocardial perfusion imaging: Impact on death, myocardial infarction, and coronary revascularization procedures. *Am Heart J* 2011;161:900-7.
10. Faselis C, Doumas M, Pittaras A, Narayan P, Myers J, Tsimploulis A, et al. Exercise capacity and all-cause mortality in male veterans with hypertension aged ≥ 70 years. *Hypertension* 2014;64:30-5.
11. Bourque JM, Holland BH, Watson DD, Beller GA. Achieving an exercise workload of $>$ or $= 10$ metabolic equivalents predicts a very low risk of inducible ischemia: Does myocardial perfusion imaging have a role? *J Am Coll Cardiol* 2009;54:538-45.
12. Bourque JM, Charlton GT, Holland BH, Belyea CM, Watson DD, Beller GA. Prognosis in patients achieving ≥ 10 METS on exercise stress testing: Was SPECT imaging useful? *J Nucl Cardiol* 2011;18:230-7.
13. Smith L, Myc L, Watson D, Beller GA, Bourque JM. A high exercise workload of ≥ 10 METS predicts a low risk of significant ischemia and cardiac events in older adults. *J Nucl Cardiol* 2018. <https://doi.org/10.1007/s12350-018-1376-7>.
14. Duvall WL, Levine EJ, Moonthungal S, Fardanesh M, Croft LB, Henzlova MJ. A hypothetical protocol for the provisional use of perfusion imaging with exercise stress testing. *J Nucl Cardiol* 2013;20:739-47.
15. Hung RK, Al-Mallah MH, McEvoy JW, Whelton SP, Blumenthal RS, Nasir K, et al. Prognostic value of exercise capacity in patients with coronary artery disease: The FIT (Henry Ford Exercise Testing) project. *Mayo Clin Proc* 2014;89:1644-54.
16. Diamond GA, Forrester JS, Hirsch M, Staniloff HM, Vas R, Berman DS, et al. Application of conditional probability analysis to the clinical diagnosis of coronary artery disease. *J Clin Investig* 1980;65:1210-21.
17. Lima R, Ronaldo L, De Lorenzo A, Andrea DL, Camargo G, Gabriel C, et al. Prognostic value of myocardium perfusion imaging with a new reconstruction algorithm. *J Nucl Cardiol* 2014;21:149-57.
18. Lima RSL, Peclat TR, Souza ACAH, Nakamoto AMK, Neves FM, Souza VF, et al. Prognostic value of a faster, low-radiation myocardial perfusion SPECT protocol in a CZT camera. *Int J Cardiovasc Imaging* 2017;33:2049-56.
19. Lima R, Peclat T, Soares T, Ferreira C, Souza AC, Camargo G. Comparison of the prognostic value of myocardial perfusion imaging using a CZT-SPECT camera with a conventional angler camera. *J Nucl Cardiol* 2017;24:245-51.
20. Berman DS, Kang X, Van Train KF, Lewin HC, Cohen I, Arceeda J, et al. Comparative prognostic value of automatic quantitative analysis versus semiquantitative visual analysis of exercise myocardial perfusion single-photon emission computed tomography. *J Am Coll Cardiol* 1998;32:1987-95.
21. Henzlova MJ, Duvall WL, Einstein AJ, Travin MI, Verberne HJ. ASNC imaging guidelines for SPECT nuclear cardiology procedures: Stress, protocols, and tracers. *J Nucl Cardiol* 2016;23:606-39.
22. Berman DS, Hachamovitch R, Kiat H, Cohen I, Cabico JA, Wang FP, et al. Incremental value of prognostic testing in patients with known or suspected ischemic heart disease: A basis for optimal utilization of exercise technetium-99m sestamibi myocardial perfusion single-photon emission computed tomography. *J Am Coll Cardiol* 1995;26:639-47.
23. Hachamovitch R, Berman DS, Shaw LJ, Kiat H, Cohen I, Cabico JA, et al. Incremental prognostic value of myocardial perfusion single photon emission computed tomography for the prediction of cardiac death: Differential stratification for risk of cardiac death and myocardial infarction. *Circulation* 1998;97:535-43.
24. Thygesen K, Alpert JS, White HD. Infarction JEAATWffRoM. Universal definition of myocardial infarction. *J Am Coll Cardiol* 2007;50:2173-95.
25. Gimelli A, Rossi G, Landi P, Marzullo P, Iervasi G, L'abbate A, et al. Stress/test myocardial perfusion abnormalities by gated SPECT: Still the best predictor of cardiac events in stable ischemic heart disease. *J Nucl Med* 2009;50:546-53.

Publisher's Note Springer Nature remains neutral with regard to jurisdictional claims in published maps and institutional affiliations.

1 Introdução e revisão da literatura

1.1 Doença Arterial Coronariana

1.1.1 Epidemiologia e relevância

A doença arterial coronariana (DAC) é um dos tipos mais comuns de doença cardiovascular (DCV) e representa um grave problema de saúde pública tanto em países desenvolvidos quanto em países subdesenvolvidos, devido a sua alta morbimortalidade(1).

Estima-se que 153,5 milhões de pessoas vivam com DAC em todo o mundo, com prevalência maior em homens (86,5 milhões)(2). Segundo estatísticas publicadas pela American Heart Association em 2019, a prevalência de DAC nos Estados Unidos é de 6,7% em adultos acima de 20 anos de idade, aproximadamente 18,2 milhões de pessoas. De acordo com este mesmo órgão, calcula-se que um infarto agudo do miocárdio (IAM) ocorra, aproximadamente, a cada 40 segundos, com incidência de 605.000 novos casos e 200.000 casos recorrentes. Desse total, estima-se que 170.000 sejam silenciosos(3).

Apesar da mortalidade por DAC estar em constante declínio ao longo das últimas quatro décadas(3, 4) — em geral atribuído aos diversos avanços ocorridos na medicina no tangente à prevenção, diagnóstico, prognóstico e tratamento e à melhora de variáveis socioeconômicas como o índice de desenvolvimento humano - ela permanece como líder das causas de morte no mundo(2). Nos Estados Unidos, a DAC é responsável por um terço das mortes que ocorrem em pessoas acima de 35 anos(1). No Brasil, as DCV foram responsáveis por 31,2% das mortes em 2015 e também apresentam declínio em relação a dados de 1990(5). Devido a sua relevante morbimortalidade, a DAC gera altos custos ao sistema de saúde mundial. Os custos diretos estimados gerados pela DAC nos Estados Unidos entre 2014 e 2015 foi de US\$109,4 bilhões segundo dados obtidos através do Medical Expenditure Panel Survey, gerado pelo National Heart, Lung, and Blood Institute. Ademais, projeta-se um aumento de aproximadamente 100% nos custos médicos relacionados a DAC entre 2015 e 2030(3). No Brasil, foi estimado um custo direto de R\$ 500 milhões associado a IAM em 2011 sob a perspectiva do Sistema Único de Saúde (SUS). Quando considerados custos diretos e indiretos (reabilitação, efeitos sociais da doença crônica, etc.) o custo foi de R\$ 3,8 bilhões neste mesmo ano(6).

1.1.2 Fisiopatologia e classificação

A DAC ocorre por consequência do depósito e acúmulo de placas de ateroma na parede interna das artérias coronárias, resultando em progressiva diminuição do lúmen ou alteração do tônus arterial. A aterosclerose é uma doença inflamatória crônica, progressiva e dinâmica e sua manifestação clínica na DAC mostra-se de forma correspondente ao seu caráter patológico, apresentando-se sob as formas subclínica, estável ou aguda.

A fase subclínica caracteriza-se por um estágio assintomático no qual a lesão ateromatosa está presente, porém não provoca redução significativa do lúmen arterial. A DAC aguda está presente no contexto das síndromes coronarianas agudas (SCA) que abrangem o IAM com e sem supradesnivelamento de ST e a angina instável. Estes ocorrem tipicamente devido a um processo agudo de aterotrombose secundário a ruptura ou erosão de uma placa de ateroma. A DAC estável é considerada aquela na qual há DAC suspeita com presença de sintomas anginosos estáveis ou DAC conhecida, porém com sintomatologia controlada ou estabilizada através de tratamento clínico otimizado. Em diretriz publicada recentemente, a European Society of Cardiology (ESC)(7) revisou o termo “estável”, optando por adotar a terminologia “crônica”. Segundo este documento, os grupos de pacientes considerados como portadores da síndrome coronariana crônica (SCC) são:

- Pacientes com DAC suspeita ou sintomas de angina estável e/ou dispneia;
- Pacientes com DAC suspeita e início recente de insuficiência cardíaca ou disfunção de ventrículo esquerdo;
- Pacientes com DAC conhecida (SCA e/ou revascularização prévia) assintomáticos ou com sintomas estáveis;
- Pacientes sintomáticos com suspeita de angina vasoespástica ou doença microvascular;
- Pacientes assintomáticos nos quais DAC é encontrada em exames solicitados como “*screening*”.

1.1.3 Abordagem diagnóstica e estratificação de risco na DAC crônica

A definição do teste a ser usado para diagnóstico de DAC crônica varia em função da probabilidade pré-teste de o paciente ter a doença. Em pacientes nos quais o diagnóstico de DAC é incerto ou não pode ser excluído apenas com avaliação clínica, o uso de testes não-invasivos é recomendado para estabelecimento do diagnóstico e estratificação de risco.

A Cintilografia de Perfusão Miocárdica (CMP) é um dos principais testes não-invasivos para avaliação de DAC, apresentando importância tanto no cenário de DAC suspeita (nova ou por mudança de estágio de uma doença conhecida estável) quanto para estratificação de risco em pacientes com DAC conhecida.(8) Além de sua importância pelo estabelecido valor diagnóstico e prognóstico, a CMP se destaca por ser um teste funcional, capaz de detectar mudanças mínimas no fluxo coronariano. De acordo com as diretrizes das sociedades americana e brasileira de cardiologia para diagnóstico e manejo da DAC crônica ou estável(8, 9), as recomendações para a utilização deste teste diagnóstico são:

No caso de pacientes referenciados ao teste com objetivo diagnóstico para DAC suspeita:

- Em pacientes com probabilidade pré-teste intermediária ou alta e que tenham eletrocardiograma não interpretável e capacidade de exercício ao menos moderada ou não tenham comorbidade incapacitante (Classe I, nível de evidência B).
- CPM com estresse farmacológico em pacientes com probabilidade pré-teste intermediária ou alta e que tenham eletrocardiograma não interpretável ou incapacidade de exercício físico (Classe I, nível de evidência B).
- Em pacientes com probabilidade pré-teste intermediária ou alta e que tenham eletrocardiograma interpretável e capacidade de exercício ao menos moderada sem comorbidade incapacitante (Classe IIa, nível de evidência B).
- CPM não é recomendada como teste inicial em pacientes com probabilidade pré-teste baixa e que tenham eletrocardiograma interpretável e capacidade de exercício físico (Classe III, nível de evidência C).
- CPM com estresse farmacológico não é recomendada para pacientes com ECG interpretável e capacidade de exercício ao menos moderada e sem comorbidade incapacitante (Classe III, nível de evidência C).

No caso de pacientes com DAC conhecida referenciados ao teste para estratificação de risco:

- Em pacientes com capacidade de exercício físico e que tenham eletrocardiograma não interpretável (Classe I, nível de evidência B).

- CPM com estresse farmacológico em pacientes com incapacidade de exercício físico independentemente da possibilidade de interpretação do ECG (Classe I, nível de evidência B).
- Em pacientes com bloqueio de ramo esquerdo no ECG, independentemente da capacidade de exercício (Classe I, nível de evidência B).
- CPM por estresse físico ou farmacológico em pacientes que estejam sendo considerados para revascularização de estenosa coronariana conhecida de significância fisiológica incerta. (Classe I, nível de evidência B).
- Em pacientes com capacidade de exercício físico e que tenham eletrocardiograma interpretável (Classe IIa, nível de evidência B).
- Não é recomendada a realização de CPM por estresse farmacológico em pacientes com incapacidade de exercício e tem ECG interpretável (Classe III, nível de evidência C)

1.2 Cintilografia Miocárdica de perfusão

1.2.1 Origem da Cardiologia Nuclear

Foi Hermann Blumgart, auxiliado por Otto C. Yens, em 1925, o responsável pelas pioneiras descobertas envolvendo radioatividade e cardiologia. Utilizando, elegantemente, radônio dissolvido em soro como marcador radionuclídeo e uma câmara Wilson modificada como detector, suas invenções permitiram os primeiros estudos hemodinâmicos não invasivos, capazes de, ainda que sem formação de imagem, medir o tempo da circulação sanguínea de um membro superior ao outro(10). Pouco depois, na década de 1940, Myron Prinzmetal desenvolveu o conceito da radiocardiografia, permitindo a medição do débito cardíaco, volume sanguíneo e tempo de trânsito circulatório através de uma sonda de iodeto de sódio marcada com albumina. As descobertas de Blumgart e Prinzmetal foram a base inicial para os posteriores estudos hemodinâmico em modelos fisiológicos e patológicos, nas décadas de 1950 e 1960(11). Contudo, Hal O Anger foi quem, em 1957, revolucionou a radiologia e propiciou o surgimento da cardiologia nuclear como especialidade, ao inventar a primeira câmara de cintilação. A gamacâmara (GC) Anger possibilitou a obtenção de imagens com alta resolução, dinâmicas e capazes de capturar todo um órgão em uma mesma imagem, essas sendo suas mais significativas vantagens em relação ao escâner retilíneo inventado por Benedict Cassen, poucos anos antes.

O modelo de GC desenvolvido por Anger é utilizado até os dias de hoje e consiste em um colimador de chumbo capaz de focalizar a radiação gama proveniente do corpo do paciente sobre placas formadas por cristais detectores de iodeto de sódio, que cintilam ao receber esta radiação. A cintilação é então captada por tubos fotomultiplicadores capazes de amplificar o sinal recebido e o transformar em pulso eletrônico, que é então reconhecido por um computador acoplado à GC. O somatório da contagem dos pulsos eletrônicos quantifica a presença do fármaco utilizado em cada ponto da imagem(12).

1.2.2 Estabelecimento do valor diagnóstico e prognóstico da CPM

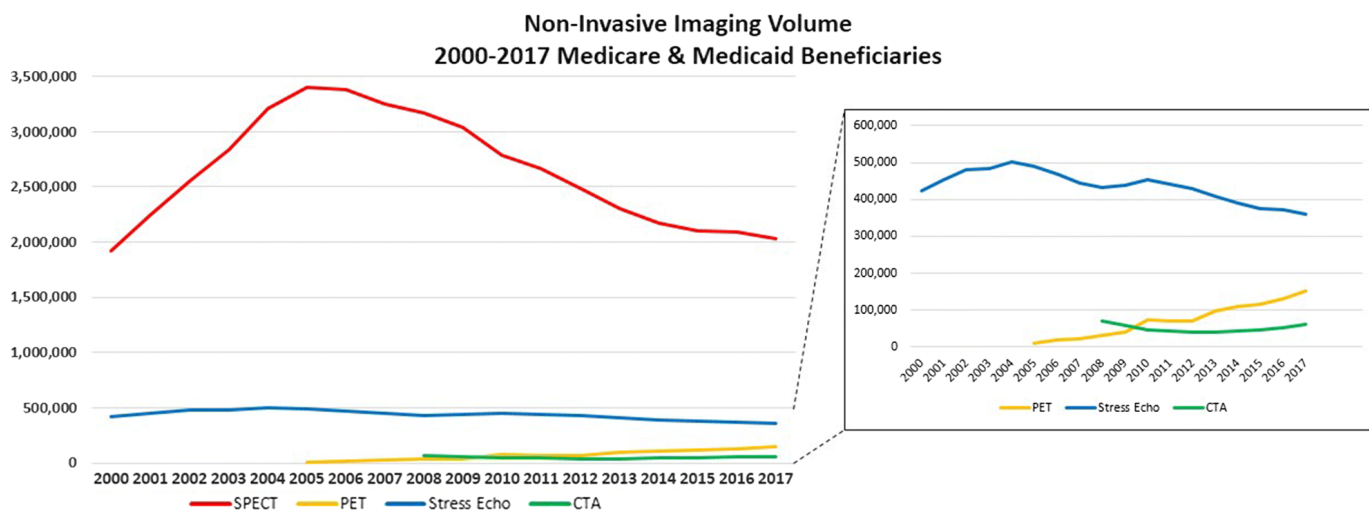
Foi em 1973 que o conceito de isquemia induzida por exercício foi capturado em imagem por Zaret, Strauss e colegas. Estes demonstraram pela primeira vez a heterogeneidade de distribuição do radiotraçador após estresse físico e sua reversão nas imagens obtidas em repouso. No mesmo ano, a introdução do Tálcio-201 como radiotraçador de baixa energia possibilitou uma série de avanços no desenvolvimento da cardiologia nuclear, que culminariam no estabelecimento do valor diagnóstico da CPM(13-16).

Ao estabelecerem de forma pioneira a capacidade de estratificação de risco de IAM com uso de Tálcio, Gibson e Beller inauguraram, em 1983, uma nova era de descobertas no campo da imagem cardiovascular(17). Foi a partir de então, que o valor prognóstico da CPM passou a ser amplamente investigado, em concomitância com o surgimento de sucessivas tecnologias que aperfeiçoaram a qualidade e complexidade da CPM, como o Single Photon Emission Computed Tomography (SPECT) e o ECG-gated.

Em função de ser um método não invasivo, capaz de fornecer informação funcional e territorial e com valor diagnóstico e prognóstico estabelecidos, a CPM se tornou um método cada vez mais difundido e utilizado, apesar do surgimento de novas modalidades de imagem cardiovascular e de sucessivas ameaças, ao longo dos últimos 25 anos, de se tornar um método obsoleto. Em recente publicação, Henzlova, M.J. et al. compila dados dos maiores estudos realizados nos Estados Unidos (país onde mais são utilizados testes não-invasivos para diagnóstico de DAC) e Itália. Este estudo mostra que, conforme dados advindos do sistema Medicare e Medicaid, o número de CPMs realizadas nos EUA apresentou crescimento significativo até meados da década de 2000, chegando a aproximadamente 3.500.000 nos anos de 2005 e 2006. Posteriormente, houve um decréscimo no número de exames realizados e a partir de 2017 houve estabilização na curva de utilização da CPM. Durante o mesmo período não houve aumento significativo nos demais métodos de imagem e

a CPM permaneceu como a modalidade de imagem não invasiva mais utilizada, conforme apresentado na Figura 1. Ademais, em outros países como Itália, Austrália e Alemanha, não houve o decréscimo observado nos dados do sistema norte-americano, indicando que a substituição da CPM por outros métodos de imagem não-invasivos não parece ser o motivador do decréscimo observado nos EUA(18).

Figura 1 Curva Temporal de volume de exames de imagem não-invasivos



Fonte: HENZLOVA, M. J.; DUVALL, W. L. Temporal changes in cardiac SPECT utilization and imaging findings: Where are we going and where have we been? J Nucl Cardiol, Mar 2019.

1.3 Radiação e Cintilografia Miocárdica de Perfusão

O aumento na realização de exames de CPM foi concomitante ao crescimento no uso de radiação em outras áreas da medicina, gerando preocupação e maior ponderação em relação aos efeitos consequentes da exposição à radiação.

1.3.1 Radiação Absorvida, Equivalente e Efetiva

Para melhor entendimento dos efeitos da radiação e dos protocolos de regulação da mesma, é necessário pontuar os princípios pelos quais ela é medida e definida. Algumas das definições básicas necessárias para este entendimento são as de radiação absorvida, equivalente e efetiva.

Radiação absorvida é a quantidade de energia absorvida por unidade de massa por qualquer tipo de material e é representada pela unidade Gray (Gy) no Sistema Internacional de Unidades (SI). Ainda que exposto a mesma quantidade de energia, cada tipo de tecido pode

apresentar uma resposta biológica diferente. A dose de radiação que um tecido biológico absorve, ajustada pelo nível de sensibilidade do tecido ao tipo de radiação empregada, é chamada de dose equivalente. O risco de radiação para o paciente é medido a partir da dose efetiva, que representa o somatório das doses equivalentes. Ambas são representadas pela unidade Sievert (Sv) no SI.

Após a administração de um radiofármaco a um paciente, não é possível medir diretamente a dose a que um tecido ou órgão foi especificamente exposto. Em geral, é feito um cálculo baseado em um modelo computadorizado(11).

1.3.2 Riscos associados à radiação

Hermann Muller foi o primeiro cientista a demonstrar, em 1927, a associação entre a exposição à radiação e a mutação genética e o câncer. Foi ele quem determinou que o risco imposto pela radiação é diretamente proporcional à dosimetria a que se é exposto, não havendo uma dose limiar(19-21).

A partir do princípio estabelecido por Hermann, configurou-se um modelo de dose-resposta para calcular a probabilidade de ocorrência de efeitos estocásticos a saúde, chamado *Linear no-threshold model* (LNT). Efeitos estocásticos são aqueles que ocorrem ao acaso e cuja probabilidade é proporcional a dose, porém a severidade independe da mesma. O modelo LNT assume que a radiação tem potencial de causar injúria em qualquer dosagem e que a soma de pequenas exposições tem efeito equivalente a uma única exposição de maior dose.

Apesar de haver escassa evidência da acurácia do modelo em relação aos efeitos relacionados à baixa dose de radiação, na década de 1970, o modelo LNT foi aceito como padrão na prática de proteção contra a radiação. No entanto, a aplicação desse modelo para baixas dosagens manteve-se controversa na comunidade científica, com diversos trabalhos que suportam(22, 23) ou que se opõe(24) ao seu uso como padrão. Em função dessa falta de consenso, o *United States Congress Joint Committee on Atomic Energy* estabeleceu, como princípio das políticas de proteção à radiação, o conceito "*As Low As Reasonably Achievable*" (ALARA), o que determinou o emprego de todos os esforços razoáveis para manter as exposições à radiação ionizante tão baixas quanto possível, corroborando assim o modelo LNT.

1.3.3 Riscos associados à radiação na medicina e na cardiologia nuclear

Ao se considerar o uso de métodos de imagem que envolvem o uso de radiação, é preciso balancear os riscos, a curto e médio prazo, relacionados à doença em investigação; e os riscos a longo prazo associados à exposição do paciente à radiação(25).

Ao mesmo tempo em que a CPM é um método de imagem capaz de obter informação funcional e anatômica do coração, ela exige que o paciente seja exposto a doses de radiação que produzem um potencial risco à saúde a longo prazo.

Este risco decorre da interação entre a radiação ionizante e o DNA. Apesar de a maioria dos danos induzidos pela radiação nas cadeias de DNA serem rapidamente reparados, em alguns casos ocorrem falhas no reparo, levando a mutações pontuais, translocação de genes e fusão de genes que podem estar ligados ao desenvolvimento de câncer(26). O intervalo de tempo típico entre a exposição à radiação e o diagnóstico de câncer é de no mínimo 5 anos(27) e na maioria dos casos pode ser de 1 a 2 décadas ou mais(28).

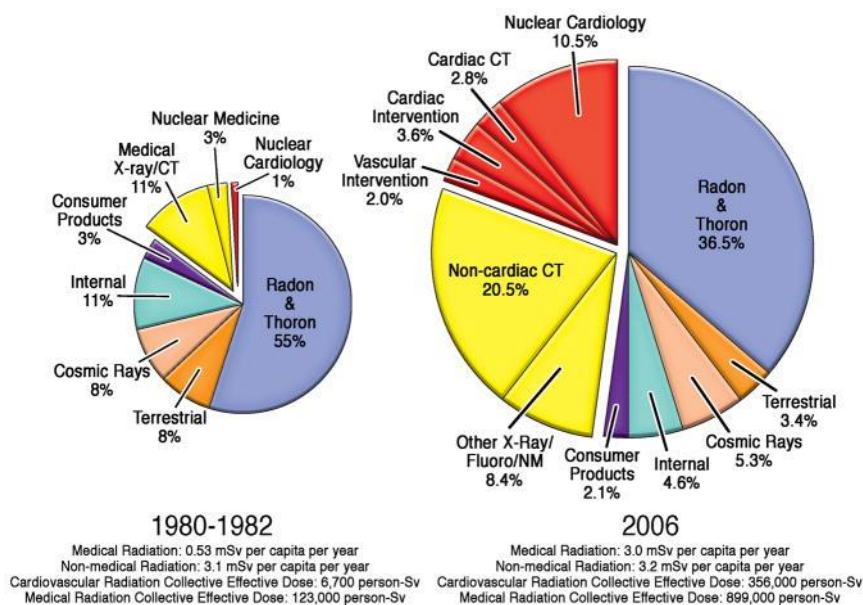
As evidências que embasam a correlação entre a exposição à radiação e o risco de câncer advém principalmente de estudos feitos em populações expostas à radiação médica, ocupacional, ambiental e dos sobreviventes das bombas atômicas no Japão(28). Os dados obtidos dos sobreviventes das bombas atômicas suportam com (29) doses efetivas maiores ou iguais a 100 mSv(29,30) *Scientific Committee on the Effects of Atomic Radiation* (UNSCEAR) estabelece o valor limite de 100 mSv como referência de dose efetiva baixa em uma exposição aguda.

A faixa de exposição anual com maior relevância médica e na cardiologia nuclear é a de 10-100 mSv, sendo também a que apresenta maior controvérsia na literatura. Alguns autores sugerem que há aumento do risco de câncer nesta faixa de dosagem(29, 31), enquanto outros discordam, sugerindo que outros fatores de confundimento podem explicar o suposto efeito carcinogênico observado em baixas doses nos sobreviventes das bombas atômicas(32).

De acordo com o UNSCEAR entre os anos de 1980 e 1982 a dose efetiva não-médica per capita era de 3 mSv por ano, enquanto a médica era de 0.54 mSv por ano. No ano de 2006, a dose efetiva não médica permaneceu constante, enquanto a de origem médica tornou-se 6 vezes maior (3mSv). Deste total, a radiação advinda da cardiologia nuclear correspondeu a 10,5%, 10 vezes maior do que sua representatividade na década de 1980(33), conforme mostrado na

Figura 2.

Figura 2 Aumento da participação da cardiologia nuclear como fonte de radiação



Fonte: EINSTEIN, A. J. Effects of radiation exposure from cardiac imaging: how good are the data? J Am Coll Cardiol, v. 59, n. 6, p. 553-65, Feb 2012.

Este último relatório contextualiza a contribuição da radiação advinda da cardiologia nuclear na população norte-americana no mesmo ano em que o número de exames solicitados atingiu seu pico. Apesar do decréscimo no volume de exames desde 2006, a CPM ainda é amplamente utilizada e permanece como a modalidade de exame de imagem não-invasivo mais utilizado na cardiologia nuclear. Destarte, é coerente o entendimento de que o decréscimo da participação da CPM como fonte de radiação desde de 2006 é significativamente menor que o acréscimo percebido entre 1980 e 2006. Esse entendimento suporta o porquê da busca de estratégias de redução da exposição à radiação na CPM ter permanecido um tema relevante nas últimas duas décadas.

Na tomada de decisão a respeito da utilização da CPM tornou-se necessário então, balancear o risco já sabido da DAC com as recomendações vigentes em relação a minimizar sempre que possível a exposição à radiação. Dessa forma, iniciou-se a busca pelo estabelecimento de novas tecnologias, estratégias e diretrizes visando a otimização deste método de imagem no que tange à dose utilizada e apropriação de indicação.

1.3.4 As novas tecnologias na CPM e a busca por estratégias de redução de radiação

Anos antes do estabelecimento de novas diretrizes relacionadas à otimização do uso de radiação na CPM, a preocupação com o fenômeno do aumento da exposição mundial à radiação médica já existia. Cada vez mais se via o desdobramento dessa preocupação nas novas tecnologias que eram desenvolvidas no campo da cardiologia nuclear. Estas se tornaram alvo de diversos estudos para comprovação da manutenção do valor prognóstico da CPM em se utilizando desses novos recursos.

Dentre estas inovações, destacaram-se os avanços nos *softwares* de reconstrução da imagem cintilográfica. Contrapondo-se aos algoritmos tradicionais, como o *Filtered backprojection* (FBP), estes novos algoritmos foram desenvolvidos para melhorar a relação sinal-ruído e aumentar a resolução da imagem. Para isso, utilizam métodos de recuperação de resolução e técnicas de otimização matemática iterativas, a fim de compensar as limitações impostas por fatores intrínsecos ao tipo de GC utilizada(34). Por consequência, tornaram possível a aquisição de imagens de qualidade equivalente às obtidas com algoritmos de reconstrução mais tradicionais, utilizando um menor tempo de exame(35, 36) e menor dosimetria. A utilização destes novos algoritmos não altera o valor prognóstico da CPM(37).

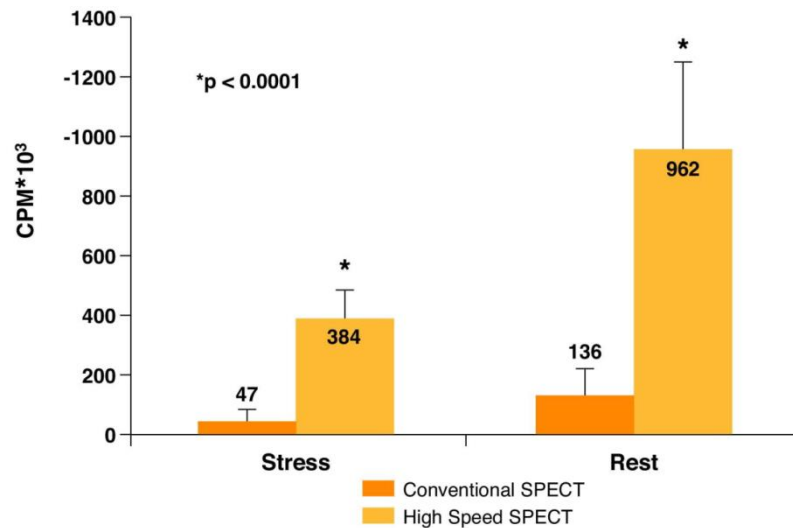
Paralelamente, os avanços na pesquisa também incluíram inovações no equipamento que compõe a GC. Em especial, podemos citar a utilização de detectores de Telureto de Cadmio e Zinco (do inglês, Cadmium-Zinc-Telluret [CZT]), que revolucionou o padrão de formação do pulso eletrônico - até então baseada no mesmo princípio, desde o advento das GCs Anger.

A GC com utilização de detectores CZT, conhecida como GC CZT, é formada por um colimador e por arranjos de detectores de estado sólido compostos por cristais de CZT. Estes detectores apresentam maior sensibilidade à radiação gama quando comparados aos cristais de iodeto de sódio. Ademais, são capazes de converter diretamente o fóton de radiação gama emitido pelo paciente em pulso eletrônico, dispensando o uso de tubos fotomultiplicadores e sendo, por isso, mais compactos. Essa característica permitiu a construção de GCs dedicadas a captação de imagens cardíacas(38, 39).

As GC CZT podem apresentar uma sensibilidade ao fóton até 8 vezes maior(39) que as GCs tradicionais, como mostrado na Figura 3, reduzindo assim o tempo de aquisição de forma significativa. Com isso, a GC CZT proporciona uma maior tolerância do paciente ao teste, diminuindo os artefatos de técnica relacionados à movimentação do mesmo, além de facilitar a realização do exame em duas posições - supina e prona. Tudo isso associado à

possibilidade de um aumento de até 1,7 a 2,5 vezes da resolução(40), gera imagens de melhor qualidade quando comparadas às geradas em GCs tradicionais.

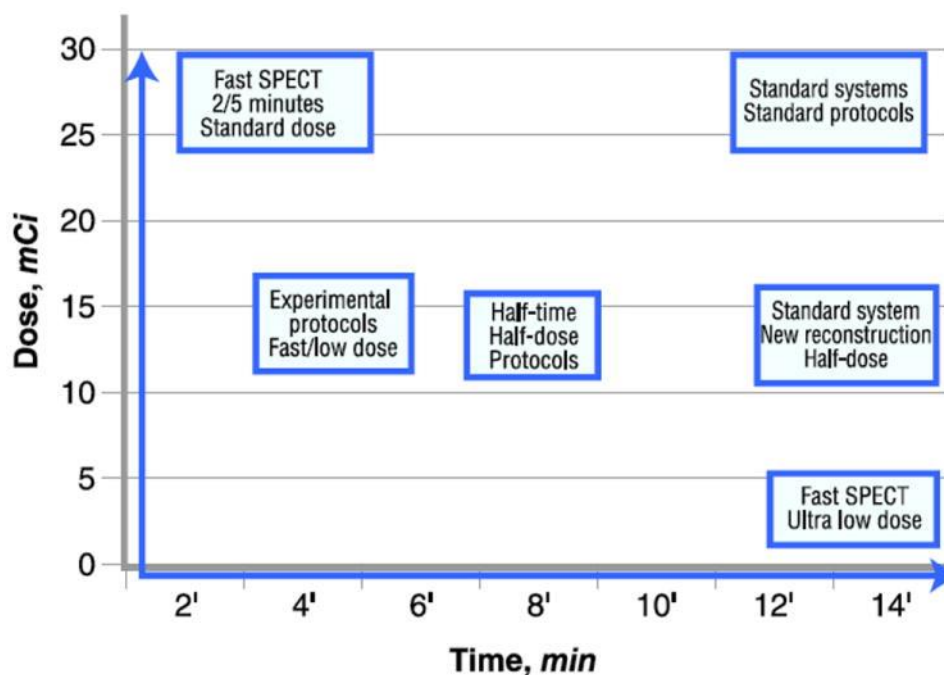
Figura 3 Comparação da sensibilidade entre a GC CZT e GCs tradicionais



Fonte: SHARIR, T. et al. High-speed myocardial perfusion imaging initial clinical comparison with conventional dual detector angler camera imaging. JACC Cardiovasc Imaging, v. 1, n. 2, p. 156-63, Mar 2008.

O advento da GC CZT possibilitando exames ultrarrápidos suscitou o aprofundamento da discussão a respeito da possibilidade de reduzir a dosimetria em detrimento da redução do tempo de exame(41-44). Do ponto de vista físico, a redução do tempo ou da dose resultam no mesmo somatório de contagem de pulsos eletrônicos. Portanto, é possível obter uma redução de dose proporcional à redução de tempo, se mantido o tempo padrão utilizado em protocolos tradicionais. A flexibilidade da manipulação da proporção tempo-dosimetria, propicia a existência de diferentes protocolos com resultados teoricamente equivalentes, conforme mostrado na Figura 4.

Figura 4 Relação entre a dose e o tempo de captura de imagens e possíveis novos protocolos investigativos utilizando as novas tecnologias da cintilografia miocárdica de perfusão



Fonte: SLOMKA, P. J. et al. Advances in nuclear cardiac instrumentation with a view towards reduced radiation exposure. *Curr Cardiol Rep*, v. 14, n. 2, p. 208-16, Apr 2012.

O princípio da flexibilização da proporção tempo-dosimetria se aplica não somente na utilização das GC CZT, mas também na utilização combinada ou não dos diferentes recursos que se desenvolveram ao longo do tempo, que incluem as novas tecnologias em softwares, GCs e a evolução nos diferentes radiofármacos que podem ser utilizados. Dessa forma, foi possibilitada a criação de diferentes protocolos que atendessem a necessidade de reduzir a exposição do paciente à radiação, cumprindo as 8 melhores práticas estabelecidas como recomendação pelo International Atomic Energy Agency (IAEA)(45), a saber:

- Evitar o uso de Tálcio, devido ao entendimento de que este está associado a uma considerável maior dose de radiação em comparação ao Tecnécio.
- Evitar a realização de exames com duplo isótopo, pois esta prática está associada a maior dosagem de radiação entre todos os tipos de protocolos.
- Evitar o uso de dose acima da necessária de Tecnécio (atividade > 36 mCi ou dose efetiva ≥ 15 mCi).
- Evitar o uso de dose acima da necessária de Tálcio (atividade > 3.5 mCi).
- Realizar quando possível apenas a fase de estresse.

- Utilizar estratégias de redução de dose baseadas na aplicação de recursos relacionados ao equipamento, quais sejam: 1) correção de atenuação, 2) Realização da imagem em múltiplas posições (supina e prona), 3) Uso de “*softwares*” de alta tecnologia (e.g. incorporação de reconstrução iterativa, redução de ruído, recuperação de resolução), 4) Uso de “*hardwares*” de alta tecnologia (e.g. PET, câmaras SPECT de estado sólido de alta eficiência ou um colimador específico para a imagem cardíaca). Todas estas possibilitam a redução de dose de radiação.
- Ajustar a dosagem de Tecnécio ao peso do paciente, pois o ajuste da atividade administrada para cada paciente possibilita redução de doses recebidas de forma desnecessária.
- Evitar o uso de dose inapropriada que pode levar a artefato de “*shine through*”. Este artefato ocorre em protocolos de mesmo dia, quando a radioatividade residual da primeira fase do estudo interfere na interpretação das imagens provenientes da segunda injeção. Para evitar que isto ocorra é recomendado que a atividade da segunda injeção seja ao menos 3 vezes maior que a da primeira, evitando artefatos que venham a inutilizar o exame.

Os protocolos criados variam combinações de tempo; dose; ordem das fases de estresse e repouso; realização de apenas estresse e radiofármaco utilizado.

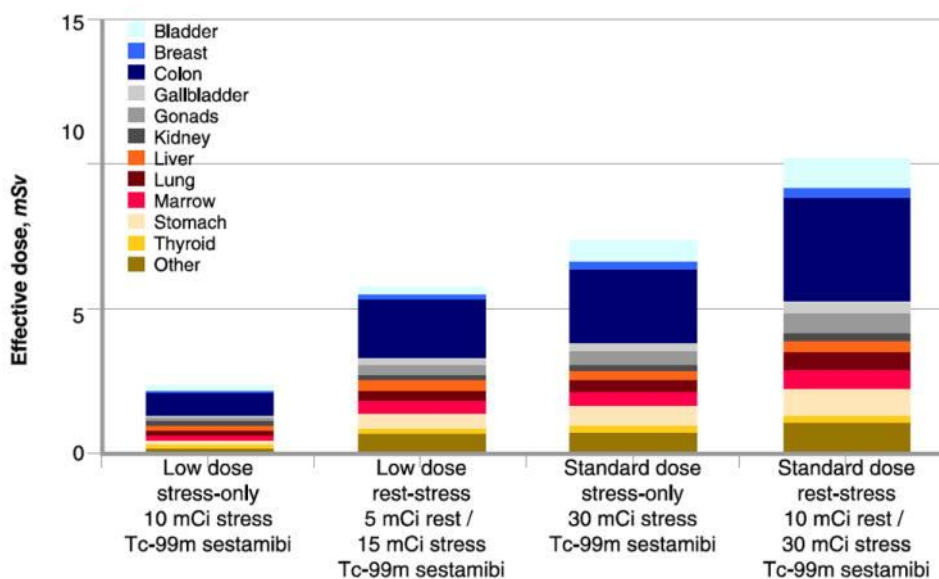
Diferentes órgãos reguladores e sociedades, recomendam então o uso de protocolos consoantes com o princípio ALARA e com estas recomendações, determinando como objetivo crucial o uso $\leq 9\text{mSv}$ em pelo menos 50% dos exames realizados nos laboratórios de imagem(46). A *American Society of Nuclear Cardiology* (ASNC), em recente recomendação(46), reforça os diferentes tipos de protocolos que podem ser utilizados para o cumprimento deste objetivo, como mostrado na Figura 5 expõe o impacto de alguns destes diferentes protocolos na dose efetiva(47).

Tabela 1 Protocolos atuais em Cintilografia Miocárdica de Perfusão: Radiofármacos recomendados e suas respectivas doses efetivas.

	First injection				Second injection				Total Dose (mSv)	Total dose if Stress only (mSv)
	Given at	Activity (mCi)	Activity (MBq)	Dose (mSv)	Given at	Activity (mCi)	Activity (MBq)	Dose (mSv)		
Tc-99m protocols										
Tc-99m one-day stress-first/stress-only	Stress	8-12	296-444	2.0-3.0	(Rest)	24-36	888-1332	7.0-10.5	9.0-13.5	2.0-3.0
Tc-99m one-day rest/stress	Rest	8-12	296-444	2.3-3.5	Stress	24-36	888-1332	6.1-9.1	8.4-12.6	n/a
Tc-99m two-day stress/rest	Stress	8-12	296-444	2.0-3.0	(Rest)	8-12	888-1332	2.3-3.5	4.3-6.5	2.0-3.0
Tc-99m two-day stress/rest—large patient	Stress	18-30	666-1110	4.5-7.6	(Rest)	18-30	666-1110	5.2-8.7	9.8-16.3	4.5-7.6
Tc-99m two-day rest/stress	Rest	8-12	296-444	2.3-3.5	Stress	8-12	296-444	2.0-3.0	4.3-6.5	n/a
Tc-99m two-day rest/stress large patient	Rest	18-30	666-1110	5.2-8.7	Stress	18-30	666-1110	4.5-7.6	9.8-16.3	n/a
Tl-201 protocols										
Tl-201 stress/redistribution rest	Stress	2.5-3.5	92.5-129.5	10.9-15.3	n/a	n/a	n/a	n/a	10.9-15.3	10.9-15.3
Tl-201 stress/redistribution rest/reinjection	Stress	2.5-3.5	92.5-129.5	10.9-15.3	Rest	1-2	37-74	4.4-8.8	15.3-24.1	n/a
Tl-201 rest/redistribution	Rest	2.5-3.5	92.5-129.5	10.9-15.3	n/a	n/a	n/a	n/a	10.9-15.3	n/a
Dual-isotope Tl-201 rest/Tc-99m stress	Rest	2.5-3.5	92.5-129.5	10.9-15.3	Stress	8-12	296-444	2.0-3.0	13.0-18.3	n/a
Dual-isotope Tl-201 rest/Tc-99m stress—large patient	Rest	3.0-3.5	111-129.5	13.1-15.3	Stress	18-30	666-1110	4.5-7.6	17.7-22.9	n/a
I-123 protocol										
MIBG	Rest	10	370	4.6	n/a	n/a	n/a	n/a	4.6	n/a
Newer technology reduced-dose protocols										
Tc-99m one-day stress-first/stress-only	Stress	4-6	148-222	1.0-1.5	(Rest)	12-18	444-666	3.5-5.2	4.5-6.7	1.0-1.5
Tc-99m one-day rest/stress	Rest	4-6	148-222	1.2-1.7	Stress	12-18	444-666	3.0-4.5	4.2-6.3	n/a
Tc-99m two-day stress/rest	Stress	4-6	148-222	1.0-1.5	(Rest)	4-6	148-222	1.2-1.7	2.2-3.3	1.0-1.5
Tc-99m two-day stress/rest—large patient	Stress	9-15	333-555	2.3-3.8	(Rest)	9-15	333-555	2.6-4.4	4.9-8.1	2.3-3.8
Tc-99m two-day rest/stress	Rest	4-6	148-222	1.2-1.7	Stress	4-6	148-222	1.0-1.5	2.2-3.3	n/a
Tc-99m two-day rest/stress—large patient	Rest	9-15	333-555	2.6-4.4	Stress	9-15	333-555	2.3-3.8	4.9-8.1	n/a

Fonte: HENZLOVA, M. J. et al. ASNC imaging guidelines for SPECT nuclear cardiology procedures: Stress, protocols, and tracers. J Nucl Cardiol, v. 23, n. 3, p. 606-39, Jun 2016

Figura 5 Efeito de diferentes protocolos na dose efetiva



Fonte: SLOMKA, P. J. et al. Advances in nuclear cardiac instrumentation with a view towards reduced radiation exposure. Curr Cardiol Rep, v. 14, n. 2, p. 208-16, Apr 2012.

1.3.5 A apropriação da CPM como estratégia de redução de exposição à radiação

Além dos avanços tecnológicos e modificações protocolares e metodológicas, outras estratégias para redução da exposição à radiação foram apresentadas em diretriz recente publicada pela ESC(48). Dentre estas, destaca-se a seleção ótima do tipo de teste mais adequado para cada paciente e situação, baseando-se na probabilidade pré-teste e características intrínsecas a cada tipo de teste. Essa recomendação suscita a discussão do quão apropriadamente a CPM é aplicada visando a uma maior criteriosidade na indicação do exame e na frequência com que é utilizado.

Dessa forma, tornou-se determinante certificar-se de que os critérios de adequação do teste para os diferentes subgrupos de pacientes com risco intermediário de DAC eram apropriados. Nesse sentido, um grupo que tem despertado a atenção da comunidade médica científica são os pacientes com alta capacidade de exercício no teste ergométrico (TE).

A capacidade de exercício é um preditor estabelecido de mortalidade(49-54) e, nas duas últimas décadas, vários autores discutiram se esse parâmetro seria suficiente para apoiar a decisão clínica. Pacientes que atingiram ≥ 10 equivalentes metabólicos (METs) demonstraram ter excelente prognóstico, com baixas taxas de eventos cardiovasculares e baixa prevalência de $\geq 10\%$ de isquemia do ventrículo esquerdo(55, 56). Posteriormente, o uso da capacidade de exercício como critério para evitar a realização da CPM foi discutido continuamente.

Protocolos provisórios foram estudados para melhor atender os grupos de pacientes que poderiam ser selecionados para essa abordagem e resguardados da exposição desnecessária à radiação(57, 58). Apesar de tanto a CPM quanto o TE serem indicados para população de intermediário risco para DAC, sabe-se que a CPM apresenta uma sensibilidade maior para a detecção de isquemia(59). A demonstração na literatura da alta capacidade de exercício como um preditor de melhor prognóstico ressalta a relevância de se confirmar os subgrupos de pacientes e os fatores que devem ser considerados para a escolha entre a CPM e o TE.

2 Motivação e Justificativa

A DAC é uma das principais doenças cardiovasculares e tem fundamental relevância epidemiológica devido à sua morbimortalidade. Nesse cenário, a CPM se estabeleceu como um dos principais métodos diagnósticos e prognósticos na avaliação de pacientes com DAC suspeita e conhecida, levando ao aumento da utilização desse método de imagem. Este novo cenário associado à utilização dos protocolos de dosimetria tradicionais, opõem-se ao princípio de exposição mínima necessária à radiação. Diante disto é notória a necessidade de avaliar mecanismos que reduzam o tempo do exame, a atividade do radiofármaco utilizado nele ou a sua frequência de realização.

O advento das GC CZT iniciou uma nova era na cardiologia nuclear, possibilitando a aplicação de diferentes protocolos e flexibilizando o tempo de aquisição das imagens e a atividade de radiofármaco utilizado na CPM. Estabelecida a capacidade das GC CZT em usar menos tempo e dose, sem comprometer a qualidade da imagem gerada e a acurácia diagnóstica do método, questiona-se se o mesmo ocorreria com seu valor prognóstico em sendo realizada com um protocolo mais rápido e com menor dose. Este valor não foi estabelecido, tampouco comparado ao utilizado nas GC tradicionais. Até o momento, a comparação realizada entre os dois tipos de GCs somente fez uso do protocolo tradicional de dosimetria e tempo, confirmando neste caso a equivalência do valor prognóstico(60). O estabelecimento deste valor traz benefícios tanto na perspectiva do paciente, por ser submetido a um exame mais confortável e sob menor dosimetria, quanto da equipe médica, por assegurar a confiabilidade do resultado obtido na estratificação de risco do paciente.

No tangente à possibilidade de redução da frequência de utilização da CPM, destacam-se as linhas de pesquisa desenvolvidas ao longo dos últimos anos para explorar os critérios de apropriação de sua indicação. Dentre estas, os estudos que correlacionaram a capacidade de

exercício à predição de melhor prognóstico representam um refinamento da apropriação dos critérios de indicação entre a utilização da CPM e do TE.

Pacientes com DAC conhecida são uma porcentagem importante da população comumente referida à CPM devido ao seu valor prognóstico bem estabelecido, digno de ser utilizado na estratificação de risco desses pacientes. Uma associação entre capacidade de exercício e mortalidade geral em pacientes com condições cardiovasculares conhecidas foi demonstrada anteriormente(61). No entanto, nenhuma investigação adicional foi feita para entender como a carga de exercício se relaciona com os resultados da CPM em relação à sua capacidade prognóstica ao avaliar esse grupo em particular.

3 Objetivos

- Estabelecer o valor prognóstico de um novo protocolo realizado em menos tempo e com menor dose de radiação em GC CZT.
- Comparar o valor prognóstico desse novo protocolo de Cintilografia de perfusão miocárdica realizado de forma mais rápida e com menor dose de radiação em GC CZT com aquele realizado em GCs tradicionais.
- Avaliar o valor prognóstico incremental da Cintilografia Miocárdica de Perfusão em relação à realização do TE apenas, em pacientes com DAC conhecida que atingiram alta performance aeróbica (>10 METs).

4 Artigos

A pesquisa é apresentada na forma de 3 artigos sucedidos de considerações finais e conclusão.

Artigo 1: “*Prognostic value of a faster, low-radiation myocardial perfusion SPECT protocol in a CZT camera*”

Este artigo foi publicado na revista *International Journal of Cardiovasc Imaging*.

Lima RSL, Peclat TR, Souza ACAH, Nakamoto AMK, Neves FM, Souza VF, et al.

Prognostic value of a faster, low-radiation myocardial perfusion SPECT protocol in a CZT camera. *Int J Cardiovasc Imaging.* 2017;33(12):2049-56.

Artigo 2: “*Comparison of the prognostic value of myocardial perfusion imaging using a CZT-SPECT camera with a conventional angier camera.*”

Esse artigo foi publicado na revista *Journal of Nuclear Cardiology*.

Lima R, Peclat T, Soares T, Ferreira C, Souza AC, Camargo G. **Comparison of the prognostic value of myocardial perfusion imaging using a CZT-SPECT camera with a conventional angier camera.** *J Nucl Cardiol.* 2017;24(1):245-51.

Artigo 3: “*The additional Prognostic Value of Myocardial Perfusion SPECT in Patients with Known Coronary Artery Disease with high exercise capacity*”

Esse manuscrito foi aceito para publicação na revista *Journal of Nuclear Cardiology*.

5 Referências bibliográficas

1. Sanchis-Gomar F, Perez-Quilis C, Leischik R, Lucia A. Epidemiology of coronary heart disease and acute coronary syndrome. *Ann Transl Med.* 2016;4(13):256.
2. Seattle, WA: Institute for Health Metrics and Evaluation (IHME) Uo, Washington. Global Burden of Disease Study 2016. Global Burden of Disease Study 2016 (GBD 2016) results <http://ghdx.healthdata.org/gbd-results-tool2016>
3. Benjamin EJ, Muntner P, Alonso A, Bittencourt MS, Callaway CW, Carson AP, et al. Heart Disease and Stroke Statistics-2019 Update: A Report From the American Heart Association. *Circulation.* 2019;139(10):e56-e528.
4. Murphy SL XJ, Kochanek KD. Deaths: final data for 2010. National vital statistics report: from the Centers for Disease Control and Prevention, National Center for Health Statistics, National Vital Statistics System. 2013. p. 1-117.
5. Brant LCC, Nascimento BR, Passos VMA, Duncan BB, Bensenõr IJM, Malta DC, et al. Variations and particularities in cardiovascular disease mortality in Brazil and Brazilian states in 1990 and 2015: estimates from the Global Burden of Disease. *Rev Bras Epidemiol.* 2017;20Suppl 01(Suppl 01):116-28.
6. Teich V, Araujo DV. Estimativa de Custo da Síndrome Coronariana Aguda no Brasil. *Rev Bras Cardiol;* 2011. p. 85-94.
7. Knuuti J, Wijns W, Saraste A, Capodanno D, Barbato E, Funck-Brentano C, et al. 2019 ESC Guidelines for the diagnosis and management of chronic coronary syndromes. *Eur Heart J.* 2019.
8. Fihn SD, Gardin JM, Abrams J, Berra K, Blankenship JC, Dallas AP, et al. 2012 ACCF/AHA/ACP/AATS/PCNA/SCAI/STS Guideline for the diagnosis and management of patients with stable ischemic heart disease: a report of the American College of Cardiology Foundation/American Heart Association Task Force on Practice Guidelines, and the American College of Physicians, American Association for Thoracic Surgery, Preventive Cardiovascular Nurses

Association, Society for Cardiovascular Angiography and Interventions, and Society of Thoracic Surgeons. *J Am Coll Cardiol*. 2012;60(24):e44-e164.

9. Cesar LA, Ferreira JF, Armaganijan D, Gowdak LH, Mansur AP, Bodanese LC, et al. Guideline for stable coronary artery disease. *Arq Bras Cardiol*. 2014;103(2 Suppl 2):1-56.

10. Patton DD. The birth of nuclear medicine instrumentation: Blumgart and Yens, 1925. *J Nucl Med*. 2003;44(8):1362-5.

11. Iskandrian AE, Garcia EV. *Nuclear Cardiac Imaging - Principles and Applications*. 4 ed: Oxford university Press, Inc.

12. Anger HO. Scintillation camera. 1958;29(1).

13. Bailey IK, Griffith LS, Rouleau J, Strauss W, Pitt B. Thallium-201 myocardial perfusion imaging at rest and during exercise. Comparative sensitivity to electrocardiography in coronary artery disease. *Circulation*. 1977;55(1):79-87.

14. Ritchie JL, Trobaugh GB, Hamilton GW, Gould KL, Narahara KA, Murray JA, et al. Myocardial imaging with thallium-201 at rest and during exercise. Comparison with coronary arteriography and resting and stress electrocardiography. *Circulation*. 1977;56(1):66-71.

15. Rigo P, Bailey IK, Griffith LS, Pitt B, Wagner HN, Becker LC. Stress thallium-201 myocardial scintigraphy for the detection of individual coronary arterial lesions in patients with and without previous myocardial infarction. *Am J Cardiol*. 1981;48(2):209-16.

16. Okada RD, Boucher CA, Strauss HW, Pohost GM. Exercise radionuclide imaging approaches to coronary artery disease. *Am J Cardiol*. 1980;46(7):1188-204.

17. Pamela FX, Gibson RS, Watson DD, Craddock GB, Sirowatka J, Beller GA. Prognosis with chest pain and normal thallium-201 exercise scintigrams. *Am J Cardiol*. 1985;55(8):920-6.

18. Henzlova MJ, Duvall WL. Temporal changes in cardiac SPECT utilization and imaging findings: Where are we going and where have we been? *J Nucl Cardiol*. 2019.

19. Muller HJ. ARTIFICIAL TRANSMUTATION OF THE GENE. *Science*. 1927;66(1699):84-7.

20. MULLER HJ. The production of mutations. *J Hered*. 1947;38(9):258-70.

21. Crow JF, Abrahamson S. Seventy years ago: mutation becomes experimental. *Genetics*. 1997;147(4):1491-6.

22. Agency USEP. EPA Radiogenic Cancer Risk Models and Projections for the U.S. Population. April 2011.

23. Effects UNSCot, Radiation oA. SOURCES AND EFFECTS OF IONIZING RADIATION - UNSCEAR 2000 Report to the General Assembly, with Scientific Annexes - Annex G. 2000.

24. Society HP. Radiation Risk in Perspective - Position Statement of the Health Physics Society. January 1996.

25. Knuuti J, Bengel F, Bax JJ, Kaufmann PA, Le Guludec D, Perrone Filardi P, et al. Risks and benefits of cardiac imaging: an analysis of risks related to imaging for coronary artery disease. *Eur Heart J*. 2014;35(10):633-8.

26. Brenner DJ, Hall EJ. Computed tomography--an increasing source of radiation exposure. *N Engl J Med*. 2007;357(22):2277-84.
27. Berrington de González A, Mahesh M, Kim KP, Bhargavan M, Lewis R, Mettler F, et al. Projected cancer risks from computed tomographic scans performed in the United States in 2007. *Arch Intern Med*. 2009;169(22):2071-7.
28. Amis ES, Butler PF, Applegate KE, Birnbaum SB, Brateman LF, Hevezi JM, et al. American College of Radiology white paper on radiation dose in medicine. *J Am Coll Radiol*. 2007;4(5):272-84.
29. Pierce DA, Preston DL. Radiation-related cancer risks at low doses among atomic bomb survivors. *Radiat Res*. 2000;154(2):178-86.
30. Radiation UNSCotEoA. BIOLOGICAL MECHANISMS OF RADIATION ACTIONS AT LOW DOSES: A white paper to guide the Scientific Committee's future programme of work. 2012.
31. Preston DL, Ron E, Tokuoka S, Funamoto S, Nishi N, Soda M, et al. Solid cancer incidence in atomic bomb survivors: 1958-1998. *Radiat Res*. 2007;168(1):1-64.
32. Tubiana M, Feinendegen LE, Yang C, Kaminski JM. The linear no-threshold relationship is inconsistent with radiation biologic and experimental data. *Radiology*. 2009;251(1):13-22.
33. Einstein AJ. Effects of radiation exposure from cardiac imaging: how good are the data? *J Am Coll Cardiol*. 2012;59(6):553-65.
34. De Lorenzo A, Fonseca LM, Landesmann MC, Lima RS. Comparison between short-acquisition myocardial perfusion SPECT reconstructed with a new algorithm and conventional acquisition with filtered backprojection processing. *Nucl Med Commun*. 2010;31(6):552-7.
35. Borges-Neto S, Pagnanelli RA, Shaw LK, Honeycutt E, Shwartz SC, Adams GL, et al. Clinical results of a novel wide beam reconstruction method for shortening scan time of Tc-99m cardiac SPECT perfusion studies. *J Nucl Cardiol*. 2007;14(4):555-65.
36. DePuey EG, Gadiraju R, Clark J, Thompson L, Anstett F, Shwartz SC. Ordered subset expectation maximization and wide beam reconstruction "half-time" gated myocardial perfusion SPECT functional imaging: a comparison to "full-time" filtered backprojection. *J Nucl Cardiol*. 2008;15(4):547-63.
37. Lima R, Ronaldo L, De Lorenzo A, Andrea dL, Camargo G, Gabriel C, et al. Prognostic value of myocardium perfusion imaging with a new reconstruction algorithm. *J Nucl Cardiol*. 2014;21(1):149-57.
38. Bocher M, Blevis IM, Tsukerman L, Shrem Y, Kovalski G, Volokh L. A fast cardiac gamma camera with dynamic SPECT capabilities: design, system validation and future potential. *Eur J Nucl Med Mol Imaging*. 2010;37(10):1887-902.
39. Sharir T, Ben-Haim S, Merzon K, Prochorov V, Dickman D, Berman DS. High-speed myocardial perfusion imaging initial clinical comparison with conventional dual detector angler camera imaging. *JACC Cardiovasc Imaging*. 2008;1(2):156-63.
40. Harrison SD, Harrison MA, Duvall WL. Stress myocardial perfusion imaging in the emergency department--new techniques for speed and diagnostic accuracy. *Curr Cardiol Rev*. 2012;8(2):116-22.

41. DePuey EG, Bommireddipalli S, Clark J, Leykekhman A, Thompson LB, Friedman M. A comparison of the image quality of full-time myocardial perfusion SPECT vs wide beam reconstruction half-time and half-dose SPECT. *J Nucl Cardiol.* 2011;18(2):273-80.
42. Duvall WL, Croft LB, Godiwala T, Ginsberg E, George T, Henzlova MJ. Reduced isotope dose with rapid SPECT MPI imaging: initial experience with a CZT SPECT camera. *J Nucl Cardiol.* 2010;17(6):1009-14.
43. Duvall WL, Croft LB, Ginsberg ES, Einstein AJ, Guma KA, George T, et al. Reduced isotope dose and imaging time with a high-efficiency CZT SPECT camera. *J Nucl Cardiol.* 2011;18(5):847-57.
44. Gimelli A, Bottai M, Genovesi D, Giorgetti A, Di Martino F, Marzullo P. High diagnostic accuracy of low-dose gated-SPECT with solid-state ultrafast detectors: preliminary clinical results. *Eur J Nucl Med Mol Imaging.* 2012;39(1):83-90.
45. Einstein AJ, Pascual TN, Mercuri M, Karthikeyan G, Vitola JV, Mahmarian JJ, et al. Current worldwide nuclear cardiology practices and radiation exposure: results from the 65 country IAEA Nuclear Cardiology Protocols Cross-Sectional Study (INCAPS). *Eur Heart J.* 2015;36(26):1689-96.
46. Henzlova MJ, Duvall WL, Einstein AJ, Travin MI, Verberne HJ. ASNC imaging guidelines for SPECT nuclear cardiology procedures: Stress, protocols, and tracers. *J Nucl Cardiol.* 2016;23(3):606-39.
47. Slomka PJ, Dey D, Duvall WL, Henzlova MJ, Berman DS, Germano G. Advances in nuclear cardiac instrumentation with a view towards reduced radiation exposure. *Curr Cardiol Rep.* 2012;14(2):208-16.
48. Gimelli A, Achenbach S, Buechel RR, Edvardsen T, Francone M, Gaemperli O, et al. Strategies for radiation dose reduction in nuclear cardiology and cardiac computed tomography imaging: a report from the European Association of Cardiovascular Imaging (EACVI), the Cardiovascular Committee of European Association of Nuclear Medicine (EANM), and the European Society of Cardiovascular Radiology (ESCR). *Eur Heart J.* 2018;39(4):286-96.
49. Peterson PN, Magid DJ, Ross C, Ho PM, Rumsfeld JS, Lauer MS, et al. Association of exercise capacity on treadmill with future cardiac events in patients referred for exercise testing. *Arch Intern Med.* 2008;168(2):174-9.
50. Morise AP, Jalisi F. Evaluation of pretest and exercise test scores to assess all-cause mortality in unselected patients presenting for exercise testing with symptoms of suspected coronary artery disease. *J Am Coll Cardiol.* 2003;42(5):842-50.
51. Goraya TY, Jacobsen SJ, Pellikka PA, Miller TD, Khan A, Weston SA, et al. Prognostic value of treadmill exercise testing in elderly persons. *Ann Intern Med.* 2000;132(11):862-70.
52. Kodama S, Saito K, Tanaka S, Maki M, Yachi Y, Asumi M, et al. Cardiorespiratory fitness as a quantitative predictor of all-cause mortality and cardiovascular events in healthy men and women: a meta-analysis. *JAMA.* 2009;301(19):2024-35.
53. Lee DS, Verocai F, Husain M, Al Khadair D, Wang X, Freeman M, et al. Cardiovascular outcomes are predicted by exercise-stress myocardial perfusion imaging: Impact on death, myocardial infarction, and coronary revascularization procedures. *Am Heart J.* 2011;161(5):900-7.

54. Faselis C, Doumas M, Pittaras A, Narayan P, Myers J, Tsimploulis A, et al. Exercise capacity and all-cause mortality in male veterans with hypertension aged ≥ 70 years. *Hypertension*. 2014;64(1):30-5.
55. Bourque JM, Holland BH, Watson DD, Beller GA. Achieving an exercise workload of $>$ or $=$ 10 metabolic equivalents predicts a very low risk of inducible ischemia: does myocardial perfusion imaging have a role? *J Am Coll Cardiol*. 2009;54(6):538-45.
56. Bourque JM, Charlton GT, Holland BH, Belyea CM, Watson DD, Beller GA. Prognosis in patients achieving ≥ 10 METS on exercise stress testing: was SPECT imaging useful? *J Nucl Cardiol*. 2011;18(2):230-7.
57. Smith L, Myc L, Watson D, Beller GA, Bourque JM. A high exercise workload of ≥ 10 METS predicts a low risk of significant ischemia and cardiac events in older adults. *J Nucl Cardiol*. 2018.
58. Duvall WL, Levine EJ, Moonthungal S, Fardanesh M, Croft LB, Henzlova MJ. A hypothetical protocol for the provisional use of perfusion imaging with exercise stress testing. *J Nucl Cardiol*. 2013;20(5):739-47.
59. Klocke FJ, Baird MG, Lorell BH, Bateman TM, Messer JV, Berman DS, et al. ACC/AHA/ASNC guidelines for the clinical use of cardiac radionuclide imaging--executive summary: a report of the American College of Cardiology/American Heart Association Task Force on Practice Guidelines (ACC/AHA/ASNC Committee to Revise the 1995 Guidelines for the Clinical Use of Cardiac Radionuclide Imaging). *J Am Coll Cardiol*. 2003;42(7):1318-33.
60. Oldan JD, Shaw LK, Hofmann P, Phelan M, Nelson J, Pagnanelli R, et al. Prognostic value of the cadmium-zinc-telluride camera: A comparison with a conventional (Anger) camera. *J Nucl Cardiol*. 2016;23(6):1280-7.
61. Hung RK, Al-Mallah MH, McEvoy JW, Whelton SP, Blumenthal RS, Nasir K, et al. Prognostic value of exercise capacity in patients with coronary artery disease: the FIT (Henry Ford Exercise Testing) project. *Mayo Clin Proc*. 2014;89(12):1644-54.

6 Artigo 1

Prognostic value of a faster, low-radiation myocardial perfusion SPECT protocol in a CZT camera

Ronaldo S. L. Lima; Thaís R. Peclat; Ana Carolina A. H. Souza; Aline M. K. Nakamoto; Felipe M. Neves; Victor F. Souza; Letícia B. Glerian; Andrea De Lorenzo

6.1 Abstract

Background and objective: To determine the prognostic value of a new, ultrafast, low dose myocardial perfusion SPECT (MPS) protocol in a cadmium-zinc telluride (CZT) camera. CZT cameras have introduced significant progress in MPS imaging, offering high-quality images despite lower doses and scan time. Yet, it is unknown if, with such protocol changes, the prognostic value of MPS is preserved.

Methods: Patients had a 1-day ^{99m}Tc -sestamibi protocol, starting with the rest (5–6 mCi) followed by stress (18–20 mCi). Acquisition times were 6 and 3 min, respectively. MPS were classified as normal or abnormal perfusion scans and summed scores of stress, rest, and difference (SSS, SRS and SDS), calculated.

Results: Patients were followed with 6-month phone calls. Hard events were defined as death or nonfatal myocardial infarction. Late revascularization was that occurring after 60 days of MPS. 2930 patients (age 64.0 ± 12.1 years, 53.3% male) were followed for 30.7 ± 7.5 months. Mean dosimetry was 6 mSv and mean total study time, 48 ± 13 min. The annual hard event and late revascularization rates were higher in patients with greater extension of defect and ischemia. SSS was higher in patients with hard events compared to those without events (2.6 ± 4.9 vs. 5.0 ± 6.3 , $p < 0.001$), as well as the SDS (0.7 ± 1.9 vs 1.7 ± 3.4 , $p < 0.001$). The same was true for patients with or without late revascularization (SSS: 2.5 ± 4.7 vs. 6.6 ± 7.1 ; SDS: 0.6 ± 1.7 vs. 2.9 ± 3.8 , $p < 0.01$).

Conclusion: A new, faster, low radiation MPS protocol in a CZT camera maintain the ability to stratify patients with increased risk of events, showing that, in the presence of greater extension of defect or ischemia, patients presented higher rates of hard events and late revascularization.

6.2 Introduction

Over the past 30 years, successive technical innovations including, but not limited to, SPECT acquisition, ECG gating, among others, have granted myocardial perfusion imaging the status of a reliable, widely applicable, and increasingly useful technique (1). The excellent diagnostic and prognostic values of myocardial perfusion SPECT (MPS) have led it to be extensively employed to evaluate patients with suspected or known coronary artery disease (CAD) (2).

Nonetheless, traditional MPS has two important limitations: Prolonged image acquisition time, leading to long procedural times, and relatively large radiation doses. The available literature demonstrates the possibility of high-speed cameras to reduce acquisition times, improving patient's tolerance to the test, and reducing radiation dose (3). These new cameras rely on a pinhole collimation design and multiple cadmium zinc telluride (CZT) crystal arrays. Compared to the traditional SPECT camera, this type of collimation provides a three- to five-fold increase in photon sensitivity, thereby reducing imaging times significantly, while providing a 1.7 to 2.5-fold increase in spatial resolution. This makes shorter scans or lower doses (or even both) a reality, without the loss of image quality (3-5).

However, the prognostic value of MPS imaging with this new protocol is still unknown. This study therefore sought to assess the prognostic value of a new faster, low-radiation MPS protocol performed in a CZT gamma camera (CZT-GC).

6.3 Materials and methods

Consecutive patients who underwent CZT MPS for the assessment of suspected or known CAD at a single laboratory in Rio de Janeiro, Brazil, between November 2011 and December 2012 were prospectively enrolled and followed by 6-month phone calls.

Those who underwent myocardial revascularization (either by coronary angioplasty or coronary artery bypass grafting surgery) < 60 days after MPS were later excluded.

Prior to scanning, patient's medical history and physical examination data were collected by a team of experienced cardiologists.

All procedures performed were in accordance with the ethical standards of the institutional research committee and with the 1964 Declaration of Helsinki and its later

amendments. Informed consent was obtained from all individual participants included in the study.

6.4 Study protocol

Patients were instructed to abstain from any products containing caffeine for 24 h before the test. Beta-blockers, calcium-channel antagonists, and nitrates were terminated 48 h before testing. A 1-day protocol was employed, with 5–6 mCi of ^{99m}Tc -sestamibi used for the resting phase and 18–20 mCi for stress. Initially, to determine the best duration for the acquisition of MPS scans, 24 patients (13 men) were selected for a pilot study in which scan acquisition was performed for 6 min in list mode. The scans were then processed using 1–6 min of the total scan time for reconstruction. Images were analyzed by two experienced readers unaware of the time range used for reconstruction, who had their readings evaluated for agreement. The study protocol was then defined according to best combination of reading agreements for stress and rest MPS studies among time ranges.

All patients underwent a 1-day, gated, rest/stress ^{99m}Tc -sestamibi protocol. Ten min after tracer injection, image acquisition was performed in the supine position. The second phase (the stress study), in which either symptom-limited exercise treadmill test using the standard Bruce protocol with 13-lead electrocardiographic or pharmacologic stress were performed, occurred immediately after. Upon 5 min of stress phase completion, patients underwent image acquisition in the supine and prone positions (6, 7). The CZT-GC (Discovery NM 530c, GE Healthcare, Haifa, Israel) was equipped with a multiple pinhole collimator and 19 stationary cadmium-zinc-telluride detectors simultaneously imaging 19 cardiac views. Each detector contained 32×32 pixelated 5-mm thick (2.46×2.46 mm) elements. The system design enabled high-quality imaging of a three-dimensional volume by all detectors (quality field-of-view), where the patient's heart should be positioned. Once acquisition was initiated, no detector or collimator motion occurred.

6.4.1 Image analysis

All images were interpreted by a consensus of two experienced readers. Image processing was performed using Evolution for Cardiac® software. Images were reconstructed without scatter or attenuation correction. Short axis, vertical and horizontal long-axis

tomograms, as well as polar maps, were generated and analyzed. The image reconstruction method used allows extra-cardiac activity to be isolated more easily. Still, two readers analyzed the image before the patient was removed from the camera. The repetition rate of the images was less than 5%. A semi quantitative 17-segment visual interpretation of the gated myocardial perfusion images was performed (8). Each segment was scored by consensus of the two observers using a standard five-point scoring system (9) (0=normal, 1=equivocal, 2=moderate, 3=severe reduction of uptake, and 4=absence of detectable tracer uptake). Summed stress scores (SSS) were obtained by adding the scores of the 17 segments of the stress images. Summed rest scores (SRS) were obtained by adding scores of the 17 segments of the rest images and a summed difference score (SDS) was calculated by segmental subtraction (SSS-SRS). For evaluating the SSS and the SDS as predictors of events, we performed separate analyses with different cut points for each perfusion variable. We created four groups of SSS and SDS with the purpose of evaluating the prognostic value and the stratification power of this new protocol on a CZT-GC based not only in positive or negative MPI results, but specially, based on the extension of defect and ischemia, which is widely established to be achieved by using this type of classification (10, 11). A normal study was considered when $SSS < 3$ and $SDS < 1$.

Post-stress eight frames gated short-axis images were processed using quantitative gated SPECT software (Cedars-Sinai Medical Center, Los Angeles, California). Left ventricular ejection fraction (LVEF), end-systolic and end-diastolic volumes (ESV and EDV, respectively) were automatically calculated.

6.4.2 Follow-up

Follow-up was performed by telephone interview every 6 months after MPS. All-cause death, nonfatal myocardial infarction, or late revascularization (>60 days after MPS) were registered. Evaluation of hospital records and/or review of civil registries confirmed these events. Nonfatal myocardial infarction was defined based on the criteria of typical chest pain, elevated cardiac enzyme levels and typical alterations of the electrocardiogram (12). Death and nonfatal myocardial infarction were classified as hard events. Late revascularization was studied separately

6.4.3 Statistical analyses

Categorical variables are presented as frequencies and continuous variables as mean \pm SD. The annual event rate was calculated as the % of events divided by person-years, and was compared among groups using the log-rank test. Kaplan–Meier curves were generated to visually assess survival in different groups. A Cox proportional hazards analysis was done to evaluate predictors of hard events and late revascularization, using variables with p value < 0.05 in univariable analysis or clinical relevance.

Analyses were performed with SPSS software, version 17.0. A p value < 0.05 was considered significant.

6.5 Results

Among 3265 patients, 235 were excluded due to early revascularization, and 100 were lost to follow-up, leaving 2930 patients who were followed for 30.7 ± 7.5 months. Mean age was 64.0 ± 12.1 years and 53.5% were male. Among these patients, 2072 (70.7%) were asymptomatic. The most frequent indications in asymptomatic patients were a previous treadmill test with intermediate-high risk Duke Score, pre-op risk stratification and a previous calcium score >100. The most prevalent risk factor for CAD was hypertension (61.6%), followed by hypercholesterolemia (52.2%), smoking (36.4%) and family history of CAD (31.2%). Diabetes was present in 22.7% and previous myocardial infarction in 12.5%. From the 2930 patients, 501 (17.1%) had already been submitted to coronary angioplasty and 222 (7.6%) to coronary artery bypass grafting (CABG). About regularly medications, 37.9% was in use of ACE inhibitors, 28.6% was using beta-blocker and 10.9% Calcium receptor

blockers. Mean perfusion scores were overall low and mean LVEF was normal with only 6% of patients with a LVEF < 40%. These characteristics are summarized in Table 1.

Table 1 Baseline data

Variables	All patients n (%) or Mean \pm SD
Age (years)	64 \pm 12.1
Male gender	1568 (53.5%)
Chest pain	865 (29.5%)
Hypertension	1807 (61.6%)
Hypercholesterolemia	1530 (52.2%)
Diabetes Mellitus	667 (22.7%)
Family history of coronary disease	915 (31.2%)
Smoking	1069 (36.4%)
Previous MI	367 (12.5%)
Previous CABG	222 (7.6%)
Previous PCI	501 (17.1%)
Exercise stress	1706 (58.2%)
Pharmacologic test	1224 (41.8%)
ACEi	1112 (37.9%)
Beta-blocker	839 (28.6%)
Calcium receptor blockers	320 (10.9%)
MPS	
SSS	1.7 \pm 3.0 (0-26)
SRS	1.1 \pm 2.1 (0-23)
SDS	0.6 \pm 1.7 (0-18)
LVEF (<40%)	176 (6.0%)
LVEF (%)	62.4 \pm 8.1
EDV (ml)	68 \pm 17.0
ESV (ml)	26.4 \pm 10.6

CABG coronary artery bypass grafting, *MI* myocardial infarction, *MPS* myocardial perfusion SPECT, *PCI* percutaneous coronary intervention, *SDS* summed difference score, *SRS* summed rest score, *SSS* summed stress score

For the definition of optimal scan time, acquired scans were processed using 1, 2, 3, 4, 5 or 6 min of the total list-mode acquisition previously performed for the pilot study. Intra and inter-observer agreement rates of MPS readings among time ranges are shown in Table 2. Based on those, the best combination, which was chosen for the subsequent MPS studies, was 6 min for the rest acquisition, 3 min for post-stress supine acquisition and 1.5 min for post-stress prone acquisition. Figure 1 shows an example of six post-stress images processed using a 6, 5, 4, 3, 2, and 1 min acquisition with a progressive degradation of image quality as we reduced the acquisition time. Considering all MPS studies performed thereafter, mean radiation dose was 6 mSv and mean scan time was 48 ± 13 min.

Table 2 Intra- and interobserver agreement rates of MPS readings using 1 to 6 min time frames

Duration	6 min		5 min		4 min		3 min		2 min		1 min	
Agreement	Inter (%)	Intra (%)	Inter (%)	Intra (%)	Inter (%)	Intra (%)	Inter (%)	Intra (%)	Inter (%)	Intra (%)	Inter (%)	Intra (%)
Stress	100	100	100	100	100	100	100	100	100	96	96	92
Rest	100	100	100	100	100	96	100	92	92	92	92	88

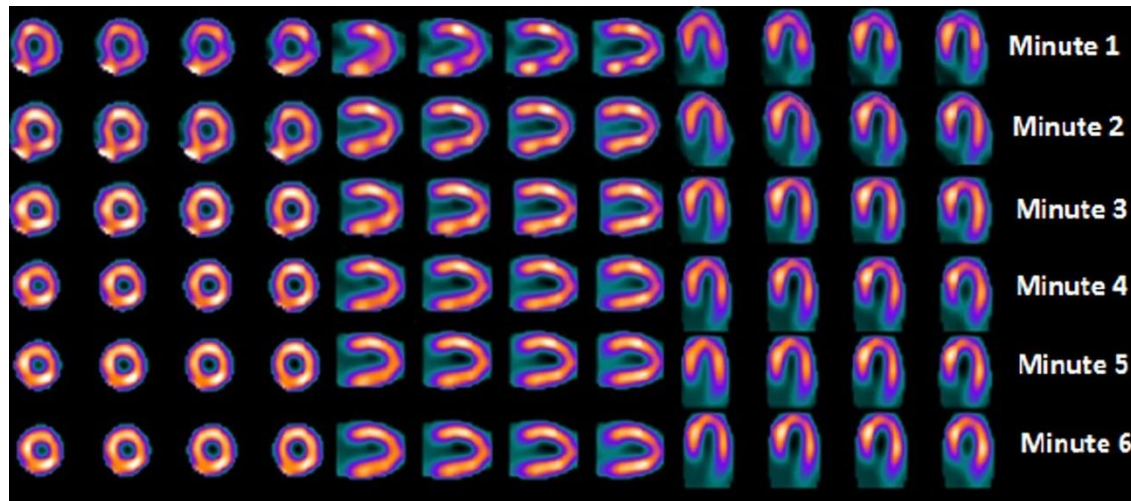


Figure 1 Example of six post-stress short-axis, vertical long axis and longitudinal long axis images processed using a 6, 5, 4, 3, 2 and 1 min acquisition, with a progressive reduction on image quality from to 6 to 1 min.

During follow-up there were 61 deaths, 29 nonfatal infarctions (90 hard events), 148 coronary angioplasty procedures and 22 bypass surgeries (170 late revascularization procedures). Table 3 shows the comparison between patients with or without hard events. The former were older, more frequently male, with prior myocardial infarction or prior CABG and less frequently able to perform exercise stress. Perfusion scores were higher, as well as left ventricular volumes, and LVEF was lower in patients with hard events. In Table 4, comparisons between patients with or without late revascularization are shown. Similarly, to patients with hard events, those with late revascularization were older, more frequently male, with cardiovascular risk factors, known coronary artery disease, and less frequently able to perform exercise stress, with higher perfusion scores, left ventricular volumes, and lower LVEF.

Table 3 Characteristics of patients with or without hard events

Variables	Univariate analysis			Cox regression	
	Patients without HE (n= 2844)	Patients with HE (n= 86)	p value	HR [95% CI]	p value
Age (years)	64.5 ± 11.7	70.7 ± 12.3	< 0.001	1.03 [1.01-1.06]	0.001
Male gender	1515 (53.2%)	57 (66.3%)	<0.01	2.26 [1.33-3.80]	0.030
Chest pain	844 (29.6%)	21 (24.4%)	0.338	1.30 [0.76-2.23]	0.336
Hypertension	1748 (61.4%)	59 (68.6%)	0.173	1.01 [0.61-1.66]	0.955
Hypercholesterolemia	1483 (52.1%)	47 (54.7%)	0.660	1.00 [0.63-1.57]	0.999
Diabetes Mellitus	633 (22.2%)	34 (39.5%)	<0.001	1.69 [1.09-2.62]	0.02
Family history of CAD	887 (31.1%)	28 (32.6%)	0.906		
Smoking	1041 (36.6%)	28 (32.6%)	0.063	0.44 [0.23-1.08]	0.105
Previous MI	347 (12.2%)	20 (23.3%)	<0.01	0.71 [0.42-1.23]	0.229
Previous CABG	208 (7.3%)	14 (16.3%)	<0.01	0.67 [0.36-1.22]	0.196
Previous PCI	480 (16.8%)	21 (24.4%)	0.058	0.88 [0.53-1.45]	0.619
Exercise stress	1682 (59.1%)	24 (27.9%)	<0.01		
Pharmacologic test	1169 (41.1%)	62 (72.1%)	<0.01	2.91 [1.75-4.80]	0.000
MPS					
SSS ^a	2.6 ± 4.9	5.0 ± 6.3	<0.001	1.36 [1.07-1.73]	0.01
SRS	1.9 ± 4.2	3.2 ± 4.8	<0.001		
SDS ^a	0.7 ± 1.9	1.7 ± 3.4	<0.001	1.09 [1.02-1.17]	0.010
LVEF (%)	59.4 ± 11.0	55.5 ± 12.7	<0.01	0.75 [0.39-1.44]	0.392
EDV (ml)	81.4 ± 33.5	87.0 ± 34.6			
ESV (ml)	35.6 ± 25.5	42.0 ± 29.8			

HE hard events; *CABG* coronary artery bypass graft; *MI* myocardial infarction; *MPS* myocardial perfusion *SPECT*; *PCI* percutaneous coronary intervention; *SDS* summed difference score; *SRS* summed rest score; *SSS* summed stress score
^a*SSS* and *SDS* were analyzed separately in the cox regression, each one with other selected variables

Table 4 Characteristics of patients with or without late revascularization

Variables	Univariate analysis			Cox regression	
	Patients w/o late revascularization (n= 2763)	Patients w/ late revascularization (n= 167)	p value	HR [95% CI]	p value
Age (years)	63.9 ± 12.2	66.4 ± 10.3	< 0.001	1.00 [0.99-1.02]	0.397
Male gender	1462 (52.8%)	110 (65.5%)	<0.01	1.35 [0.97-1.88]	0.068
Chest pain	812 (29.3%)	53 (31.5%)			
Hypertension	1690 (61.0%)	117 (69.6%)	0.044	1.07 [0.75-1.51]	0.689
Hypercholesterolemia	1425 (51.5%)	105 (62.5%)	<0.01	1.47 [1.06-2.04]	0.020
Diabetes Mellitus	598 (21.6%)	69 (41.1%)	<0.001	1.94 [1.41-2.66]	0.000
Family history of CAD	861 (31.1%)	54 (32.1%)			
Smoking	1001 (36.2%)	68 (40.5%)		0.77 [0.46-1.28]	0.314
Previous MI	317 (11.4%)	50 (29.8%)	<0.001	2.01 [1.43-2.83]	0.000
Previous CABG	208 (7.5%)	14 (8.3%)		1.60 [0.92-2.79]	0.095
Previous PCI	429 (15.5%)	72 (42.9%)	<0.001	2.54 [1.76-3.68]	0.000
Exercise stress	1624 (59.0%)	82 (48.8%)	<0.01		
Pharmacologic test	1955 (41.4%)	86 (51.2%)	<0.01	1.20 [0.86-1.67]	0.264
MPS					
SSS ^a	2.5 ± 4.7	6.6 ± 7.1	<0.001	1.06 [1.04-1.08]	0.000
SRS	1.9 ± 4.1	3.7 ± 5.6	<0.001		
SDS ^a	0.6 ± 1.7	2.9 ± 3.8	<0.001	1.22 [1.17-1.26]	0.000
LVEF (%)	59.6 ± 10.9	54.8 ± 12.0	<0.01	1.00 [0.99-1.00]	0.887
EDV (ml)	81.4 ± 33.5	88.5 ± 36.9	<0.01		
ESV (ml)	35.6 ± 25.5	43.0 ± 30.2	<0.01		

CABG coronary artery bypass graft; MI myocardial infarction; MPS myocardial perfusion SPECT; PCI percutaneous coronary intervention; SDS summed difference score; SRS summed rest score; SSS summed stress score

^aSSS and SDS were analyzed separately in the cox regression, each one with other selected variables

Based on the SSS, 4 patient groups were created: group 1 with SSS values from 0 to 2 [n=2098 (71.6%)]; group 2, SSS values from 3 to 5 [n=430 (14.6%)]; group 3, SSS values from 6 to 11 [n=220 (7.5%)] and group 4, SSS ≥ 12 [n=182 (6.2%)]. Kaplan–Meier survival curves (Fig. 2a, b) showed that the highest the SSS, the lowest the survival free of hard events ($p < 0.001$) or late revascularization ($p < 0.001$), respectively. Table 5 shows the annualized hard events and late revascularization rates for individual groups of SSS, with highest rates in the group of highest SSS values.

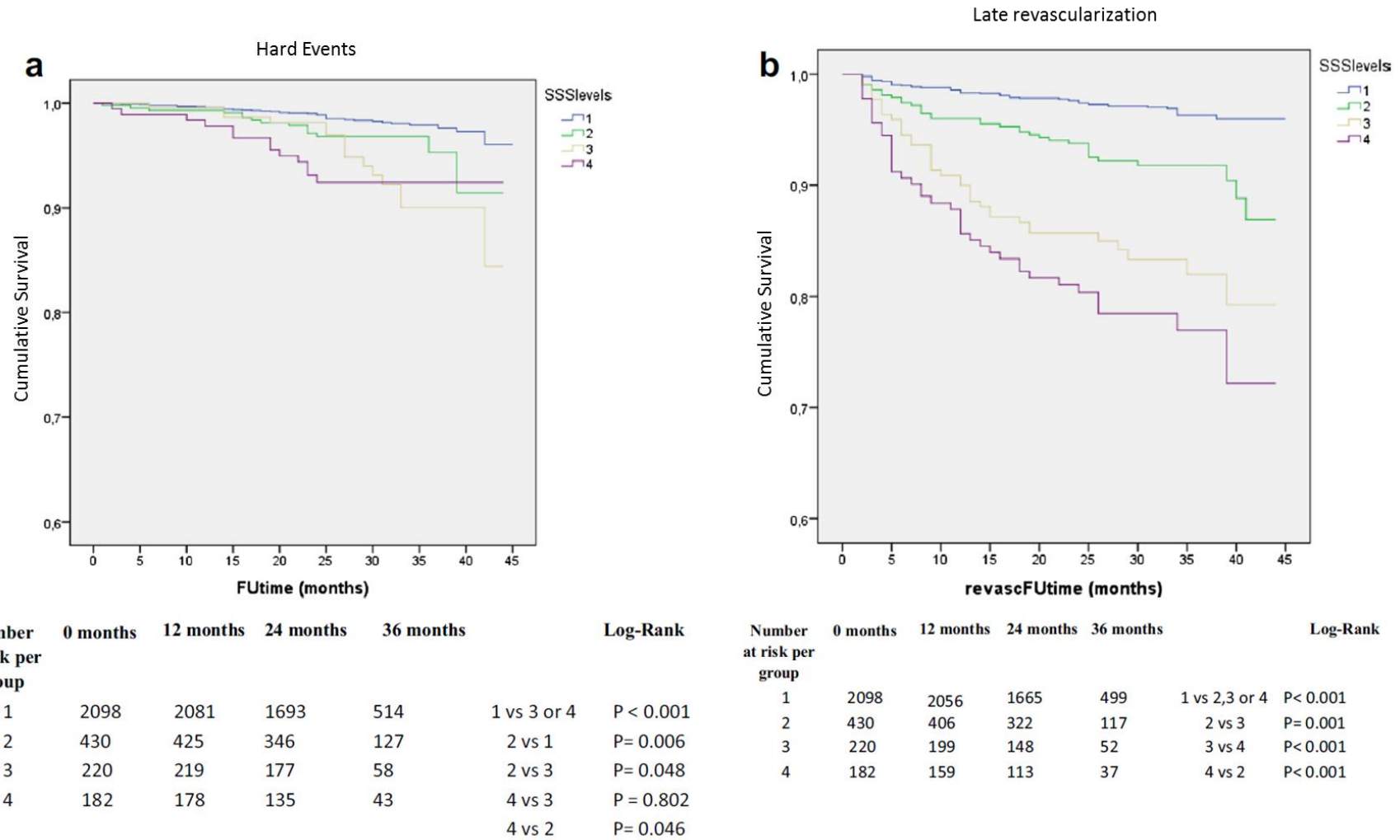
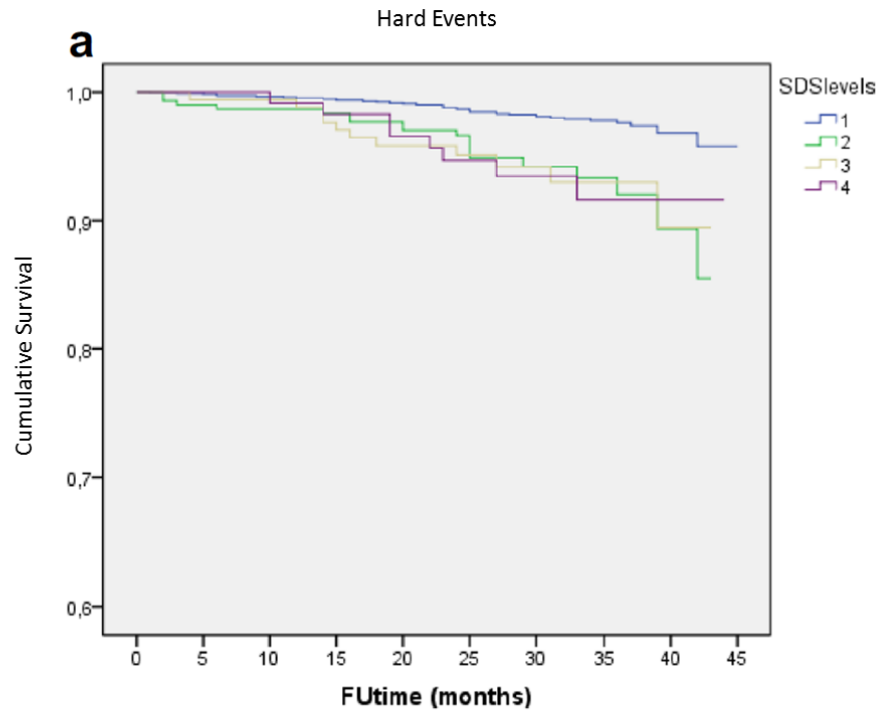


Figure 2 Kaplan-Meier curves of hard events (a) or late revascularization (b) according to SSS categories. Blue line SSS 0-2, green line SSS 3-5; yellow line SSS 6-11; purple line SSS ≥ 12

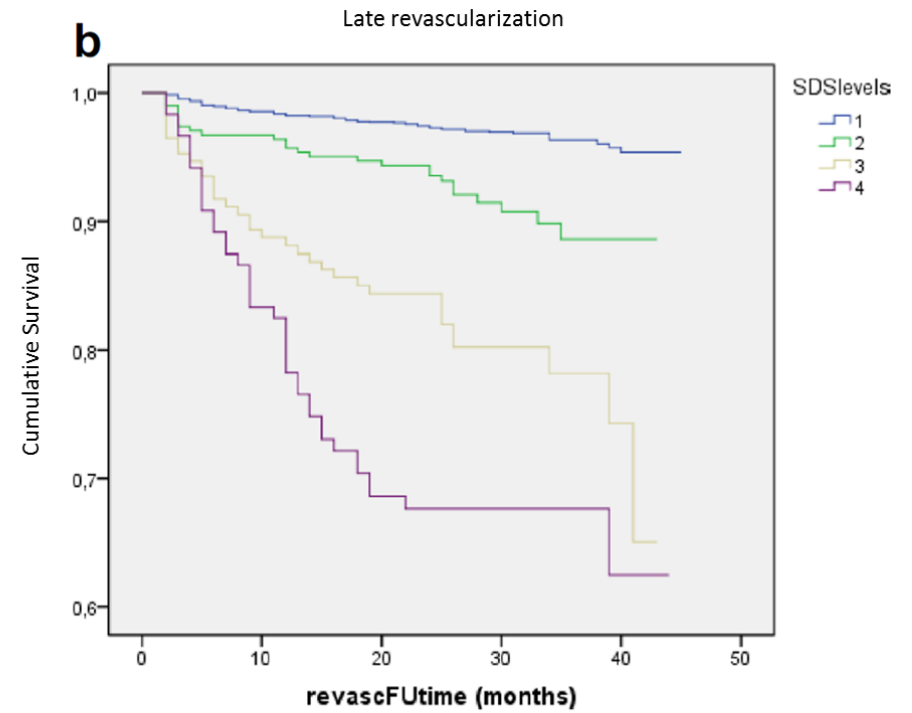
Table 5 Annualized hard events and late revascularization rates for

SSS groups	Annualized hard event rates	Annualized late revascularization rates
1	0.57	0.90
2	1.27	2.45
3	2.06	4.96
4	2.15	6.48

Four groups were also created according to SDS values: group 1 with SDS=0 [n=2334 (79.6.0%)]; group 2, SDS values from 1 to 2 [n=305 (10.4%)]; group 3, SDS from 3 to 5 [n=171 (5.8%)] and group 4, SDS \geq 6 [n=120 (4.0%)]. Kaplan–Meier survival curves also showed that, with increasing SDS, event-free survival was reduced, both for hard events (Fig 3a) (p<0.001) or late revascularization (Fig. 3b) (p<0.001). Also, the annualized events rates, both for hard events or late revascularization, showed the same behavior presented on SSS groups for SDS groups, with higher rates in groups with higher values of SDS (Table 6). For all Kaplan Meier survival curves, p values were demonstrated in a pairwise comparison, below the graphs, to express the statistical differences in events rates between individual groups.



Number at risk per group	0 months	12 months	24 months	36 months	Log-Rank
1	2334	2316	1867	603	1 vs 2,3 or 4 p≤ 0.001
2	305	300	249	71	2 vs 3 P= 0.931
3	171	168	139	38	3 vs 4 P= 0.957
4	120	119	96	30	4 vs 2 P= 0.926



Number at risk per group	0 months	12 months	24 months	36 months	Log-Rank
1	2334	2283	1828	587	2,3 or 4 P< 0.001
2	305	292	238	62	2 vs 3 P< 0.001
3	171	147	118	31	3 vs 4 P= 0.018
4	120	98	64	25	4 vs 2 P< 0.001

Figure 3 Kaplan-Meier curves of hard events (a) or late revascularization (b) according to SDS categories. Blue line SDS 0, green line SDS 1-2; yellow line SDS 3-5; purple line SDS ≥6

Table 6 Annualized hard events and late revascularization rates for individual SDS groups

SDS groups	Annualized hard evnt rates	Annualized late revascularizatio rates
1	0.6	0.96
2	1.87	2.57
3	1.93	6.03
4	2.03	9.84

Finally, in the Cox analysis, male gender (hazard ratio=2.26 [1.33–3.8], $p=0.03$), age (hazard ratio=1.03 [1.01–1.06], $p=0.001$), diabetes (hazard ratio=1.69 [1.09–2.62], $p=0.02$), pharmacologic stress (hazard ratio=2.91 [1.75–4.8], $p<0.001$) and the SSS (hazard ratio=1.36 [1.07–1.73], $p=0.01$) were independently associated with hard events. SDS, when substituting SSS in the cox analysis, also showed to be an independent predictor of hard events (hazard ratio=1.09 [1.02–1.17], $p=0.01$) and maintained the results of the other variables. Table 3 shows all the variables used in the cox regression for hard events, with their respective hazard ratio and confidence interval.

For late revascularization, diabetes (hazard ratio=1.94 [1.41–2.66], $p<0.001$), prior percutaneous coronary intervention (hazard ratio=2.54 [1.76–3.68], $p<0.001$) and the SSS (hazard ratio=1.06 [1.04–1.08], $p<0.001$) were the independent predictors. Again, SDS also showed to be an independent predictor of late revascularization (hazard ratio=1.22 [1.17–1.26], $p<0.001$) when analyzed substituting the SSS with no modification in the other variables. Table 4 shows the variables used for this cox regression, with their respective hazard ratio and confidence interval.

6.6 Discussion

Previous studies have shown that CZT cameras are able to perform ultrafast and low-dose MPS studies, with even higher sensitivity and image quality when compared to traditional cameras (13). However, there is still incomplete evidence supporting the prognostic value of MPS performed in CZT cameras. This study shows, in a large patient population, that the prognostic value of a new MPS protocol in a high-speed CZT-GC could be comparable to what literature has shown about the prognostic value traditionally provided

by conventional MPS (9). Our group had already demonstrated the prognostic value of MPS with a new reconstruction algorithm (11) in traditional Anger cameras, which also allowed faster scans. However, with the advent of CZT technology, it became imperative to define if these new cameras would provide MPS studies with reliable prognostic value, which might be reliably used to manage patients with suspected or known CAD.

Dolan et al. demonstrated the prognostic value of MPS in a CZT camera, but as these authors recognized, they used the conventional activity of radiotracers (14). The radiation dose used in this study was considerably lower than standard dose used in traditional protocols, and we initially tested different acquisition times to obtain the best possible images with low radiation. Total procedure time was reduced to less than one hour, with imaging time of 6 min for rest and 3 min for stress phase.

After establishing these parameters, we then studied the prognostic value of this protocol. Male gender, increasing age and the use of pharmacologic stress were significant predictors of hard events, as previously described (15, 16). Diabetes was independently associated both with hard events or late revascularization. Of note, LVEF was not associated with events, what might be explained by the overall normal left ventricular function of the study population. Importantly, the extent and intensity of myocardial ischemia, as expressed by the SDS, was significantly associated with outcomes, what supports the prognostic value of this new protocol.

It is worth noting the characteristics of the study population, composed of outpatients, most asymptomatic (performing MPS as part of a preoperative evaluation or general screening due to cardiac risk factors) with normal left ventricular function. Nonetheless, the prevalence of diabetes was > 20%, and over 10% had a history of myocardial infarction, what increases overall risk and may improve the generalizability of these results. Therefore, we believe that CZT MPS may be reliably used to evaluate patients for CAD, with the advantages of reduced imaging time and lower radiation dose.

We recognize, as a limitation, that the best method to establish the prognostic value of this new protocol in a CZT-GC would be a comparison between new and traditional cameras, with each patient being studied in both cameras and being control for themselves. However, it assumes that the same protocol would be used for both cameras (14). Since the new low radiation dose and acquisition time protocol could not be used for traditional cameras, the study would not verify the protocol that this study aims to establish.

6.7 Conclusion

A new, faster, low-radiation, MPS protocol in a CZT camera was able to maintain the ability of stratifying patients with increased risk of events, showing that, in the presence of greater extension of defect or ischemia, patients presented higher rates of hard events and late revascularization.

Compliance with ethical standards

Conflict of interest: The authors declare that they have no conflict of interest.

6.8 References

1. Verberne HJ, Acampa W, Anagnostopoulos C, Ballinger J, Bengel F, De Bondt P, et al. EANM procedural guidelines for radionuclide myocardial perfusion imaging with SPECT and SPECT/CT: 2015 revision. *Eur J Nucl Med Mol Imaging*. 2015;42(12):1929-40.
2. Hansen CL, Goldstein RA, Akinboboye OO, Berman DS, Botvinick EH, Churchwell KB, et al. Myocardial perfusion and function: single photon emission computed tomography. *J Nucl Cardiol*. 2007;14(6):e39-60.
3. Oddstig J, Hedeer F, Jögi J, Carlsson M, Hindorf C, Engblom H. Reduced administered activity, reduced acquisition time, and preserved image quality for the new CZT camera. *J Nucl Cardiol*. 2013;20(1):38-44.
4. Duvall WL, Sweeny JM, Croft LB, Ginsberg E, Guma KA, Henzlova MJ. Reduced stress dose with rapid acquisition CZT SPECT MPI in a non-obese clinical population: comparison to coronary angiography. *J Nucl Cardiol*. 2012;19(1):19-27.
5. Mouden M, Timmer JR, Ottervanger JP, Reiffers S, Oostdijk AH, Knollemans S, et al. Impact of a new ultrafast CZT SPECT camera for myocardial perfusion imaging: fewer equivocal results and lower radiation dose. *Eur J Nucl Med Mol Imaging*. 2012;39(6):1048-55.
6. Hayes SW, De Lorenzo A, Hachamovitch R, Dhar SC, Hsu P, Cohen I, et al. Prognostic implications of combined prone and supine acquisitions in patients with equivocal or abnormal supine myocardial perfusion SPECT. *J Nucl Med*. 2003;44(10):1633-40.
7. Burrell S, MacDonald A. Artifacts and pitfalls in myocardial perfusion imaging. *J Nucl Med Technol*. 2006;34(4):193-211; quiz 2-4.
8. Berman DS, Kang X, Van Train KF, Lewin HC, Cohen I, Areeda J, et al. Comparative prognostic value of automatic quantitative analysis versus semiquantitative visual analysis of exercise myocardial perfusion single-photon emission computed tomography. *J Am Coll Cardiol*. 1998;32(7):1987-95.
9. Berman DS, Hachamovitch R, Kiat H, Cohen I, Cabico JA, Wang FP, et al. Incremental value of prognostic testing in patients with known or suspected ischemic heart disease: a basis for optimal utilization of exercise technetium-99m sestamibi myocardial perfusion single-photon emission computed tomography. *J Am Coll Cardiol*. 1995;26(3):639-47.

10. Hachamovitch R, Berman DS, Shaw LJ, Kiat H, Cohen I, Cabico JA, et al. Incremental prognostic value of myocardial perfusion single photon emission computed tomography for the prediction of cardiac death: differential stratification for risk of cardiac death and myocardial infarction. *Circulation*. 1998;97(6):535-43.
11. Lima R, Ronaldo L, De Lorenzo A, Andrea dL, Camargo G, Gabriel C, et al. Prognostic value of myocardium perfusion imaging with a new reconstruction algorithm. *J Nucl Cardiol*. 2014;21(1):149-57.
12. Thygesen K, Alpert JS, White HD, Infarction JEAATFftRoM. Universal definition of myocardial infarction. *J Am Coll Cardiol*. 2007;50(22):2173-95.
13. Duvall WL, Croft LB, Ginsberg ES, Einstein AJ, Guma KA, George T, et al. Reduced isotope dose and imaging time with a high-efficiency CZT SPECT camera. *J Nucl Cardiol*. 2011;18(5):847-57.
14. Oldan JD, Shaw LK, Hofmann P, Phelan M, Nelson J, Pagnanelli R, et al. Prognostic value of the cadmium-zinc-telluride camera: A comparison with a conventional (Anger) camera. *J Nucl Cardiol*. 2016;23(6):1280-7.
15. Hachamovitch R, Berman DS, Kiat H, Bairey CN, Cohen I, Cabico A, et al. Effective risk stratification using exercise myocardial perfusion SPECT in women: gender-related differences in prognostic nuclear testing. *J Am Coll Cardiol*. 1996;28(1):34-44.
16. Navare SM, Mather JF, Shaw LJ, Fowler MS, Heller GV. Comparison of risk stratification with pharmacologic and exercise stress myocardial perfusion imaging: a meta-analysis. *J Nucl Cardiol*. 2004;11(5):551-61.

7 Artigo 2

Comparison of the prognostic value of myocardial perfusion imaging using a CZT-SPECT camera with a conventional angler camera

Ronaldo Lima; Thais Peclat; Thalita Soares; Caio Ferreira; Ana Carolina Souza;
Gabriel Camargo

7.1 Abstract

Background: Recent studies have shown that myocardial perfusion imaging (MPI) in cadmium-zinc-telluride (CZT) cameras allow faster exams with less radiation dose but there are little data comparing its prognosis information with that of dedicated cardiac Na-I SPECT cameras

Objective: The objective of this study is to compare the prognostic value of MPI using an ultrafast protocol with low radiation dose in a CZT-SPECT and a traditional one.

Methods: Group 1 was submitted to a two-day MIBI protocol in a conventional camera, and group 2 was submitted to a 1-day MIBI protocol in CZT camera. MPI were classified as normal or abnormal, and perfusion scores were calculated. Propensity score matching methods were performed

Results: 3554 patients were followed during 33±8 months. Groups 1 and 2 had similar distribution of age, gender, body mass index, risk factors, previous revascularization, and use of pharmacological stress. Group 1 had more abnormal scans, higher scores than group 2. Annualized hard events rate was higher in group 1 with normal scans but frequency of revascularization was similar to normal group 2. Patients with abnormal scans had similar event rates in both groups

Conclusion: New protocol of MPI in CZT-SPECT showed similar prognostic results to those obtained in dedicated cardiac Na-I SPECT camera, with lower prevalence of hard events in patients with normal scan.

(J Nucl Cardiol 2016)

Key Words: myocardial perfusion imaging; coronary artery disease; SPECT

7.2 Introduction

It is well known that myocardial perfusion imaging (MPI) with stress testing is an independent predictor of prognosis in patients with suspected or known coronary artery disease (CAD). The gated single-photon emission computed tomography (SPECT) appears to be the best predictor of cardiac event-free survival in this population.(1) Also, compared with other methods such as stress-ECG and coronary angiography, SPECT-based strategies seem to be more cost-effective.(2)

Over time, numerous technological advances have increased MPI's performance, with the most meaningful being the introduction of tomographic imaging and, later, of the multi-detector gamma cameras. Recent developments have allowed for reductions in scan time and radiation dose used to its acquisition.(3) Specifically, new multipinhole cameras with cadmium-zinc-telluride solid state detectors (CZT-SPECT) technology allow for faster image acquisition and lower radiation doses in comparison with traditional Sodium-Iodine Anger cameras. This allows for 1-day stress/rest MPI protocols, preserving diagnostic image quality and diagnostic accuracy.(4, 5) The CZT technology improves the energy and spatial resolutions, while using simultaneously acquired views improves the overall sensitivity, resulting in high-quality images.(6)

Previous examination of the prognostic value in specific groups, like the obese, demonstrated that CZT SPECT provides adequate risk stratification.(7) However, there is little data comparing the prognostic value between ultrafast protocol CZT-SPECT and dedicated cardiac Na-I SPECT cameras. That could impair the broad use of this technology. Our objective is to compare the prognostic value of MPI using these two camera protocols.

7.3 Methods

7.3.1 Population and Study Design

We analyzed two different groups of patients clinically referred to a SPECT-MPI in an outpatient clinic between 2008 and 2012. Patients in group 1 were scanned in Na-I SPECT cameras from 2008 to 2010, and in group 2 were scanned using CZT SPECT from 2011 to 2012.

Ninety-nine patients who underwent revascularization in the first 60 days after nuclear testing were excluded. History of significant cardiac valve disease or severe nonischemic cardiomyopathy (33 patients) or any condition which might adversely affect short-term prognosis were also considered exclusion criteria (Figure 1). Three patients were

excluded because the images acquired in gamma camera CZT were inadequate for interpretation (BMI>45). The research was approved by the institutional review board, and all subjects signed informed consent.

Prior to scanning, a team of cardiologists collected information on the presence of categorical cardiac risk factors in each individual including hypertension, diabetes, hypercholesterolemia, smoking, and family history of CAD using a standard questionnaire.

Cardiac symptoms were based on Diamond and Forrester criteria,(8) divided as asymptomatic, non-anginal pain, atypical angina, typical angina, and shortness of breath.

From a total of 6128 patients meeting inclusion criteria, follow-up was complete in 5828 (95.1% of the total). We selected 3554 using propensity score matching based on sex, age, body mass index (BMI), symptoms, cardiac risk factors, history of coronary events, and type of stress used. A 1 to 1 nearest neighbor matching with no replacement was performed to produce two groups with 1777 individuals in each, divided according to the type of gamma camera used.

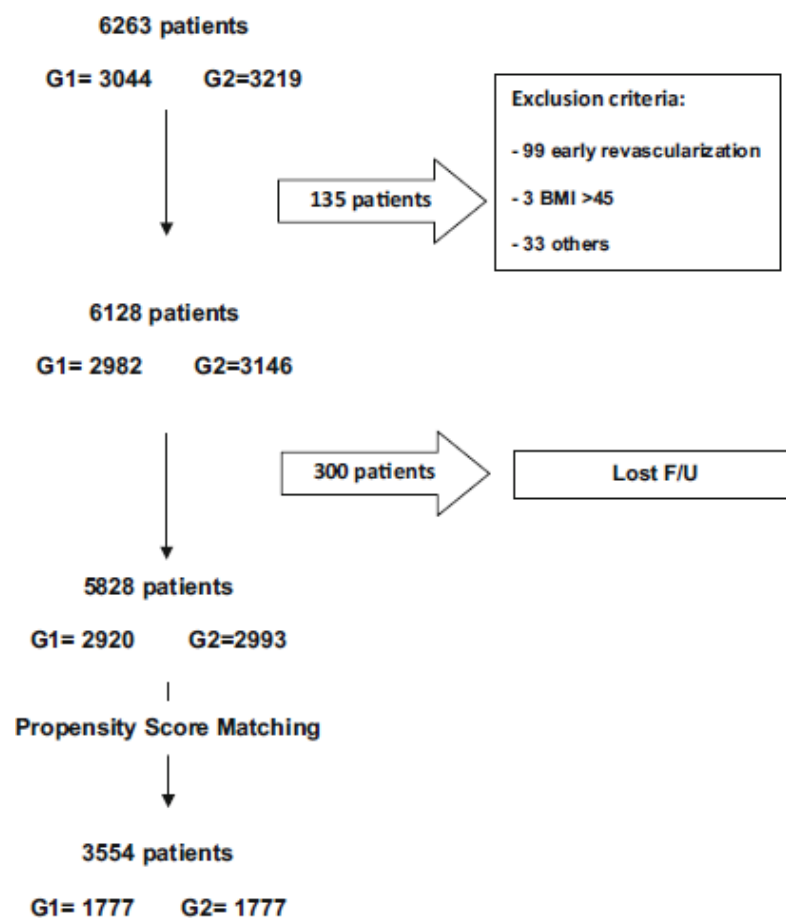


Figure 1 Flow diagram of the study

7.3.2 Cardiac Imaging and Stress Protocol

Patients were instructed to abstain from any products containing caffeine for 24 hours before the test. Beta-blockers and calcium-channel antagonists were terminated 48 hours before testing, and nitrates were withheld for at least 6 hours before testing. Stress testing was performed with a symptom limited Bruce treadmill exercise protocol or pharmacologic protocol (dipyridamole or dobutamine). In general, whenever pharmacologic stress test was used, dipyridamole was the first choice, while dobutamine was reserved for patients with contraindications to vasodilator stress (mainly bronchospastic airway disease).

Patients in group 1 underwent 2-day ^{99m}Tc -sestamibi (near-maximal exercise, 10-12 mCi was injected intravenously, and exercise was continued at maximal workload for at least 1 minute) gated MPS with scan time of 6 minutes stress and rest studies (15-18 mCi). Mean radiation dose was 9.5 mSv. Stress-only imaging was not performed due to reimbursement issues. Three minutes prone images were acquired in all male patients but gating was not performed. All supine images were gated. The full protocols used have been previously described.⁽⁹⁾ MPI studies were classified as normal or abnormal, and perfusion scores (SSS, SRS, and SDS) were calculated. Images were acquired using a two-headed gamma camera equipped with 90°-angled detectors (Ventri, GE Healthcare, Waukesha, WI, USA) equipped with a low-energy, high-resolution collimator, and 30 stops in a 64 x 64 matrix. Image acquisition began 15-45 minutes after tracer injection. Scans were reconstructed with Evolution for CardiacTM (GE healthcare), using 12 iterations. Post stress gated short-axis images were processed using quantitative gated SPECT software (QGS; Cedars-Sinai Medical Center, Los Angeles, California), and left ventricular ejection fraction (LVEF) was automatically calculated after inspection of myocardial contours.

Patients in group 2 underwent treadmill exercise or pharmacological stress using standard dipyridamole or dobutamine infusion protocols,⁽¹⁰⁾ Exercise testing was performed using a symptom-limited Bruce protocol. A 1-day ^{99m}Tc -sestamibi, rest/stress protocol was used, starting with rest study (injection of 5 mCi) followed by stress (15 mCi) in a CZT camera. Mean radiation dose was 6 mSv. The MPI were also classified as normal or abnormal and perfusion scores (SSS, SRS, and SDS) were also calculated. Post-stress prone acquisitions were performed in all patients. CZT-SPECT was performed using a camera with multipinhole collimator (Discovery 530, GE Healthcare, Milwaukee, USA). The system design allows acquisition without detector or collimator motion. Images were acquired in 6, 3,

and 1 minute, respectively, for rest, supine stress and prone stress, as previously described(11). A 10% symmetric energy window at 140 keV was used. Images were reconstructed on a dedicated Xeleris workstation (GE Healthcare) applying an iterative reconstruction algorithm with maximum-likelihood expectation maximization. Assessment of image quality and perfusion abnormalities was performed visually by two experienced nuclear cardiologists blinded to patient characteristics. Post-stress left ventricular volumes and ejection fraction were calculated from the post-stress-gated images using commercially available software (QGS, Cedars-Sinai Medical Center, Los Angeles, California, USA).

In both groups, semiquantitative visual interpretation of MPI images was performed with short-axis and vertical long axis tomograms divided into 17 segments.(10) Each segment was scored by consensus of two expert observers (aware of clinical and stress data) using a 5-point scale (0 = normal; 1 = equivocal; 2 = moderate; 3 = severe reduction of tracer uptake; 4 = the absence of detectable radiotracer activity in a segment). Then, perfusion scores were calculated to express the extent and severity of myocardial perfusion abnormalities. The summed stress score (SSS, a measure of the total post-stress perfusion defect) and summed rest score (SRS, a measure of rest defect or myocardial fibrosis) were obtained by means of adding the scores for the 17 segments of the stress and rest images, respectively. The difference between the SSS and SRS was defined as the summed difference score (SDS, a measure of reversible defect or myocardial ischemia). For the purpose of evaluating the SSS and the SDS as predictors of events, we performed separate analyses with different cut points for each perfusion variable. We classified SSS as abnormal when it was >3 and SDS when it was >1 .

7.3.3 Follow-Up

Follow-up was performed by telephone interview every 6 months after MPI. Events were defined as all-cause death and nonfatal myocardial infarction (classified as hard events) and late revascularization (>60 days after MPI), by percutaneous coronary intervention (PCI) or bypass surgery (CABG). Events were confirmed through review of hospital charts or physician's records. Nonfatal myocardial infarction was defined based on the criteria of typical chest pain, elevated cardiac enzyme levels, and typical alterations of the electrocardiogram.(12)

7.3.4 Statistical Analysis

All statistical calculations were performed using SPSS (Version 17). Categorical variables are presented as frequencies and continuous variables as mean \pm SD. Variables were compared with Pearson Chi-squared test for categorical variables and by Student's two sample t test for continuous variables. Event-free survival curves were constructed using the Kaplan-Meier methods to account for censored survival times and were compared with the log-rank test.

7.4 Results

Patients were divided into group 1 and 2, each with of 1777 subjects, and its overall baseline characteristics are summarized in Table 1. There were no statistically significant differences between groups in regard of gender, prevalence of hypertension, diabetes, smoking, hypercholesterolemia, previous revascularization, and use of pharmacological stress. The more frequent indications in asymptomatic patients were a previous treadmill test with intermediate-high risk Duke Score, pre-op risk stratification and a previous calcium score >100 . Patients with previous MI or revascularization were considered to have known CAD. The mean follow-up interval was 34 ± 9 months in group 1 and 33 ± 8 months in group 2.

Comparing the two groups, the classification as normal or abnormal scans and the perfusion scores (SSS, SRS, and SDS) were statistically different. Group 1 had more abnormal scans (27.4% vs 21.6%; $p < 0.001$) and higher SSS, SRS, and SDS than group 2. Scan results, perfusion scores, left ventricle ejection fraction, and ventricular volumes of both groups are summarized in Table 2.

Table 1 Baseline characteristics

Baseline Characteristics	Total (6128)	Select (3554)	Group 1 (1777)	Group 2 (1777)	<i>p</i> value
Age (years)	63.0 ± 12.3	62.8 ± 12.0	62 ± 12.0	62.9 ± 12.0	1
Male	3370 (55.0%)	1920 (54.0%)	949 (53.4%)	971 (54.6%)	0.46
Weight (kg)	78.5 ± 17.7	78.1 ± 16.6	77.9 ± 16.3	78.2 ± 165.9	0.47
BMI	28.0 ± 6.1	27.8 ± 5.9	27.7 ± 6.0	27.9 ± 6.0	0.26
Asymptomatic	4221 (68.9%)	2377 (66.9%)	1171 (65.9%)	1206 (67.9%)	0.21
Diabetes	1396 (22.8%)	815 (22.9%)	390 (21.9%)	425 (23.9%)	0.16
Hypertension	3908 (63.8%)	2165 (60.9%)	1081 (60.8%)	1084 (61.0%)	0.92
Hypercholesterolemia	3166 (51.7%)	1764 (49.8%)	885 (49.6%)	879 (49.5%)	0.84
Beta-blockers	1782 (29.1%)	1074 (30.2%)	541 (30.4%)	533 (30%)	0.39
ACEi	3247 ((38.6%)	1365 (38.4%)	400 (22.5%)	410 (23.1%)	0.3
Statins	3062 (50.0%)	1777 (50.0%)	886 (49.9%)	891 (50.1%)	0.78
Previous MI	767 (12.5%)	439 (12.4%)	225 (12.7%)	214 (12.0%)	0.31
Previous PCI	1195 (19.5%)	628 (17.7%)	314 (17.7%)	314 (17.7%)	1
Previous CABG	550 (9.0%)	302 (8.5%)	159 (9.0%)	143 (8.0%)	0.34
Pharmacological stress	2566 (41.9%)	1458 (41.0%)	752 (42.3%)	706 (39.7%)	0.13

p value comparison between Group 1 and 2: n (%) or mean ± Standard deviation
ACEi angiotensin-converting enzyme inhibitor; *BMI* body mass index; *CABG* coronary artery bypass graft; *MI* myocardial infarction; *PCI* percutaneous coronary intervention

Table 2 Scans results, perfusion scores, and gated SPECT measurements

	Group 1 (1777)	Group 2 (1777)	<i>p</i> value
Abnormal scans	487 (27.4%)	383 (21.6%)	<0.001
Reversible	237 (13.3%)	154 (8.7%)	
Fixed	126 (7.1%)	128 (7.2%)	
Mixed defect	124 (7.0%)	101 (5.7%)	
SSS	2 (0-4)	1 (0-3)	<0.01
SRS	1 (1-3)	0 (0-2)	<0.01
SDS	0 (0-1)	0 (0-0)	<0.01
LVEF stress	58.5 ± 11.9	59.3 ± 13.0	0.07
EDV stress	80.1 ± 33.9	82.1 ± 33.5	0.1
ESV stress	36.4 ± 28.3	36.1 ± 26.5	0.7

EDV end diastolic volume; *ESV* end systolic volume; *LVEF* left ventricle ejection fraction; *SSS* summed stress score; *SRS* summed rest score; *SDS* summed difference score
Perfusion scores are expressed as median and interquartile 25 and 75

During follow-up, 98 deaths and 48 myocardial infarctions, 188 percutaneous coronary interventions, and 48 coronary artery bypass graft surgeries occurred. Assessing data from patients with normal scans, it was found that the annualized hard events rate was higher in patients of Group 1 (1.0%/year vs 0.5%/year; $p < 0.01$), but the percentage of PCI and CABG were not different (0.9% vs 0.8%; 0.3% vs 0.1%, respectively; $p = \text{NS}$) comparing with Group 2. However, patients with abnormal scans had no significant difference between the two groups in regard of both annualized hard events (3.3%/year and 3.2%/year; $p = \text{NS}$) and percentage of revascularization (6.6% vs 6.3%, $p = \text{NS}$). Event rates comparison between two groups are demonstrated in Table 3. Kaplan-Meier cumulative survival comparing group 1 and 2 with normal or abnormal scan are shown in Figure 2 (hard events) and Figure 3 (late revascularization).

Table 3 Annualized event rate (%/year)

Variables	Group 1		Group 2	
	Normal scan (n=1290)	Abnormal scan (n= 487)	Normal scan (n=1394)	Abnormal scan (n= 383)
Hard events	1.0* (41)	3.3 (54)	0.5* (18)	3.2 (33)
Late Revascularization	1.2* (46)	4.2 (92)	0.7* (33)	3.3 (65)
Death	0.7* (26)	2.3 (33)	0.5* (16)	2.4 (23)
MI	0.4* (15)	1.5 (21)	0.06* (2)	1.0 (10)
PCI	0.9* (36)	5.0 (72)	0.8* (30)	5.1 (50)
CABG	0.3* (10)	1.6 (20)	0.1* (3)	1.2 (15)

*Significant difference between normal and abnormal scan
Significant difference between Group 1 and Group 2; (number of events)
CABG coronary artery bypass graft; MI myocardial infarction; PCI percutaneous coronary intervention

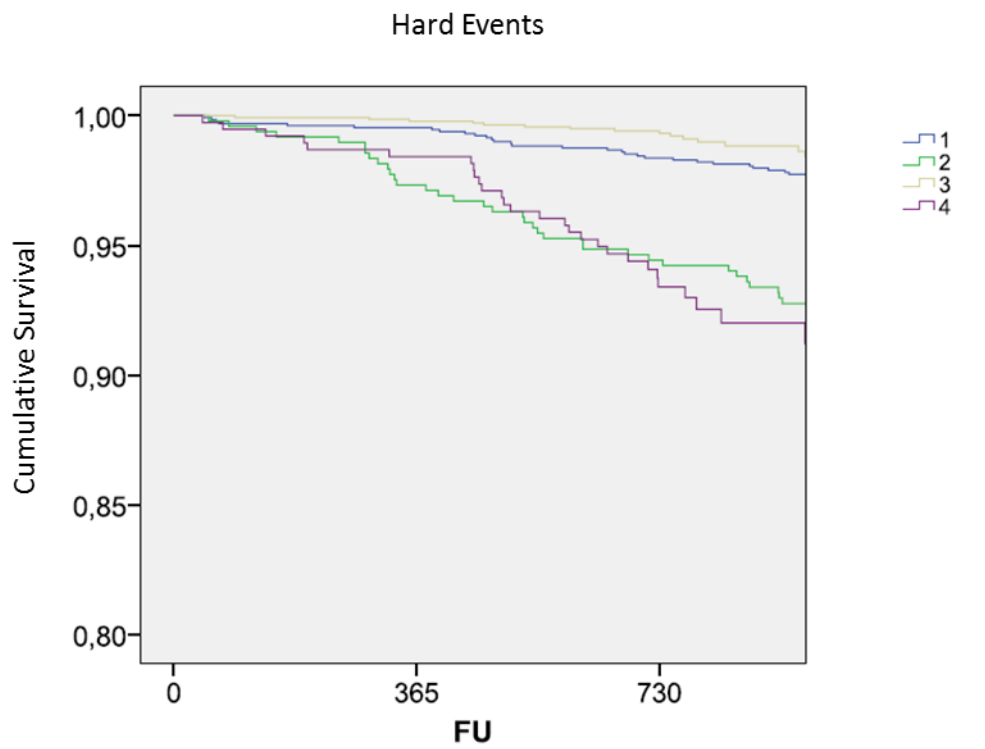
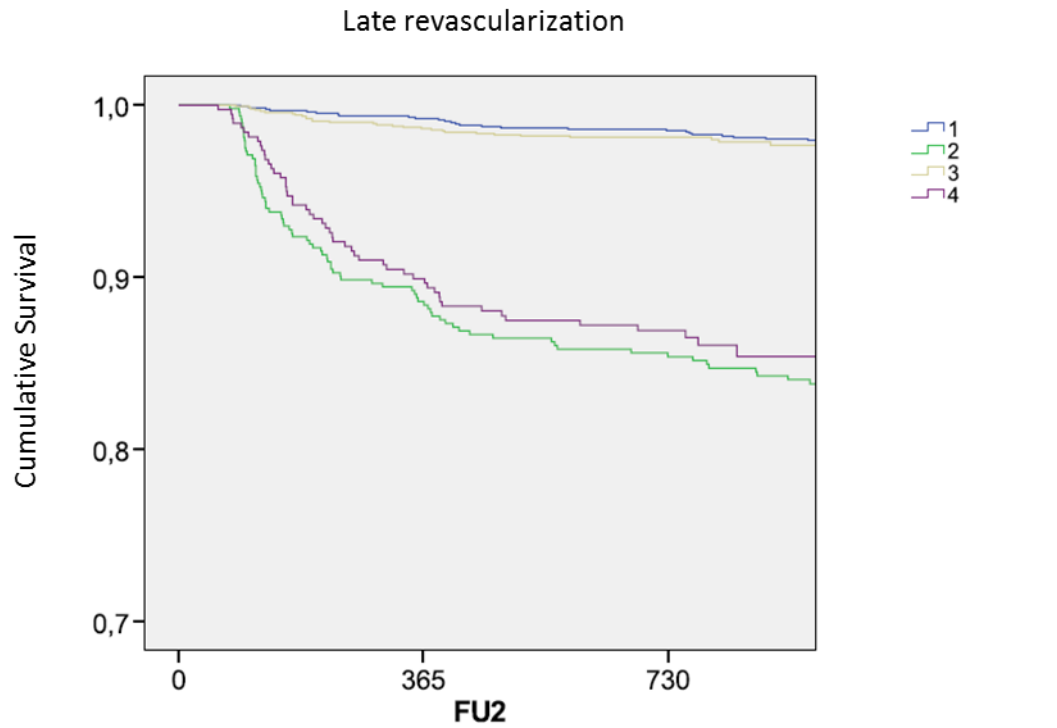


Figure 2 Kaplan-Meier curves for hard events. (1) Blue: Ventri normal scans; (2) Green: Ventri-abnormal scans; (3) Yellow: CZT normal scans; and (4) Purple: CZT abnormal scans.



Number at risk			Log-rank	
1291	1273	1242	1 vs 2	0.001
486	419	340	3 vs 4	0.001
1396	1372	1325	1 vs 3	0.292
381	336	269	2 vs 4	0.355

Figure 3 Kaplan-Meier curves for late revascularization. (1) Blue: Ventri normal scans; (2) Green: Ventri-abnormal scans; (3) Yellow: CZT normal scans; and (4) Purple: CZT abnormal scans.

7.5 Discussion

MPI is an established method for diagnostic and prognostic evaluation of patients with CAD.(1) However, two considerable limitations of this method are the prolonged time required to scan acquisition and the radiation dose.(13) New high-speed SPECT cameras using cadmium-zinc-telluride detectors are a new technology of gamma camera that allows shorter acquisition time and lower tracer activities.(14) Nevertheless, the prognostic value of this ultrafast, low-dose radiation, protocol is not yet established and has not been compared with the protocol in dedicated cardiac Na-I SPECT cameras.(15-17)

In an attempt to do this comparison, we studied two different groups with 1777 patients. They were standard to each other through a propensity score matching with the purpose of showing the association, in both groups, between scan results and the hard events rate. As can be seen in Table 1, the strict matching parameter we used produced two groups with very similar exposition to factors that could influence results.

Statistically significant differences in the distribution of perfusion scores (SSS, SRS, and SDS) and the classification as normal and abnormal scans were noted between the CZT camera and the conventional camera. The CZT camera had, on average, 6% less abnormal scans and lower SSS, SDS, and SRS as previously demonstrated by Oldan et al.(16) Results showed that the rate of events and myocardial revascularization was not higher in group 1. Someone might argue that the more frequently abnormal tests in Group 1 could mean greater accuracy of traditional equipment. In this case, a larger number of false negative tests should have occurred in Group 2, which did not happen. In fact, patients with normal examination evaluated in CZT cameras showed a lower percentage of events.

In the follow-up data, our study has found that among patients with normal scans, the annualized hard events rate was higher in patients from traditional Na-I camera. The difference among hard event rate between both cameras may be an objective representation of the already known higher sensitivity for these new cameras, reflecting in a higher negative predicted value. In the follow-up of patients with abnormal scans, the study has shown no significant difference between the two groups in regard of both annualized hard events and percentage of revascularization. These data support that in patients with a higher probability of disease; both cameras were totally able to stratify the risk of events and thereby definitely established the MPI good prognostic value for patients with CAD.

There has been controversy regarding the diagnostic value of SPECT-MPI using CZT cameras in obese patients,(7) therefore the weight and BMI were included in the propensity score. As described in Population section, three patients were excluded because the images acquired in gamma camera CZT were inadequate for interpretation but more than 300 patients with at least 220 pounds were included in group 2. De Lorenzo et al demonstrated that in obese patients CZT-SPECT camera provides prognostic discrimination with high image quality This is consistent with the results of the present study.

Our study was a retrospective analysis of outpatients who underwent CZT-SPECT or traditional Anger camera for clinical indications which carries the obvious and inherent bias of this type of study design. This is also a single-institution study and thus may not be applicable to others institutions and others types of camera designs, both CZT and conventional. Beyond that, reviewers were not blinded to clinical data. While this is necessary to clinical interpretation of scan results, it can bias the interpretation for research purposes. However, we can assume that any bias introduced by use of clinical information should affect both cameras in the same degree. Finally, it is important to mention that while the propensity score matching was successful in producing groups with similar baseline characteristics that could bias the results, there could be other potential unknown sources of bias that may not have been balanced in our two groups using this approach.

Analyzing the few data produced by similar studies,(15-17) we concluded that our study also showed a pattern of maintenance of the prognostic value of CZT comparing with traditional cameras. However, we had the opportunity to use a larger population that was matched in baseline characteristics and exposed to two totally different protocols. We used a standard protocol as mentioned before to dedicated Na-I cameras and a faster, lower-dose protocol in CZT-SPECT, something pioneer to this type of study.

7.6 New Knowledge Gained

The CZT camera has similar utility for prognostication to conventional Anger cameras even when they are using smaller radiation doses and shorter acquisition time.

7.7 Conclusion

In our study, a new protocol of MPI in CZT-SPECT camera showed similar prognostic results to those obtained in dedicated cardiac Na-I SPECT camera, with lower prevalence of hard events in patients with normal scan. According to these data, we can assume that the new ultrafast protocol, using considerable lower dose of radiation, has a reliable prognostic value and is non-inferior to traditional cameras.

7.8 Acknowledgments

The authors had no financial support for this research.

The authors would like to thank Dr. Ilan Gottlieb for his review and valuable suggestions.

7.9 Compliance with Ethical Standards

7.9.1 Disclosure

The authors declare that they have no conflict of interest.

7.9.2 Ethical standards

All procedures performed in studies involving human participants were in accordance with the ethical standards of the institutional and/or national research committee and with the 1964 Helsinki declaration and its later amendments of comparable ethical standards.

7.9.3 Informed consent

Informed consent was obtained from all individual participants included in the study.

7.10 References

1. Gimelli A, Rossi G, Landi P, Marzullo P, Iervasi G, L'abbate A, et al. Stress/Rest Myocardial Perfusion Abnormalities by Gated SPECT: Still the Best Predictor of Cardiac Events in Stable Ischemic Heart Disease. *J Nucl Med.* 2009;50(4):546-53.
2. Underwood SR, Godman B, Salyani S, Ogle JR, Ell PJ. Economics of myocardial perfusion imaging in Europe--the EMPIRE Study. *Eur Heart J.* 1999;20(2):157-66.
3. DePuey EG. Advances in SPECT camera software and hardware: currently available and new on the horizon. *J Nucl Cardiol.* 2012;19(3):551-81; quiz 85.
4. Duvall WL, Croft LB, Ginsberg ES, Einstein AJ, Guma KA, George T, et al. Reduced isotope dose and imaging time with a high-efficiency CZT SPECT camera. *J Nucl Cardiol.* 2011;18(5):847-57.
5. Herzog BA, Buechel RR, Katz R, Brueckner M, Husmann L, Burger IA, et al. Nuclear myocardial perfusion imaging with a cadmium-zinc-telluride detector technique: optimized protocol for scan time reduction. *J Nucl Med.* 2010;51(1):46-51.
6. Slomka PJ, Patton JA, Berman DS, Germano G. Advances in technical aspects of myocardial perfusion SPECT imaging. *J Nucl Cardiol.* 2009;16(2):255-76.
7. De Lorenzo A, Peclat T, Amaral AC, Lima RSL. Prognostic evaluation in obese patients using a dedicated multipinhole cadmium-zinc telluride SPECT camera. *Int J Cardiovasc Imaging.* 2016;32(2):355-61.
8. Diamond GA, Forrester JS, Hirsch M, Staniloff HM, Vas R, Berman DS, et al. Application of conditional probability analysis to the clinical diagnosis of coronary artery disease. *J Clin Invest.* 1980;65(5):1210-21.
9. Lima R, Ronaldo L, De Lorenzo A, Andrea dL, Camargo G, Gabriel C, et al. Prognostic value of myocardium perfusion imaging with a new reconstruction algorithm. *J Nucl Cardiol.* 2014;21(1):149-57.
10. Henzlova MJ, Duvall WL, Einstein AJ, Travin MI, Verberne HJ. ASNC imaging guidelines for SPECT nuclear cardiology procedures: Stress, protocols, and tracers. *J Nucl Cardiol.* 2016;23(3):606-39.
11. Lima R PT, Amaral AC, Nakamoto A, Lavagnoli D, De, A. L. Preliminary data on the prognostic value of a new protocol of ultra-fast myocardial scintigraphy with less radiation in CZT gamma camera. *Arq Bras Cardiol: Im Cardio*2016. p. 11-6.
12. Thygesen K, Alpert JS, White HD, Infarction JEAAWTFftRoM. Universal definition of myocardial infarction. *J Am Coll Cardiol.* 2007;50(22):2173-95.
13. Douglas PS, Hendel RC, Cummings JE, Dent JM, Hodgson JM, Hoffmann U, et al. ACCF/ACR/AHA/ASE/ASNC/HRS/NASCI/RSNA/SAIP/SCAI/SCCT/SCMR 2008 Health Policy Statement on Structured Reporting in Cardiovascular Imaging. *J Am Coll Cardiol.* 2009;53(1):76-90.
14. Sharir T, Pinskiy M, Pardes A, Rochman A, Prokhorov V, Kovalski G, et al. Comparison of the diagnostic accuracies of very low stress-dose with standard-dose myocardial perfusion imaging:

Automated quantification of one-day, stress-first SPECT using a CZT camera. *J Nucl Cardiol.* 2016;23(1):11-20.

15. Gimelli A, Bottai M, Giorgetti A, Genovesi D, Kusch A, Ripoli A, et al. Comparison between ultrafast and standard single-photon emission CT in patients with coronary artery disease: a pilot study. *Circ Cardiovasc Imaging.* 2011;4(1):51-8.

16. Oldan JD, Shaw LK, Hofmann P, Phelan M, Nelson J, Pagnanelli R, et al. Prognostic value of the cadmium-zinc-telluride camera: A comparison with a conventional (Anger) camera. *J Nucl Cardiol.* 2016;23(6):1280-7.

17. Yokota S, Mouden M, Ottervanger JP, Engbers E, Knollema S, Timmer JR, et al. Prognostic value of normal stress-only myocardial perfusion imaging: a comparison between conventional and CZT-based SPECT. *Eur J Nucl Med Mol Imaging.* 2016;43(2):296-301.

8 Artigo 3

The additional Prognostic Value of Myocardial Perfusion SPECT in Patients with Known Coronary Artery Disease with high exercise capacity

Thais R. Peclat, Ana Carolina A.H. Souza, Victor F. Souza, Aline K. M. Nakamoto, Felipe M. Neves, Izabella C. R. Silva, Ronaldo S. L. Lima

8.1 Abstract

Background: The prognostic value of myocardial perfusion imaging (MPI) in patients with known coronary artery disease (CAD) and high exercise capacity is still unknown. We sought to determine MPI additional prognostic value over ECG stress testing alone in patients with known CAD who achieved ≥ 10 Metabolic Equivalents (METs).

Methods and Results: We evaluated 926 patients with known CAD referred for MPI with exercise stress. Patients were followed for a mean of 32.4 ± 9.7 months for the occurrence of all-cause death or nonfatal myocardial infarction (MI). Those achieving ≥ 10 METs were younger, predominantly male, and had lower prevalence of cardiovascular risk factors. Patients reaching ≥ 10 METs had a lower annualized rate of hard events compared to their counterparts achieving < 10 METs (1.13 %/year vs 3.95 %/year, $p < 0.001$). Patients who achieved ≥ 10 METs with abnormal scans had a higher rate of hard events compared to those with normal scans (3.37 %/year vs 0.57 %/year, $p = 0.023$). Cardiac workload < 10 METs and abnormal MPI scan were independent predictors of hard events.

Conclusions: MPI is able to stratify patients with known CAD achieving ≥ 10 METs for the occurrence of all-cause death and non-fatal MI with incremental prognostic value over ECG stress test alone.

8.2 Introduction

Coronary artery disease (CAD) remains as the leading cause of death in adults in the United States, accounting for about one-third of all deaths in subjects over age 35 (1). In patients with known or suspected CAD, accurate risk stratification and management guidance is of great value to improve outcomes.

Exercise electrocardiography (ECG) stress test and myocardial perfusion imaging with single photon emission computed tomography (MPI SPECT) are both robust, widely used tools for risk stratification in stable CAD (2, 3). It is known that MPI has higher sensitivity over exercise ECG stress test for detection of ischemia in patients with an intermediate pretest likelihood of CAD (4). Moreover, MPI may provide additional clinical information on ventricular function and regional perfusion.

Exercise capacity is an established predictor of mortality (5-10) and along the past two decades several authors have brought to discussion whether this parameter would be sufficient to support clinical decision. Patients achieving ≥ 10 metabolic equivalents (METs) were shown to have excellent prognosis, with low rates of cardiovascular events and low prevalence of $\geq 10\%$ LV ischemia regardless of peak exercise heart rate. That led to questioning on the usefulness of MPI-derived information (11, 12) and later, on the use of exercise capacity as criteria to skip imaging protocols. In that context, provisional protocols were created to better address the groups of patients that could have been selected for this approach, preserving them from unnecessary radiation exposure (13, 14). However, these provisional protocols typically excluded patients with known CAD (14).

Patients with known CAD are an important segment of the population commonly referred to MPI due to its well-established prognostic value, worthy to be used in the management of those patients. An association between exercise capacity and overall mortality in patients with known cardiovascular disease has been previously demonstrated (15). However, no further investigation was done to better understand how workload relates to MPI results regarding the ability to predict outcomes in this particular group.

The aim of this study is to determine the additional MPI prognostic value over ECG stress testing alone in patients with known CAD who achieved high exercise capacity (≥ 10 METs).

8.3 Methods

8.3.1 Study Cohort

We evaluated 4187 consecutive patients with known or suspected CAD referred for clinically indicated MPI with exercise stress in an outpatient clinic in Rio de Janeiro, Brazil, between March 2008 and October 2012. The following were considered as exclusion criteria: suspected CAD, early revascularization (coronary angioplasty or coronary artery bypass grafting surgery occurring < 60 days after MPI), and history of significant cardiac valve disease, severe non-ischemic cardiomyopathy or any condition which might affect short-term prognosis.

Patients were classified as having known CAD based on reported medical history of myocardial infarction (MI); coronary artery bypass graft (CABG) or percutaneous coronary intervention (PCI). From 948 patients meeting all criteria, follow-up was completed in 926 (97.6% of the total). Study cohort flowchart is showed on Figure 1.

Prior to the scan, patients' medical history and physical examination data were collected in a standard questionnaire by a team of experienced cardiologists. Cardiac risk factors including hypertension, diabetes, hypercholesterolemia, smoking, obesity and family history of CAD were collected. Cardiac symptoms were based on Diamond and Forrester criteria (16) and classified as asymptomatic, non-cardiac pain, atypical angina, typical angina and shortness of breath.

All study procedures were in accordance with the ethical standards of the institutional research committee. Informed consent was obtained from all individual participants included in the study.

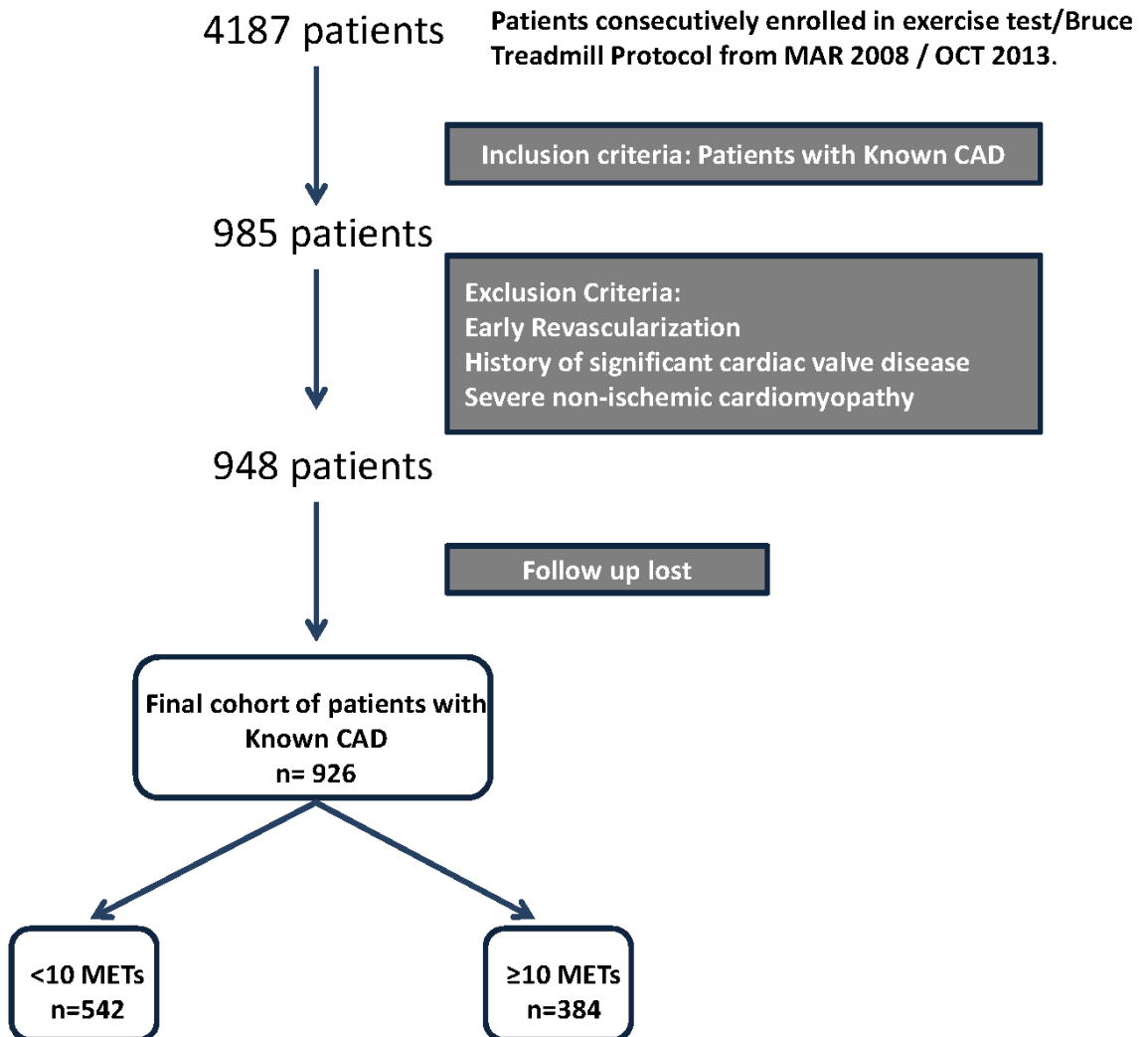


Figure 1 Study cohort derivation flowchart

8.3.2 Study Protocol

8.3.2.1 Exercise Testing

Stress ECG test was performed based on a symptom-limited Bruce treadmill protocol. Exercise workload was defined by the total METs achieved. Ischemic ST segment depression was defined as a horizontal or down-sloping depression of the ST segment with ≥ 1 mm present ≥ 80 ms after the J-point for 3 consecutive beats.

8.3.2.2 SPECT Imaging

SPECT imaging protocols have been previously described and validated (17-19), and will be summarized here. Patients underwent either a 2-day or 1-day Tc-99m-Sestamibi gated MPI protocol based on the scan date, since the camera used for most patients in our laboratory changed during the observation period. For the 2-day protocol an activity of 10-12 mCi 99mTc-sestamibi was injected with a scan time of 6 minutes. For the rest phase, images were acquired after 15 to 40 minutes. In the stress phase 99mTc-sestamibi was injected near maximal exercise, which was continued at maximal workload for at least 1 minute and image acquisition was performed after 15 to 30 minutes. MPI images were acquired through the gated-SPECT technique using a two-headed gamma camera (Ventri, GE Healthcare, Waukesha, WI, USA).

The 1-day 99mTc-sestamibi rest/stress protocol was also used, starting with rest study (injection of 5 mCi) followed by stress (15 mCi) in a CZT camera. CZT-SPECT was performed using a camera with multipinhole collimator (Discovery 530, GE Healthcare, Milwaukee, USA). Images were acquired in 6, 3, and 1 minute, respectively, for rest, supine stress and prone stress.

8.3.3 Imaging Interpretation

All images were jointly interpreted by two experienced cardiologists. Image processing was performed with the software Evolution for Cardiac® using 12 iterations. Images were reconstructed without scatter or attenuation correction. Post-stress gated short axis, vertical and horizontal long-axis tomograms as well as polar maps were generated and analyzed.

Semi quantitative 17-segment visual interpretation of the gated myocardial perfusion images was performed (20, 21). Each segment was scored by consensus using a standard five-point

scoring system (22) (0 = normal, 1 = equivocal, 2 = moderate, 3 = severe reduction of uptake, and 4 = absence of detectable tracer uptake) and each reader chose a score based on both quantitative perfusion data and qualitative visual assessment. Summed stress scores (SSS) were obtained by adding the scores of the 17 segments of the stress images. Summed rest scores (SRS) were obtained by adding scores of the 17 segments of the rest images and a summed difference score (SDS) was calculated by segmental subtraction (SSS-SRS).

For evaluating the correlation of SSS and the SDS with outcomes, we performed separate analyses with different cut points for each perfusion variable. With the purpose of evaluating the prognostic value and the stratification power based on the extent of defect and ischemia, we segmented our study population based on SSS and SDS values, as it is a widely established type of classification (17, 23) to achieve this result.

We converted SSS into percentage of total myocardial defect extension by calculating the ratio between summed stress score and its maximum possible score (68). An abnormal scan was considered as having an $SSS \geq 4$ or percentage of total defect $\geq 5\%$.

Left ventricular ejection fraction (LVEF), end-systolic and end-diastolic volumes (ESV and EDV, respectively) were automatically calculated (Cedars-Sinai Medical Center, Los Angeles, California).

8.3.4 Follow-up

Follow-up was performed by telephone interview every 6 months after MPI. All-cause death and nonfatal myocardial infarction (MI) were registered. Events were confirmed through review of hospital charts, physician's records and national death certification. Nonfatal MI was defined based on the criteria of typical chest pain, elevated cardiac enzyme levels and typical alterations of the electrocardiogram (24). All-cause death and nonfatal myocardial infarction were classified as hard events and time to first event was considered.

8.3.5 Statistical analyses

Categorical variables are presented as frequencies and were calculated using the Pearson Chi-Square or Fisher's Exact Test. Continuous variables are expressed as mean \pm SD or median and interquartile range (IQR) and were compared using Student T-Test or Mann-Whitney test, accordingly. Poisson regression was performed to calculate annualized rate of hard events. Kaplan-Meier curves were generated to visually assess survival in different clinical groups. For pairwise comparisons between these groups, the log-rank test was used. A Cox regression model was used for testing predictors of hard events. Variables with a p value <0.05 in the univariable analysis or clinical significance were considered in the model. Proportional hazard assumption was tested by using Martingale residuals and we tested for interaction among exercise capacity and MPI results. Incremental prognostic value of MPI was evaluated by sequential multivariable models, built by the addition of exercise capacity and MPI results to demographic and clinical characteristics. Final model fit was assessed with the goodness-of-fit χ^2 test. A p-value < 0.05 was considered statistically significant. All analyses were performed with IBM SPSS statistics version 22.0 Armonk, NY: IBM Corp.

8.4 Results

8.4.1 Cohort baseline Characteristics

A total of 926 patients were followed for a mean 32.4 ± 9.7 months. The clinical characteristics of this study cohort are summarized in Table 1. Patients were divided into two groups: those who achieved ≥ 10 METs (41.5%), here named Group 1, and <10 METs (58.5%), named Group 2. Patients achieving higher workloads were younger, more often male, and had lower rates of hypertension, diabetes mellitus and obesity. There was no significant difference between groups concerning the presence of angina.

Table 1 Baseline Characteristics relative to cardiac workload

Baseline Characteristics	Group 1 ≥ 10 METs 384 (41.5%)	Group 2 < 10 METs 542 (58.5%)	Entire cohort n=926	p Value*
Age	59.6 (9)	66.7 (9.2)		<0.001
Male	363 (94.5%)	379 (69.9%)	742 (80.1%)	<0.001
Symptoms:				
Asymptomatic	286 (74.5%)	396 (73.1%)	682 (73.6%)	0.630
Typical Angina	16 (4.2%)	24 (4.4%)	40 (4.3%)	0.847
Atypical angina	64 (16.7%)	93 (17.2%)	157 (16.9%)	0.844
Shortness of breath	5 (1.3%)	12 (2.2%)	17 (1.8%)	0.308
Non-cardiac chest pain	13 (3.3%)	17 (3.1%)	30 (3.4%)	0.331
Hypertension	216 (56.3%)	345 (63.7%)	561 (60.5%)	0.023
Diabetes Mellitus	67 (17.4%)	162 (29.9%)	229 (24.7%)	<0.001
Hyperlipidemia	220 (57.3%)	327 (60.3%)	547 (59%)	0.354
BMI ≥ 30	65 (17.6%)	123 (24%)	188 (20.3%)	0.023
History of tobacco use	140 (36.4%)	202 (37.3%)	342 (36.9%)	0.968
Previous MI	158 (41.1%)	240 (44.3%)	398 (42.9%)	0.342
Previous CABG	174 (32.1%)	107 (27.9%)	281 (30.3%)	0.095

BMI Body Mass Index; MI Myocardial Infarction; CABG Coronary Artery Bypass Graft; PCI Percutaneous Coronary Intervention; CAD Coronary Artery Disease.

** Values < 0.05 are considered statistically significant*

8.4.2 Stress-ECG Test and SPECT Findings

Table 2 present findings on the stress-ECG test and SPECT imaging stratified by groups of workload achievement. Maximum heart rate achieved during the test was higher in the group of patients achieving ≥ 10 METs (148 vs 137, $p < 0.001$), as well the prevalence of patients achieving $\geq 85\%$ of their Maximum age-predicted Heart Rate (MAPHR) (82.8% vs 74.1%, $p = 0.002$). The prevalence of chest pain during the ECG stress was lower in group 1 for both typical (2.3% vs 7.4%, $p = 0.003$) and atypical angina (1.8% vs 2.4%, $p = 0.003$) compared to group 2. There was no significant difference in the prevalence of exercise ST depression between groups.

Table 2 Exercise test and SPECT parameters relative to cardiac workload

Tests Parameters	Group 1 ≥ 10 METs n=384	Group 2 < 10 METs n=542	p Value *
Stress-ECG Test:			
Exercise ST depression [n(%)]	35 (9.1%)	47 (8.7%)	0.815
Maximum HR (bpm) (Median(25 th ,75 th))	148 (138,162)	137 (126,149)	<0.001
>85% MAPHR	303 (82.8%)	380 (74.1%)	0.002
Chest pain during stress [n(%)]	16 (4.1%)	53(9.7%)	0.003
SPECT imaging:			
Abnormal Scans (%)	74 (19.3%)	119 (22%)	0.322
Mean of SSS (±SD)	2.69 (4.5)	2.97 (5)	0.824
Mean of SDS (±SD)	0.69 (1.8)	0.87 (2.2)	0.424
Mean % of LV defect (±SD)	3.9 (0.33)	4.3 (0.31)	0.824
Percentage of LV defect n(%):			
< 5%	310 (80.7%)	423 (78%)	0.678
5-7%	18 (4.7%)	29 (5.4%)	
8-9%	10 (2.6%)	12 (2.2%)	
≥ 10%	46 (12%)	78 (14.4%)	
EF<40% [n(%)]	24 (6.3%)	63 (11.7%)	0.006

HR Hear Rate; MAPHR Maximum Age-Predicted Heart Rate; SSS Summed Stress Score; SDS Summed Difference Score; LV TPD Left ventricle total perfusion defect; LVEF Left ventricle ejection fraction

* Values < 0.05 are considered statistically significant

When comparing exercise capacity to SPECT imaging results there was no significant difference between groups 1 and 2, respectively, on mean SSS (2.69 vs 2.97), SDS (0.69 vs 0.87) or TPD (3.9 vs 4.3). The prevalence of patients with significant left ventricular dysfunction (EF<40%) was lower in those reaching higher cardiac workloads (6.3% vs 11.7% p=0.006).

8.4.3 Outcomes

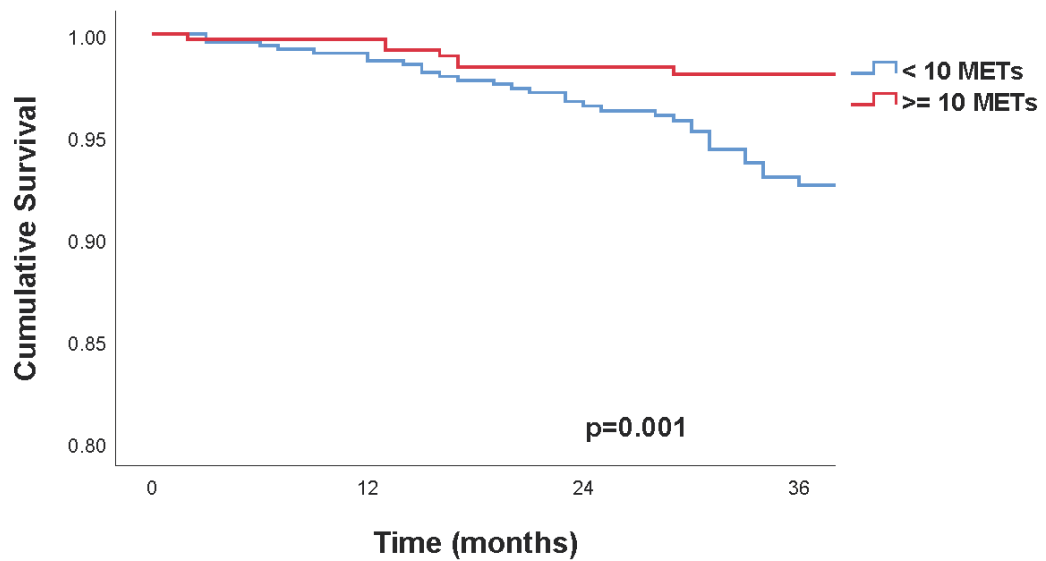
A total of 42 deaths (4.5%) and 20 nonfatal myocardial infarctions (2.1%) (58 hard events) occurred during the follow-up period, as shown on table 3. The group of patients achieving ≥ 10 METs had a lower annualized rate of hard events when compared to group 2 (1.13 %/year vs 3.95 %/year, p<0.001). The difference in cumulative survival free of hard events according to cardiac workload achievement is shown in the Kaplan-Meier survival curve (p<0.001) (Figure 2).

Table 3 Prevalence of outcomes relative to cardiac workload during the entire follow up time

Event	Group 1 ≥ 10 METs n=384	Group 2 < 10 METs n=542	Entire cohort n=926	p Value*
Hard events	10 (2.6%)	48 (8.9%)	58 (6.3%)	<0.001
All-cause mortality	6 (1.6%)	36 (6.6%)	42 (4.5%)	<0.001
Non-fatal MI	4 (1%)	16 (3%)	20 (2.1%)	0.04

MI Myocardial Infarction

** Values < 0.05 are considered statistically significant*



Number at risk

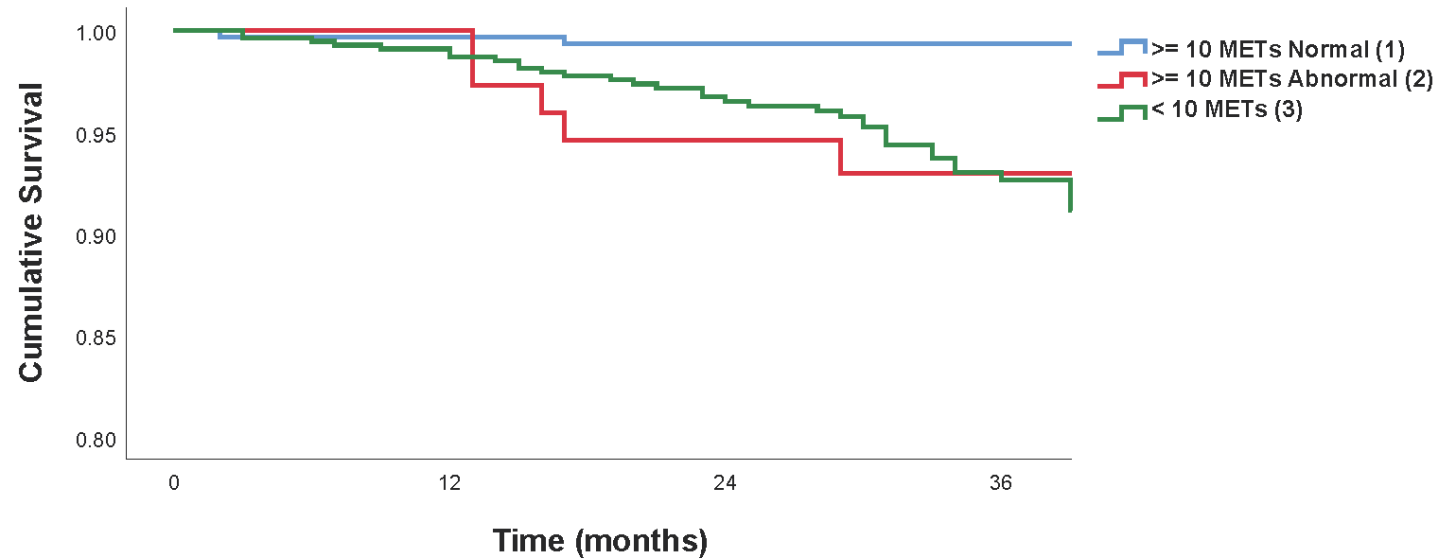
Time(months)	0	12	24	36
< 10 METs	542	524	436	233
≥10 METs	384	376	311	166

Figure 2 Survival free of hard events stratified by cardiac workload. Blue line Patients reaching < 10 METs; Red line Patients reaching \geq 10 METs.

In order to evaluate MPI prognostic contribution for patients with high exercise capacity, we analyzed survival only in patients achieving \geq 10 METs, stratified for scan results, SSS, and SDS groups. Kaplan-Meier curves show the comparison of cumulative survival among patients achieving < 10 METs, \geq 10 METs with abnormal scans and \geq 10 METs with normal scans, showing increased survival rate in the latter (Figure 3). Consistently, patients who reached \geq 10 METs with a normal scan had a significant lower annualized rate of hard events compared to those who reached \geq 10 METs with abnormal scans and those who reached < 10 METs (0.57%/year, 3.37 %/year, 3.95%/year respectively, $p=0.001$) (Figure 4). There was also a stepwise increment in the annualized rate of events according to the increase in total defect severity, based on SSS groups. There was no difference in the prevalence of these events when stratifying patients with \geq 10 METs according to the presence of ischemia (Figure 5).

Finally, in the Cox proportional hazards model, cardiac workload achievement <10 METs (2.72 [1.28-5.77], $p=0.009$) and an abnormal MPI result (1.9 [1.15-3.39], $p=0.01$) were independently associated with hard events. The variables considered in the univariable and

multivariable models are shown in Table 4. In order to assess the incremental prognostic value of MPI results, we constructed multivariable models by sequentially adding exercise capacity and MPI results to demographic and clinical characteristics. Figure 6 shows improvement in the model statistics when these two variables were added. The final model global $\chi^2 = 22.5$, $p=0.001$. No interaction between exercise capacity and MPI results was observed.



Number at risk						Pairwise comparisons	p value
Time(months)	0	12	24	36	1 vs 2	0.023	
≥ 10 METs Normal	310	302	257	137	1 vs 3	< 0.001	
≥ 10 METs Abnormal	74	74	62	39	2 vs 3	0.394	
< 10 METs	542	524	436	233			

Figure 3 Survival free of hard events stratified by patients achieving < 10 METs, ≥ 10 METs with abnormal scans and ≥ 10 METs with normal scans. Green line Patients reaching < 10 METs; Red line Patients reaching ≥ 10 METs with abnormal scans; Blue line Patients reaching ≥ 10 METs with normal scans. For the pairwise comparisons, 1 - ≥ 10 METs Normal, 2- ≥ 10 METs Abnormal and 3 - < 10 METs.

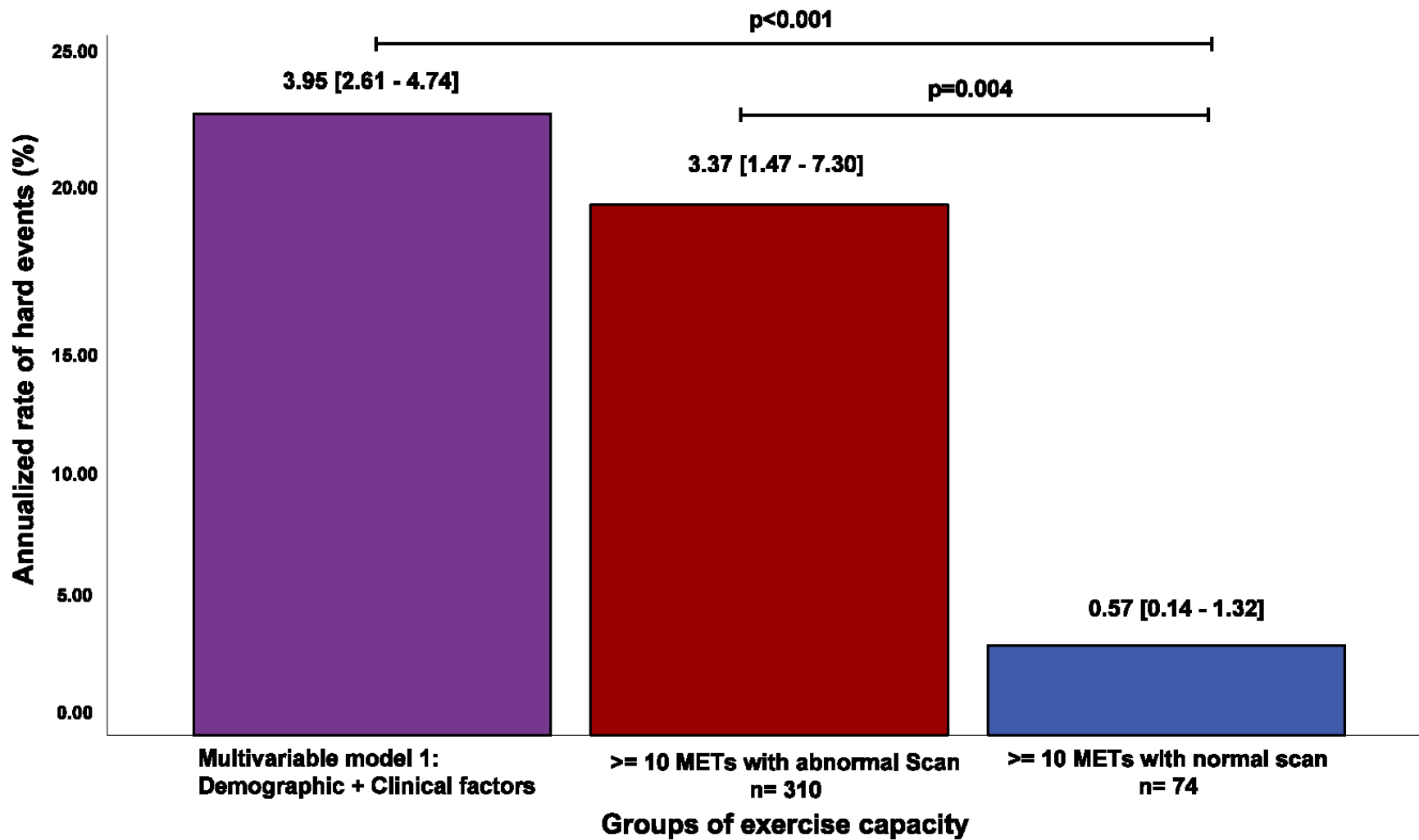
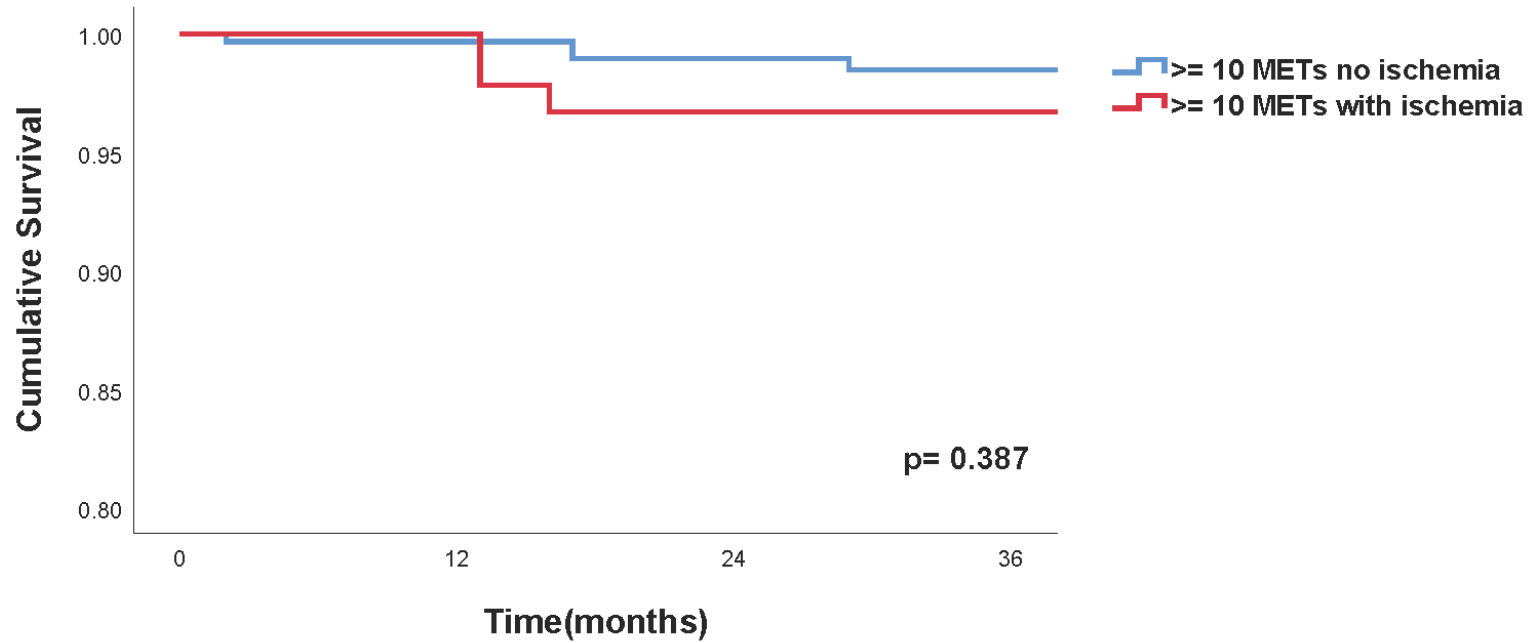


Figure 4 Annualized rate of hard events (%/year [95% CI]) per group of cardiac workload and scan results in % person-years.



Number at risk

Time(months)	0	12	24	36
≥10 METs no ischemia	292	285	240	132
≥10 METs with ischemia	92	91	79	45

Figure 5 Survival free of hard events in patients achieving ≥ 10 METs according to the presence of ischemia in MPI. Blue line Patients achieving ≥ 10 METs with no ischemia; Red line Patients achieving ≥ 10 METs with ischemia.

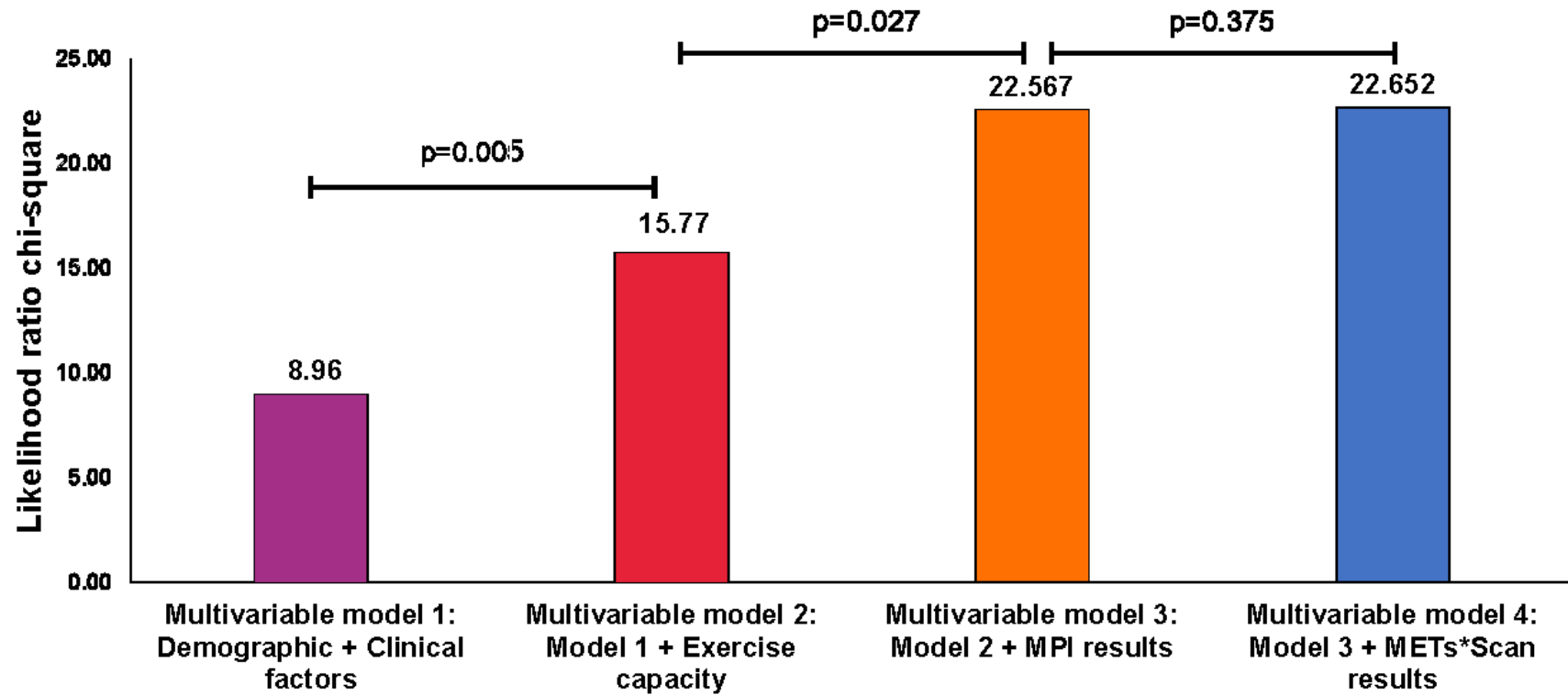


Figure 6 Multivariable-Adjusted models showing the incremental prognostic value of exercise capacity and MPI results in Patients with Known CAD.

Table 4 Univariable and Multivariate Indicators of Hard Events

Predictors	Univariable		Multivariable	
	Hazard Ratio (95% CI)	p value *	Hazard Ratio (95% CI)	p value*
Age	1.03 (1.00 – 1.07)	0.014	1.02 (0.98 – 1.05)	0.254
Male gender	1.16 (0.54 – 2.47)	0.697	0.64 (0.30 – 1.4)	0.268
Diabetes mellitus	1.66 (0.96 – 2.87)	0.068	0.64 (0.36 – 1.14)	0.133
< 10 METs	3.1 (1.55 – 6.16)	0.001	2.72 (1.28 – 5.77)	0.009
Abnormal scan	1.74 (1.03 – 2.95)	0.037	1.98 (1.15 – 3.39)	0.013
LVEF	0.99 (0.98 – 1.01)	0.818	1 (0.99 – 1)	0.876
< 10 METs * Abnormal Scan	-	-	0.51 (0.11 – 2.29)	0.386
Hypertension	0.85 (0.5 – 1.46)	0.57		
Dyslipidemia	1.01 (0.59 – 1.74)	0.958		
Previous MI	0.89 (0.52 – 1.53)	0.688		
Family history of CAD	0.83 (0.48 – 1.42)	0.5		
ST-segment depression	0.32 (0.07 – 1.31)	0.114		
SSS	0.98 (0.93 – 1.03)	0.588		
SDS	1.00 (0.99 – 1.01)	0.096		

No significant interaction was observed between exercise capacity and MPI results in the multivariable analysis CI, confidence interval; METs, metabolic equivalents; LVEF, left ventricle ejection fraction; MI, myocardial infarction; CAD, coronary artery disease; SSS, summed stress score; SDS, summed difference score.

** Values < 0.05 are considered statistically significant*

8.5 Discussion

Clinical application of exercise testing as a gatekeeper for nuclear imaging has been a matter of debate along the last decade. MPI cost-effectiveness, procedure costs and related benefits are mounting challenges in an era of advanced cardiac imaging technologies (3). In this context, it is crucial to reassess the risk stratification ability of each method in specific populations.

It is established that patients achieving ≥ 10 METs have low rates of cardiovascular events and low prevalence of $\geq 10\%$ LV ischemia on MPI regardless of peak exercise heart rate (11, 12). Duvall et al. attempted to create a provisional injection protocol, by applying the ≥ 10 METs cut-off as criterion to abstain from radiotracer injection. However, groups such as older adults and patients with known CAD were excluded (14). More recently, Smith et al. described that exercise capacity also influences outcomes in patients with ≥ 65 years old and is associated with a low occurrence of significant ischemia in MPI (13). Nonetheless, it is still not clear if patients with known CAD would show similar results.

Here we addressed the association of high exercise capacity (≥ 10 METs) with mortality and cardiovascular events in a population comprised of patients with known CAD referred for exercise ECG-stress MPI. Of most importance, we tried to determine the additional contribution of MPI prognostic value in that specific population. We showed that patients attaining higher workloads were younger, predominantly male, and had significant lower rates of cardiac risk factors. Approximately 70% of the population was asymptomatic before the test, with no significant difference on the prevalence of pre-test symptoms among Groups 1 and 2 in. This fact is suggestive of CAD follow-up as the main reason for scan referral. There was no significant difference in the prevalence of ST depression between groups 1 and 2. Also, there was no difference in the prevalence of abnormal scans or extent of ischemia in patients with ST depression compared to those without ST depression.

Survival analyses showed that patients with known CAD achieving ≥ 10 METs had a significantly better prognosis compared to those attaining < 10 METs for all-cause mortality and non-fatal MI, with a lower annualized rate of hard. This finding is similar to what has been previously described (11). To further understand how scan results predicted hard events in the study population, we performed survival analyses only in patients attaining ≥ 10 METs and found out that those with abnormal scans had a significant higher rate of events. Furthermore, the increase in the annualized rate of hard event is proportional to the extent of

defect as determined by SSS values. The results suggest that although a higher exercise capacity is associated with a lower prevalence of all-cause mortality and non-fatal MI, MPI can still provide valuable prognostic information. These findings were corroborated by Cox regression analyses, which showed that both exercise capacity and scan results were independently associated with hard events.

Regarding ischemic burden, we did not find significant difference in the survival free of hard event in this cohort with established CAD achieving ≥ 10 METs. Although it is worth mentioning that the survival analysis stratified by SDS groups was potentially limited by the number of events in this subgroup (10 events), we also believe that our study cohort peculiarities may explain the lack of prognostic value of SDS. In a previous study, Gimelli et al (25), aimed to evaluate the incremental prognostic value of MPI over other imaging methods. The group described that when focusing only in a population of ascertained known CAD, without early revascularized patients and a small number of events, SDS was also not a predictor of cardiac events.

Based on what was mentioned above and the fact that under same constraints, the percentage of total defect kept its prognostic value, we believe that for our cohort, the greater contribution of MPI is determined not only by quantification of new ischemia, but the sum of ischemia and previous myocardial scar. Nevertheless, we agree that new studies focusing exclusively on the MPI prognostic value for similar cohorts are necessary to further support this assumption. Thus, our study's results may contribute to better determine appropriate referral criteria to MPI in patients with known CAD who achieved high exercise capacity in stress-ECG test.

8.6 Limitations

Our study has some limitations, including its retrospective, observational and single-institution nature. It is worth noticing that despite having a large sample size, the prevalence of events in the group with higher exercise capacity is low and it might have limited further subgroup analyses.

Additionally, the cardiologists who interpreted the scans were not blinded to clinical data, as the protocol was part of the clinical routine. Hence, it could have been a source of bias.

8.7 New Knowledge Gained

MPI is able to stratify patients with known CAD and high exercise capacity for the occurrence of all-cause death and non-fatal MI with an incremental prognostic value over ECG stress test alone.

8.8 Conclusion

MPI was able to stratify the risk for the occurrence of all-cause death and nonfatal myocardial infarction in patients with known CAD achieving ≥ 10 METs with an incremental prognostic value compared to ECG stress test alone. These results support the performance of perfusion imaging in this subset of patients, as opposed to what had been proposed with provisional protocols that aimed to reduce patients' exposure to radiation.

8.9 References

1. Sanchis-Gomar F, Perez-Quilis C, Leischik R, Lucia A. Epidemiology of coronary heart disease and acute coronary syndrome. *Ann Transl Med.* 2016;4(13):256.
2. Hansen CL, Goldstein RA, Akinboboye OO, Berman DS, Botvinick EH, Churchwell KB, et al. Myocardial perfusion and function: single photon emission computed tomography. *J Nucl Cardiol.* 2007;14(6):e39-60.
3. Bourque JM, Beller GA. Value of Exercise ECG for Risk Stratification in Suspected or Known CAD in the Era of Advanced Imaging Technologies. *JACC Cardiovasc Imaging.* 2015;8(11):1309-21.
4. Klocke FJ, Baird MG, Lorell BH, Bateman TM, Messer JV, Berman DS, et al. ACC/AHA/ASNC guidelines for the clinical use of cardiac radionuclide imaging--executive summary: a report of the American College of Cardiology/American Heart Association Task Force on Practice Guidelines (ACC/AHA/ASNC Committee to Revise the 1995 Guidelines for the Clinical Use of Cardiac Radionuclide Imaging). *J Am Coll Cardiol.* 2003;42(7):1318-33.
5. Peterson PN, Magid DJ, Ross C, Ho PM, Rumsfeld JS, Lauer MS, et al. Association of exercise capacity on treadmill with future cardiac events in patients referred for exercise testing. *Arch Intern Med.* 2008;168(2):174-9.
6. Morise AP, Jalisi F. Evaluation of pretest and exercise test scores to assess all-cause mortality in unselected patients presenting for exercise testing with symptoms of suspected coronary artery disease. *J Am Coll Cardiol.* 2003;42(5):842-50.
7. Goraya TY, Jacobsen SJ, Pellikka PA, Miller TD, Khan A, Weston SA, et al. Prognostic value of treadmill exercise testing in elderly persons. *Ann Intern Med.* 2000;132(11):862-70.
8. Kodama S, Saito K, Tanaka S, Maki M, Yachi Y, Asumi M, et al. Cardiorespiratory fitness as a quantitative predictor of all-cause mortality and cardiovascular events in healthy men and women: a meta-analysis. *JAMA.* 2009;301(19):2024-35.

9. Lee DS, Verocai F, Husain M, Al Khdair D, Wang X, Freeman M, et al. Cardiovascular outcomes are predicted by exercise-stress myocardial perfusion imaging: Impact on death, myocardial infarction, and coronary revascularization procedures. *Am Heart J*. 2011;161(5):900-7.
10. Faselis C, Doumas M, Pittaras A, Narayan P, Myers J, Tsimploulis A, et al. Exercise capacity and all-cause mortality in male veterans with hypertension aged ≥ 70 years. *Hypertension*. 2014;64(1):30-5.
11. Bourque JM, Holland BH, Watson DD, Beller GA. Achieving an exercise workload of $>$ or $=$ 10 metabolic equivalents predicts a very low risk of inducible ischemia: does myocardial perfusion imaging have a role? *J Am Coll Cardiol*. 2009;54(6):538-45.
12. Bourque JM, Charlton GT, Holland BH, Belyea CM, Watson DD, Beller GA. Prognosis in patients achieving ≥ 10 METS on exercise stress testing: was SPECT imaging useful? *J Nucl Cardiol*. 2011;18(2):230-7.
13. Smith L, Myc L, Watson D, Beller GA, Bourque JM. A high exercise workload of ≥ 10 METS predicts a low risk of significant ischemia and cardiac events in older adults. *J Nucl Cardiol*. 2018.
14. Duvall WL, Levine EJ, Moonthungal S, Fardanesh M, Croft LB, Henzlova MJ. A hypothetical protocol for the provisional use of perfusion imaging with exercise stress testing. *J Nucl Cardiol*. 2013;20(5):739-47.
15. Hung RK, Al-Mallah MH, McEvoy JW, Whelton SP, Blumenthal RS, Nasir K, et al. Prognostic value of exercise capacity in patients with coronary artery disease: the FIT (Henry Ford Exercise Testing) project. *Mayo Clin Proc*. 2014;89(12):1644-54.
16. Diamond GA, Forrester JS, Hirsch M, Staniloff HM, Vas R, Berman DS, et al. Application of conditional probability analysis to the clinical diagnosis of coronary artery disease. *J Clin Invest*. 1980;65(5):1210-21.
17. Lima R, Ronaldo L, De Lorenzo A, Andrea dL, Camargo G, Gabriel C, et al. Prognostic value of myocardium perfusion imaging with a new reconstruction algorithm. *J Nucl Cardiol*. 2014;21(1):149-57.
18. Lima RSL, Peclat TR, Souza ACAH, Nakamoto AMK, Neves FM, Souza VF, et al. Prognostic value of a faster, low-radiation myocardial perfusion SPECT protocol in a CZT camera. *Int J Cardiovasc Imaging*. 2017;33(12):2049-56.
19. Lima R, Peclat T, Soares T, Ferreira C, Souza AC, Camargo G. Comparison of the prognostic value of myocardial perfusion imaging using a CZT-SPECT camera with a conventional angler camera. *J Nucl Cardiol*. 2017;24(1):245-51.
20. Berman DS, Kang X, Van Train KF, Lewin HC, Cohen I, Areeda J, et al. Comparative prognostic value of automatic quantitative analysis versus semiquantitative visual analysis of exercise myocardial perfusion single-photon emission computed tomography. *J Am Coll Cardiol*. 1998;32(7):1987-95.
21. Henzlova MJ, Duvall WL, Einstein AJ, Travin MI, Verberne HJ. ASNC imaging guidelines for SPECT nuclear cardiology procedures: Stress, protocols, and tracers. *J Nucl Cardiol*. 2016;23(3):606-39.
22. Berman DS, Hachamovitch R, Kiat H, Cohen I, Cabico JA, Wang FP, et al. Incremental value of prognostic testing in patients with known or suspected ischemic heart disease: a basis for optimal

utilization of exercise technetium-99m sestamibi myocardial perfusion single-photon emission computed tomography. *J Am Coll Cardiol.* 1995;26(3):639-47.

23. Hachamovitch R, Berman DS, Shaw LJ, Kiat H, Cohen I, Cabico JA, et al. Incremental prognostic value of myocardial perfusion single photon emission computed tomography for the prediction of cardiac death: differential stratification for risk of cardiac death and myocardial infarction. *Circulation.* 1998;97(6):535-43.

24. Thygesen K, Alpert JS, White HD, Infarction JEAATFftRoM. Universal definition of myocardial infarction. *J Am Coll Cardiol.* 2007;50(22):2173-95.

25. Gimelli A, Rossi G, Landi P, Marzullo P, Iervasi G, L'abbate A, et al. Stress/Rest Myocardial Perfusion Abnormalities by Gated SPECT: Still the Best Predictor of Cardiac Events in Stable Ischemic Heart Disease. *J Nucl Med.* 2009;50(4):546-53.

9 Considerações finais

Os resultados apresentados ao longo dos três artigos que compõem este trabalho convergem fundamentalmente na busca observada ao longo dos últimos 20 anos por estratégias cientificamente validadas que contribuam para a redução de radiação advinda da cardiologia nuclear.

Apesar de diferentes diretrizes direcionando o uso das estratégias e protocolos e reforçando a necessidade de aliar as práticas da CPM ao princípio do ALARA, ainda existe uma grande heterogeneidade na implementação dessas diretrizes no mundo(1, 2).

De acordo com dados do IAEA Nuclear Cardiology Protocols Cross-Sectional Study (INCAPS), a Europa apresenta a menor média e mediana de dose efetiva e a maior proporção de pacientes que cumprem a meta de dose efetiva ≤ 9 mSv (60%). Segundo o mesmo estudo, a América Latina e a Ásia apresentam as maiores doses (média e mediana) e a segunda menor proporção de pacientes com dose efetiva ≤ 9 mSv (27% e 24% respectivamente). É devido a esta disparidade que a IAEA apresenta neste estudo as 8 melhores práticas anteriormente citadas no presente trabalho(3).

Conforme estudo recente realizado para avaliar a adoção das melhores práticas recomendadas pelo IAEA nos protocolos da CPM em serviços de medicina nuclear no Brasil, um número considerável desses não chega a adotar nem 6 das 8 práticas recomendadas. Dentre as mais frequentemente adotadas estão o não uso do Tálcio e do protocolo com dois isótopos. O uso do protocolo apenas com a fase de estresse aparece como a prática menos adotada. As principais justificativas apresentadas para não utilização deste pelos prestadores de serviço avaliados no estudo estão relacionadas às questões burocráticas relativas à cobertura dos planos de saúde(4). Esta mesma justificativa explica o não uso deste protocolo em nosso trabalho.

Além disso o estudo mostra que 57% dos serviços de medicina nuclear administram atividades acima do limite recomendado pela IAEA (36 mCi) ou alcançaram doses efetivas maiores que 15 mSv. Ademais, os autores concluem que, de forma geral, uma maior adesão às recomendações não incorreria em novos custos para os prestadores de serviço(4). Estes dados reforçam a relevância de estudos correlatos à presente obra que foquem na avaliação de protocolos e critérios de indicação para redução de dose relacionada à CPM tendo como base de estudo a população brasileira.

Apesar de a distribuição de GC CZT no Brasil ainda ser escassa e heterogênea, em parte devido ao elevado custo deste equipamento, os resultados mostrados neste trabalho

contribuem com a melhor aplicação de protocolos que atendam à demanda dos órgãos reguladores mundiais e ao mesmo tempo dos diferentes prestadores de serviço. Ademais, é fundamental o entendimento de que em face da não possibilidade do uso dessas GCs, existem os demais métodos citados ao longo deste manuscrito, muitas vezes menos financeiramente dispendiosos.

Como exemplo, podemos citar que, no presente trabalho, a dose efetiva na GC CZT foi de 6 mSv, enquanto na GC tradicional - com o uso de um novo algoritmo de reconstrução, foi de 9,5 mSv, representando uma redução significativa devido à tecnologia das GCs CZT. No entanto, o uso de “*softwares*” de reconstrução em GCs tradicionais por si só já é capaz de reduzir significativamente a dose efetiva em relação à dose efetiva máxima recomendada (15 mSv). Dessa forma, entende-se que apesar de todas as vantagens das GC CZT, existe benefício na implantação de alternativas, em sendo estas mais custo acessíveis.

Entretanto, em relação à redução de tempo entre a GC CZT e a GC tradicional com o uso de “*softwares*” de reconstrução, apesar de significativa possibilidade de redução do tempo com uso deste último protocolo, não se compara à capacidade de redução com o uso da GC CZT.

Existem ainda algumas nuances do presente trabalho que merecem ser mais detalhadamente discutidas.

Primeiramente, a prática realizada em nosso estudo de avaliar revascularizações tardias como desfecho é algo reconhecidamente adotado na literatura(5). Esta decisão se baseia na tentativa de retirar o confundimento entre as revascularizações que ocorreram como consequência do resultado do exame e aquelas que ocorreram como consequência da evolução da doença, e cujo risco poderia ser ou não estratificado pelo exame (e por isso, contribuiriam para avaliar o seu valor prognóstico). É preciso ponderar, no entanto, que existe controvérsia em relação a esta abordagem. Outros autores defendem que ao excluir estes eventos perde-se a informação de desfecho em relação aos pacientes mais graves, nos quais a CPM influenciou diretamente o manejo clínico. Há ainda autores que defendem que a análise das revascularizações poderia ser realizada de forma tempo-dependente(6), já que é uma variável que pode mudar, ao longo do tempo de seguimento, a história natural da doença e consequentemente os desfechos duros. Reconhecemos que todas estas abordagens têm embasamento científico e apresentam vantagens e desvantagens.

Além disso, em relação aos resultados demonstrados no artigo 3, destaca-se o fato que apesar de o grupo com <10 METs apresentar mais fatores de risco cardiovasculares, mais

sintomas e maior disfunção ventricular, não houve diferença na quantidade de exames anormais. Uma possível explicação para este fato deve-se ao fato de que a participação de pacientes do sexo feminino entre os que atingiram < 10 METs era consideravelmente maior do que entre os que atingiram ≥ 10 METs. Estudos prévios já descreveram uma maior prevalência de doença aterosclerótica não-obstrutiva e doença microvascular coronariana na população feminina(7). Tais condições clínicas estão frequentemente associadas a sintomas semelhantes àqueles da doença arterial coronariana obstrutiva, e podem existir em um cenário de coronariografia e/ou CPM normais. Tal fenômeno se deve à resolução insuficiente destes métodos para avaliação da microvasculatura, majoritariamente responsável pela manutenção da resistência coronariana.

Atualmente, os métodos de diagnóstico da doença microvascular baseiam-se na perturbação da função vasodilatadora da árvore coronariana através de técnicas invasivas e não-invasivas, como a tomografia por emissão de pósitrons (PET). Mais recentemente, a quantificação da reserva de fluxo coronariano em gamacâmara CZT emergiu como uma possibilidade no diagnóstico de pacientes portadores de doença microvascular, e protocolos de aquisição de dinâmicas vem sendo validados(8).

Ainda que não passível de revascularização pelas técnicas atuais, a doença microvascular não se configura como um fenótipo benigno e está associada a ocorrência de eventos adversos cardiovasculares(9, 10) e insuficiência cardíaca com fração de ejeção preservada(11). Dessa forma, a predominância de mulheres sintomáticas possivelmente portadoras de doença microvascular no grupo com <10 METs poderia explicar em parte a inexistência de diferença no número de exames anormais.

9.1 Referências bibliográficas

1. Jerome SD, Tilkemeier PL, Farrell MB, Shaw LJ. Nationwide Laboratory Adherence to Myocardial Perfusion Imaging Radiation Dose Reduction Practices: A Report From the Intersocietal Accreditation Commission Data Repository. *JACC Cardiovasc Imaging*. 2015;8(10):1170-6.
2. Mercuri M, Pascual TN, Mahmarian JJ, Shaw LJ, Rehani MM, Paez D, et al. Comparison of Radiation Doses and Best-Practice Use for Myocardial Perfusion Imaging in US and Non-US Laboratories: Findings From the IAEA (International Atomic Energy Agency) Nuclear Cardiology Protocols Study. *JAMA Intern Med*. 2016;176(2):266-9.
3. Einstein AJ, Pascual TN, Mercuri M, Karthikeyan G, Vitola JV, Mahmarian JJ, et al. Current worldwide nuclear cardiology practices and radiation exposure: results from the 65 country IAEA Nuclear Cardiology Protocols Cross-Sectional Study (INCAPS). *Eur Heart J*. 2015;36(26):1689-96.
4. Rodrigues CVB, Oliveira A, Wiefels CC, Leão MS, Mesquita CT. Current Practices in Myocardial Perfusion Scintigraphy in Brazil and Adherence to the IAEA Recommendations: Results of a Cross-Sectional Study. *Arq Bras Cardiol*. 2018;110(2):175-80.
5. Berman DS, Hachamovitch R, Kiat H, Cohen I, Cabico JA, Wang FP, et al. Incremental value of prognostic testing in patients with known or suspected ischemic heart disease: a basis for optimal utilization of exercise technetium-99m sestamibi myocardial perfusion single-photon emission computed tomography. *J Am Coll Cardiol*. 1995;26(3):639-47.
6. Petretta M, Acampa W, Daniele S, Zampella E, Assante R, Nappi C, et al. Long-Term Survival Benefit of Coronary Revascularization in Patients Undergoing Stress Myocardial Perfusion Imaging. *Circ J*. 2016;80(2):485-93.
7. Bairey Merz CN, Shaw LJ, Reis SE, Bittner V, Kelsey SF, Olson M, et al. Insights from the NHLBI-Sponsored Women's Ischemia Syndrome Evaluation (WISE) Study: Part II: gender differences in presentation, diagnosis, and outcome with regard to gender-based pathophysiology of atherosclerosis and macrovascular and microvascular coronary disease. *J Am Coll Cardiol*. 2006;47(3 Suppl):S21-9.
8. Souza ACDA, Gonçalves BKD, Tedeschi A, Lima RSL. Quantification of Coronary Flow Reserve with CZT Gamma Camera in the Evaluation of Multivessel Coronary Disease. *Arq Bras Cardiol*. 2018;111(4):635-7.
9. Murthy VL, Naya M, Taqueti VR, Foster CR, Gaber M, Hainer J, et al. Effects of sex on coronary microvascular dysfunction and cardiac outcomes. *Circulation*. 2014;129(24):2518-27.
10. Taqueti VR, Shaw LJ, Cook NR, Murthy VL, Shah NR, Foster CR, et al. Excess Cardiovascular Risk in Women Relative to Men Referred for Coronary Angiography Is Associated With Severely Impaired Coronary Flow Reserve, Not Obstructive Disease. *Circulation*. 2017;135(6):566-77.
11. Taqueti VR, Solomon SD, Shah AM, Desai AS, Groarke JD, Osborne MT, et al. Coronary microvascular dysfunction and future risk of heart failure with preserved ejection fraction. *Eur Heart J*. 2018;39(10):840-9.

10 Conclusão

Neste trabalho foram avaliadas estratégias para a redução da exposição à radiação advindas da cintilografia miocárdica de perfusão. Baseando-se nos resultados encontrados na análise dessa coorte retrospectiva, pudemos concluir que é possível a aplicação de um protocolo com redução de dose e tempo em GC CZT sem comprometer o valor prognóstico da CPM. Sendo este não inferior ao valor prognóstico do método quando utilizadas as GCs tradicionais.

Além disso, em face da importância na certificação da indicação dos pacientes à CPM, exploramos a contribuição do valor prognóstico deste método em relação ao TE em pacientes com DAC conhecida que alcançaram ≥ 10 METs. Nossos resultados mostraram que a CPM possui valor na estratificação deste grupo de pacientes e que este valor é incremental em relação ao TE, ao contrário do que a literatura tem indicado em relação a outros subgrupos, em atingindo alta capacidade de exercício. Esta evidência acrescenta embasamento para uma melhor utilização do método ajustado a diferentes tipos de pacientes e situações.

11 Anexos

ANEXO A - Produção Científica

Artigo 1:

1. Publicado na revista International Journal of Cardiovascular Imaging. Lima RSL, Peclat TR, Souza ACAH, Nakamoto AMK, Neves FM, Souza VF, et al. Prognostic value of a faster, low-radiation myocardial perfusion SPECT protocol in a CZT camera. Int J Cardiovasc Imaging. 2017;33(12):2049-56.
2. Dados preliminares publicados na revista do departamento de Imagem Cardiovascular (DIC) da Sociedade Brasileira de Cardiologia. Revista DIC, n 3, vol 28.
3. Poster com dados preliminares apresentado na International Conference on Integrated Medical Imaging in Cardiovascular Diseases, International Atomic Energy Agency (IAEA), em Vienna, Austria, 2016.
4. Prêmio de melhor poster apresentando dados preliminares no Congresso do Departamento de Imagem Cardiovascular da Sociedade Brasileira de Cardiologia, 2015.

Artigo 2:

1. Publicado na revista Journal of Nuclear Cardiology. Lima R, Peclat T, Soares T, Ferreira C, Souza AC, Camargo G. Comparison of the prognostic value of myocardial perfusion imaging using a CZT-SPECT camera with a conventional angler camera. J Nucl Cardiol. 2017;24(1):245-51.

Artigo 3:

1. Publicado na revista Journal of Nuclear Cardiology. Thais R. Peclat, Ana Carolina do A. H. de Souza, Victor F. Souza, Aline M. K. Nakamoto, Felipe M. Neves, Izabella C. R. Silva, et al. The additional prognostic value of myocardial perfusion SPECT in patients with known coronary artery disease with high exercise capacity. J Nucl Cardiol. 2019.

ANEXO B – Artigo 1

Int J Cardiovasc Imaging
DOI 10.1007/s10554-017-1202-3



ORIGINAL PAPER

Prognostic value of a faster, low-radiation myocardial perfusion SPECT protocol in a CZT camera

Ronaldo S. L. Lima^{1,2} · Thaís R. Peclat² · Ana Carolina A. H. Souza² ·
Aline M. K. Nakamoto² · Felipe M. Neves² · Victor F. Souza² · Leticia B. Glerian² ·
Andrea De Lorenzo^{1,2}

Received: 19 February 2017 / Accepted: 22 June 2017
© Springer Science+Business Media B.V. 2017

Abstract To determine the prognostic value of a new, ultrafast, low dose myocardial perfusion SPECT (MPS) protocol in a cadmium-zinc telluride (CZT) camera. CZT cameras have introduced significant progress in MPS imaging, offering high-quality images despite lower doses and scan time. Yet, it is unknown if, with such protocol changes, the prognostic value of MPS is preserved. Patients had a 1-day 99 m-Tc-sestamibi protocol, starting with the rest (185–222 MBq) followed by stress (666–740 MBq). Acquisition times were 6 and 3 min, respectively. MPS were classified as normal or abnormal perfusion scans and summed scores of stress, rest, and difference (SSS, SRS and SDS), calculated. Patients were followed with 6-month phone calls. Hard events were defined as death or nonfatal myocardial infarction. Late revascularization was that occurring after 60 days of MPS. 2930 patients (age 64.0 ± 12.1 years, 53.3% male) were followed for 30.7 ± 7.5 months. Mean dosimetry was 6 mSv and mean total study time, 48 ± 13 min. The annual hard event and late revascularization rate were higher in patients with greater extension of defect and ischemia. SSS was higher in patients with hard events compared to those without events (2.6 ± 4.9 vs. 5.0 ± 6.3 , $p < 0.001$), as well as the SDS (0.7 ± 1.9 vs. 1.7 ± 3.4 , $p < 0.00$). The same was true for patients with or without late revascularization (SSS: 2.5 ± 4.7 vs. 6.6 ± 7.1 ; SDS: 0.6 ± 1.7 vs. 2.9 ± 3.8 , $p < 0.01$). A new, faster, low-radiation, MPS protocol in a CZT camera maintain the

ability to stratify patients with increased risk of events, showing that, in the presence of greater extension of defect or ischemia, patients presented higher rates of hard events and late revascularization.

Keywords Myocardial perfusion SPECT · Prognosis · CZT camera · Coronary artery disease

Introduction

Over the past 30 years, successive technical innovations-including, but not limited to, SPECT acquisition, ECG gating, among others- have granted myocardial perfusion imaging the status of a reliable, widely applicable, and increasingly useful technique [1]. The excellent diagnostic and prognostic values of myocardial perfusion SPECT (MPS) have led it to be extensively employed to evaluate patients with suspected or known coronary artery disease (CAD) [2].

Nonetheless, traditional MPS has two important limitations: Prolonged image acquisition time, leading to long procedural times, and relatively large radiation doses. The available literature demonstrates the possibility of high-speed cameras to reduce acquisition times, improving patient's tolerance to the test, and reducing radiation dose [3]. These new cameras rely on a pinhole collimation design and multiple cadmium zinc telluride (CZT) crystal arrays. Compared to the traditional SPECT camera, this type of collimation provides a three- to five-fold increase in photon sensitivity, thereby reducing imaging times significantly, while providing a 1.7 to 2.5-fold increase in spatial resolution. This makes shorter scans or lower doses (or even both) a reality, without the loss of image quality [3–5].

✉ Ronaldo S. L. Lima
ronlima@hotmail.com

¹ Clínica de Diagnóstico por Imagem, Av. Ataulfo de Paiva 669, Leblon, Rio de Janeiro, RJ, Brazil

² Universidade Federal do Rio de Janeiro, Rio de Janeiro, Brazil

However, the prognostic value of MPS imaging with this new protocol is still unknown. This study therefore sought to assess the prognostic value of a new faster, low-radiation MPS protocol performed in a CZT gamma camera (CZT-GC).

Materials and methods

Consecutive patients who underwent CZT MPS for the assessment of suspected or known CAD at a single laboratory in Rio de Janeiro, Brazil, between November 2011 and December 2012 were prospectively enrolled and followed by 6-month phone calls.

Those who underwent myocardial revascularization (either by coronary angioplasty or coronary artery bypass grafting surgery) <60 days after MPS were later excluded.

Prior to scanning, patient's medical history and physical examination data were collected by a team of experienced cardiologists.

All procedures performed were in accordance with the ethical standards of the institutional research committee and with the 1964 Declaration of Helsinki and its later amendments. Informed consent was obtained from all individual participants included in the study.

Study protocol

The patients were instructed to abstain from any products containing caffeine for 24 h before the test. Beta-blockers, calcium-channel antagonists, and nitrates were terminated 48 h before testing. A 1-day protocol was employed, with 185–222 MBq of 99 m-Tc-sestamibi used for the resting phase and 666–740 MBq for stress. Initially, to determine the best duration for the acquisition of the MPS scan, 24 patients (13 men) were selected for a pilot study in which scan acquisition was performed for 6 min in list mode. The scans were then processed using 1–6 min of the total scan time for reconstruction, and images were analyzed by two experienced readers unaware of the time range used for reconstruction, who had their readings evaluated for agreement. The study protocol was then defined according to best combination of reading agreements for stress and rest MPS studies among time ranges.

All patients underwent a 1-day, gated, rest/stress 99 m-Tc-sestamibi protocol. 10 min after tracer injection, image acquisition was performed in the supine position. The second phase was the stress study, in which either symptom-limited exercise treadmill test using the standard Bruce protocol with 13-lead electrocardiographic or pharmacologic stress were performed. Upon 5 min of stress phase completion, patients underwent image

acquisition in the supine and prone positions [6, 7]. The CZT-GC (Discovery NM 530c, GE Healthcare, Haifa, Israel) was equipped with a multiple pinhole collimator and 19 stationary cadmium-zinc-telluride detectors simultaneously imaging 19 cardiac views. Each detector contained 32 × 32 pixelated 5-mm thick (2.46 × 2.46 mm) elements. The system design enabled high-quality imaging of a three-dimensional volume by all detectors (quality field-of-view), where the patient's heart should be positioned. Once acquisition was initiated, no detector or collimator motion occurred.

Image analysis

All images were interpreted by a consensus of two experienced readers. Image processing was performed using Evolution for Cardiac[®] software. Images were reconstructed without scatter or attenuation correction. Short-axis, vertical and horizontal long-axis tomograms, as well as polar maps, were generated and analyzed. The image reconstruction method used allows extra-cardiac activity to be isolated more easily. Still, two readers analyzed the image before the patient was removed from the camera. The repetition rate of the images was less than 5%. A semi quantitative 17-segment visual interpretation of the gated myocardial perfusion images was performed [8]. Each segment was scored by consensus of the two observers using a standard five-point scoring system [9] (0 = normal, 1 = equivocal, 2 = moderate, 3 = severe reduction of uptake, and 4 = absence of detectable tracer uptake). Summed stress scores (SSS) were obtained by adding the scores of the 17 segments of the stress images. Summed rest scores (SRS) were obtained by adding scores of the 17 segments of the rest images and a summed difference score (SDS) was calculated by segmental subtraction (SSS-SRS). For evaluating the SSS and the SDS as predictors of events, we performed separate analyses with different cut points for each perfusion variable. We created four groups of SSS and SDS with the purpose of evaluating the prognostic value and the stratification power of this new protocol on a CZT-GC based not only in positive or negative MPI results, but specially, based on the extension of defect and ischemia, which is widely established to be achieved by using this type of classification [10, 11]. A normal study was considered when SSS < 3 and SDS < 1.

Post-stress eight frames gated short-axis images were processed using quantitative gated SPECT software (Cedars-Sinai Medical Center, Los Angeles, California), and left ventricular ejection fraction (LVEF), end-systolic and end-diastolic volumes (ESV and EDV, respectively) were automatically calculated.

Follow-up

Follow-up was performed by telephone interview every 6 months after MPI. All-cause death, nonfatal myocardial infarction, or late revascularization (>60 days after MPS) were registered. Evaluation of hospital records and/or review of civil registries confirmed these events. Nonfatal myocardial infarction was defined based on the criteria of typical chest pain, elevated cardiac enzyme levels and typical alterations of the electrocardiogram [12]. Death or nonfatal myocardial infarction were classified as hard events. Late revascularization was studied separately.

Statistical analyses

Categorical variables are presented as frequencies and continuous variables as mean \pm SD. The annual event rate was calculated as the % of events divided by person-years, and was compared among groups using the log-rank test. Kaplan–Meier curves were generated to visually assess survival in different groups. A Cox proportional hazards analysis was done to evaluate predictors of hard events and late revascularization, using variables with *p* value <0.05 in univariable analysis or clinical relevance.

Analyses were performed with SPSS software, version 17.0. A *p* value <0.05 was considered significant.

Results

Among 3265 patients, 235 were excluded due to early revascularization, and 100 were lost to follow-up, leaving 2930 patients who were followed for 30.7 ± 7.5 months. Mean age was 64.0 ± 12.1 years and 53.5% were male. Among these patients, 2072 (70.7%) were asymptomatic. The most frequent indications in asymptomatic patients were a previous treadmill test with intermediate-high risk Duke score, pre-op risk stratification and a previous calcium score >100. The most prevalent risk factor for CAD was hypertension (61.6%), followed by hypercholesterolemia (52.2%), smoking (36.4%) and family history of CAD (31.2%). Diabetes was present in 22.7% and previous myocardial infarction in 12.5%. From the 2930 patients, 501 (17.1%) had already been submitted to coronary angioplasty and 222 (7.6%) to coronary artery bypass grafting (CABG). About regularly medications, 37.9% was in use of ACE inhibitors, 28.6% was using beta-blocker and 10.9% Calcium receptor blockers. Mean perfusion scores were overall low and mean LVEF was normal with only 6% of patients with a LVEF <40%. These characteristics are summarized in Table 1.

For the definition of optimal scan time, acquired scans were processed using 1, 2, 3, 4, 5 or 6 min of the total

Table 1 Baseline data

Variables	All patients N (%) or mean \pm SD
Age (years)	64.0 \pm 12.1
Male gender	1568 (53.5%)
Chest pain	865 (29.5%)
Hypertension	1807 (61.6%)
Hypercholesterolemia	1530 (52.2%)
Diabetes mellitus	667 (22.7%)
Family history of coronary disease	915 (31.2%)
Smoking	1069 (36.4%)
Previous MI	367 (12.5%)
Previous CABG	222 (7.6%)
Previous PCI	501 (17.1%)
Exercise stress	1706 (58.2%)
Pharmacologic test	1224 (41.8%)
ACEi	1112 (37.9%)
Beta-blocker	839 (28.6%)
Calcium receptor blockers	320 (10.9%)
MPS	
SSS	1.7 \pm 3.0 (0–26)
SRS	1.1 \pm 2.1 (0–23)
SDS	0.6 \pm 1.7 (0–18)
LVEF (<40%)	176 (6.0%)
LVEF (%)	62.4 \pm 8.1
EDV (ml)	68.0 \pm 17.0
ESV (ml)	26.4 \pm 10.6

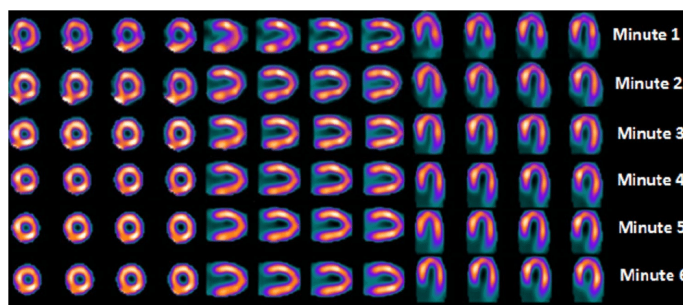
CABG coronary artery bypass grafting, MI myocardial infarction, MPS myocardial perfusion SPECT, PCI percutaneous coronary intervention, SDS summed difference score, SRS summed rest score, SSS summed stress score

list-mode acquisition previously performed for the pilot study. Intra and inter-observer agreement rates of MPS readings among time ranges are shown in Table 2. Based on those, the best combination, which was chosen for the subsequent MPS studies, was 6 min for the rest acquisition, 3 min for post-stress supine acquisition and 1.5 min for post-stress prone acquisition. Figure 1 shows an example of six post-stress images processed using a 6, 5, 4, 3, 2 and 1 min acquisition with a progressive degradation of image quality as we reduced the acquisition time. Considering all MPS studies performed thereafter, mean radiation dose was 6 mSv and mean scan time was 48 ± 13 min.

During follow-up, there were 61 deaths, 29 nonfatal infarctions (90 hard events), 148 coronary angioplasty procedures and 22 bypass surgeries (170 late revascularization procedures). Table 3 shows the comparison between patients with or without hard events. The former were older, more frequently male, with prior myocardial infarction or prior CABG and less frequently able to perform

Table 2 Intra- and interobserver agreement rates of MPS readings using 1 to 6 min time frames

Duration	6 min		5 min		4 min		3 min		2 min		1 min	
Agreement	Inter (%)	Intra (%)	Inter (%)	Intra (%)	Inter (%)	Intra (%)	Inter (%)	Intra (%)	Inter (%)	Intra (%)	Inter (%)	Intra (%)
Stress	100	100	100	100	100	100	100	100	100	96	96	92
Rest	100	100	100	100	100	96	100	92	92	92	92	88

Fig. 1 Example of six post-stress short-axis, vertical long axis and longitudinal long axis images processed using a 6, 5, 4, 3, 2 and 1 min acquisition, with a progressive reduction on image quality from 6 to 1 min

exercise stress. Perfusion scores were higher, as well as left ventricular volumes, and LVEF was lower in patients with hard events. In Table 4, comparisons between patients with or without late revascularization are shown. Similarly to patients with hard events, those with late revascularization were older, more frequently male, with cardiovascular risk factors, known coronary artery disease, and less frequently able to perform exercise stress, with higher perfusion scores, left ventricular volumes, and lower LVEF.

Based on the SSS, 4 patient groups were created: group 1 with SSS values from 0 to 2 [$n=2098$ (71.6%)]; group 2, SSS values from 3 to 5 [$n=430$ (14.6%)]; group 3, SSS values from 6 to 11 [$n=220$ (7.5%)]; and group 4, SSS ≥ 12 [$n=182$ (6.2%)]. Kaplan–Meier survival curves (Fig. 2a, b) showed that the highest the SSS, the lowest the survival free of hard events ($p<0.001$) or late revascularization ($p<0.001$), respectively. Table 5 shows the annualized hard events and late revascularization rates for individual groups of SSS, with highest rates in the group of highest SSS values. Four groups were also created according to SDS values: group 1 with SDS = 0 [$n=2334$ (79.6.0%)]; group 2, SDS values from 1 to 2 [$n=305$ (10.4%)]; group 3, SDS from 3 to 5 [$n=171$ (5.8%)]; and group 4, SDS ≥ 6 [$n=120$ (4.0%)]. Kaplan–Meier survival curves also showed that, with increasing SDS, event-free survival was reduced, both for hard events (Fig. 3a) ($p<0.001$) or late revascularization (Fig. 3b) ($p<0.001$). Also, the annualized events rates,

both for hard events or late revascularization, showed the same behavior presented on SSS groups for SDS groups, with higher rates in groups with higher values of SDS (Table 6). For all Kaplan Meier survival curves, p values were demonstrated in a pairwise comparison, below the graphs, to express the statistical differences in events rates between individual groups.

Finally, in the Cox analysis, male gender (hazard ratio = 2.26 [1.33–3.8], $p=0.03$), age (hazard ratio = 1.03 [1.01–1.06], $p=0.001$), diabetes (hazard ratio = 1.69 [1.09–2.62], $p=0.02$), pharmacologic stress (hazard ratio = 2.91 [1.75–4.8], $p<0.001$) and the SSS (hazard ratio = 1.36 [1.07–1.73], $p=0.01$), were independently associated with hard events. SDS, when substituting SSS in the cox analysis, also showed to be an independent predictor of hard events (hazard ratio = 1.09 [1.02–1.17], $p=0.01$) and maintained the results of the other variables. Table 3 shows all the variables used in the cox regression for hard events, with their respective hazard ratio and confidence interval.

For late revascularization, diabetes (hazard ratio = 1.94 [1.41–2.66], $p<0.001$), prior percutaneous coronary intervention (hazard ratio = 2.54 [1.76–3.68], $p<0.001$), and the SSS (hazard ratio = 1.06 [1.04–1.08], $p<0.001$) were the independent predictors. Again, SDS also showed to be an independent predictor of late revascularization (hazard ratio = 1.22 [1.17–1.26], $p<0.001$) when analyzed substituting the SSS with no modification in

Table 3 Characteristics of patients with or without hard events

Variables	Univariate analysis			Cox regression	
	Patients without HE (n = 2844)	Patients with HE (n = 86)	p value	HR [95% CI]	p value
Age (years)	64.5 ± 11.7	70.7 ± 12.3	<0.001	1.03 [1.01–1.06]	0.001
Male gender	1515 (53.2%)	57 (66.3%)	<0.01	2.26 [1.33–3.80]	0.030
Chest pain	844 (29.6%)	21 (24.4%)	0.338	1.30 [0.76–2.23]	0.336
Hypertension	1748 (61.4%)	59 (68.6%)	0.173	1.01 [0.61–1.66]	0.955
Hypercholesterolemia	1483 (52.1%)	47 (54.7%)	0.660	1.00 [0.63–1.57]	0.999
Diabetes mellitus	633 (22.2%)	34 (39.5%)	<0.001	1.69 [1.09–2.62]	0.020
Family history of CAD	887 (31.1%)	28 (32.6%)	0.906		
Smoking	1041 (36.6%)	28 (32.6%)	0.063	0.44 [0.23–1.08]	0.105
Previous MI	347 (12.2%)	20 (23.3%)	<0.01	0.71 [0.42–1.23]	0.229
Previous CABG	208 (7.3%)	14 (16.3%)	<0.01	0.67 [0.36–1.22]	0.196
Previous PCI	480 (16.8%)	21 (24.4%)	0.058	0.88 [0.53–1.45]	0.619
Exercise stress	1682 (59.1%)	24 (27.9%)	<0.01		
Pharmacologic test	1169 (41.1%)	62 (72.1%)	<0.01	2.91 [1.75–4.80]	0.000
MPS					
SSS ^a	2.6 ± 4.9	5.0 ± 6.3	<0.001	1.36 [1.07–1.73]	0.01
SRS	1.9 ± 4.2	3.2 ± 4.8	<0.001		
SDS ^a	0.7 ± 1.9	1.7 ± 3.4	<0.001	1.09 [1.02–1.17]	0.010
LVEF (%)	59.4 ± 11.0	55.5 ± 12.7	<0.01	0.75 [0.39–1.44]	0.392
EDV (ml)	81.4 ± 33.5	87.0 ± 34.6			
ESV (ml)	35.6 ± 25.5	42.0 ± 29.8			

HE hard events, CABG coronary artery bypass grafting, MI myocardial infarction, MPS myocardial perfusion SPECT, PCI percutaneous coronary intervention, SDS summed difference score, SRS summed stress score, SSS summed stress score

^aSSS and SDS were analyzed separately in the cox regression, each one with all other selected variables

the other variables. Table 4 shows the variables used for this cox regression, with their respective hazard ratio and confidence interval.

Discussion

Previous studies have shown that CZT cameras are able to perform ultrafast and low-dose MPS studies, with even higher sensitivity and image quality when compared to traditional cameras [13]. However, there is still incomplete evidence supporting the prognostic value of MPS performed in CZT cameras. This study shows, in a large patient population, that the prognostic value of a new MPS protocol in a high-speed CZT-GC could be comparable to what literature has shown about the prognostic value traditionally provided by conventional MPS [9]. Our group had already demonstrated the prognostic value of MPS with a new reconstruction algorithm [11] in traditional Anger cameras, which also allowed faster scans. However, with the advent of CZT technology, it became imperative to define if these new cameras would provide MPS studies

with reliable prognostic value, which might be reliably used to manage patients with suspected or known CAD.

Dolan et al. demonstrated the prognostic value of MPS in a CZT camera, but as these authors recognized, they used the conventional dose of radiotracers [14]. The radiation dose used in this study was considerably lower than standard dose used in traditional protocols, and we initially tested different acquisition times to obtain the best possible images with low radiation. Total procedure time was reduced to less than one hour, with imaging time of 6 min for rest and 3 min for stress phase.

After establishing these parameters, we then studied the prognostic value of this protocol. Male gender, increasing age, the use of pharmacologic stress were significant predictors of hard events, as previously described [15, 16]. Diabetes was independently associated both with hard events or late revascularization. Of note, LVEF was not associated with events, what might be explained by the overall normal left ventricular function of the study population. Importantly, the extent and intensity of myocardial ischemia, as expressed by the SDS, was significantly

Table 4 Characteristics of patients with or without late revascularization

Variables	Univariate analysis			Cox regression	
	Patients w/o late revascularization (n = 2763)	Patients w/late revascularization (n = 167)	p value	HR [95% CI]	p value
Age (years)	63.9 ± 12.2	66.4 ± 10.3	<0.001	1.00 [0.99–1.02]	0.397
Male gender	1462 (52.8%)	110 (65.5%)	<0.01	1.35 [0.97–1.88]	0.068
Chest pain	812 (29.3%)	53 (31.5%)			
Hypertension	1690 (61.0%)	117 (69.6%)	0.044	1.07 [0.75–1.51]	0.689
Hypercholesterolemia	1425 (51.5%)	105 (62.5%)	<0.01	1.47 [1.06–2.04]	0.020
Diabetes mellitus	598 (21.6%)	69 (41.1%)	<0.001	1.94 [1.41–2.66]	0.000
Family history of CAD	861 (31.1%)	54 (32.1%)			
Smoking	1001 (36.2%)	68 (40.5%)		0.77 [0.46–1.28]	0.314
Previous MI	317 (11.4%)	50 (29.8%)	<0.001	2.01 [1.43–2.83]	0.000
Previous CABG	208 (7.5%)	14 (8.3%)		1.60 [0.92–2.79]	0.095
Previous PCI	429 (15.5%)	72 (42.9%)	<0.001	2.54 [1.76–3.68]	0.000
Exercise stress	1624 (59.0%)	82 (48.8%)	<0.01		
Pharmacologic test	1955 (41.4%)	86 (51.2%)	<0.01	1.20 [0.86–1.67]	0.264
MPS					
SSS ^a	2.5 ± 4.7	6.6 ± 7.1	<0.001	1.06 [1.04–1.08]	0.000
SRS	1.9 ± 4.1	3.7 ± 5.6	<0.001		
SDS ^a	0.6 ± 1.7	2.9 ± 3.8	<0.001	1.22 [1.17–1.26]	0.000
LVEF (%)	59.6 ± 10.9	54.8 ± 12.0	<0.01	1.00 [0.99–1.00]	0.887
EDV (ml)	81.1 ± 33.3	88.5 ± 36.9	<0.01		
ESV (ml)	35.3 ± 25.3	43.0 ± 30.2	<0.01		

CABG coronary artery bypass grafting, MI myocardial infarction, MPS myocardial perfusion SPECT, PCI percutaneous coronary intervention, SDS summed difference score, SRS summed rest score, SSS summed stress score

^aSSS and SDS were analyzed separately in the cox regression, each one with all other selected variables

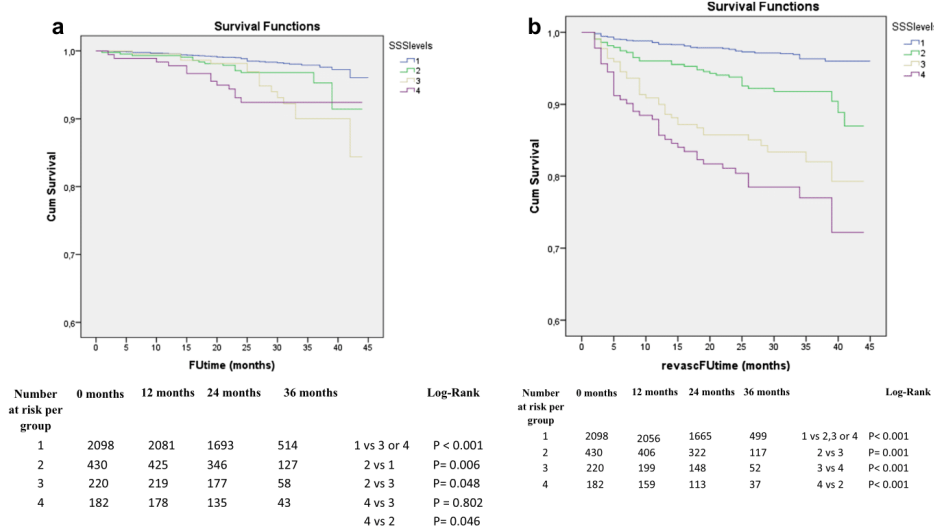


Fig. 2 Kaplan–Meier curves of hard events (a) or late revascularization (b) according to SSS categories. Blue line SSS 0–2; green line SSS 3–5; yellow line SSS 6–11; purple line SSS ≥ 12

Table 5 Annualized hard events and late revascularization rates for individual SSS groups

SSS groups	Annualized hard event rates	Annualized late revascularization rates
1	0.57	0.90
2	1.27	2.45
3	2.06	4.96
4	2.15	6.48

associated with outcomes, what supports the prognostic value of this new protocol.

It is worth noting the characteristics of the study population, composed of outpatients, most asymptomatic (performing MPS as part of a preoperative evaluation or general screening due to cardiac risk factors) with normal left ventricular function. Nonetheless, the prevalence of diabetes was >20%, and over 10% had a history of myocardial infarction, what increases overall risk and may improve the generalizability of these results. Therefore, we believe that CZT MPS may be reliably used to evaluate patients for CAD, with the advantages of reduced imaging time and lower radiation dose.

We recognize, as a limitation, that the best method to establish the prognostic value of this new protocol in a CZT-GC would be a comparison between new and traditional cameras, with each patient being studied in both

Table 6 Annualized hard events and late revascularization rates for individual SDS groups

SDS groups	Annualized hard event rates	Annualized late revascularization rates
1	0.60	0.96
2	1.87	2.57
3	1.93	6.03
4	2.03	9.84

cameras and being control for themselves. However, it assumes that the same protocol would be used for both cameras [14]. Since the new low radiation dose and acquisition time protocol could not be used for traditional cameras, the study would not verify the protocol that this study aim to establish.

Conclusion

A new, faster, low-radiation, MPS protocol in a CZT camera was able to maintain the ability of stratifying patients with increased risk of events, showing that, in the presence of greater extension of defect or ischemia, patients presented higher rates of hard events and late revascularization.

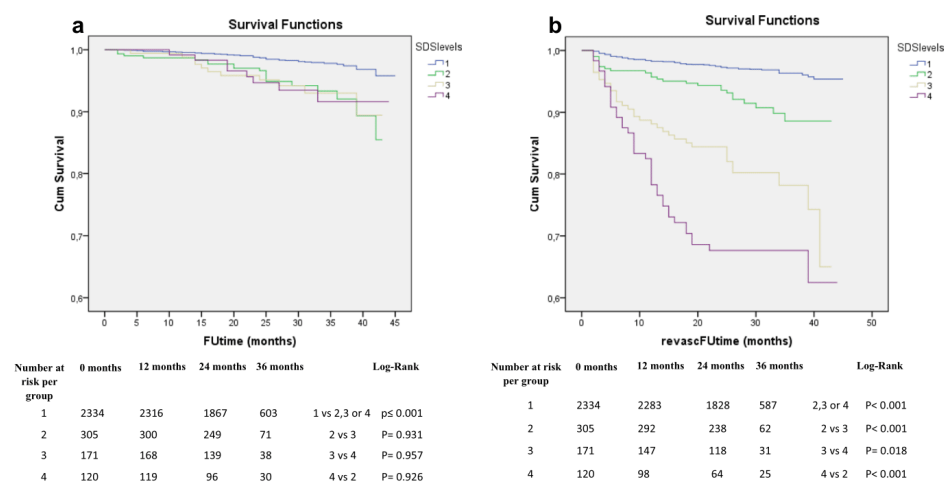


Fig. 3 Kaplan–Meier curves of hard events (a) or late revascularization (b) according to SDS categories. Blue line SDS 0; green line SDS 1–2; yellow line SDS 3–5; purple line SDS ≥6

Compliance with ethical standards

Conflict of interest The authors declare that they have no conflict of interest.

References

1. Verberne HJ, Acampa W, Anagnostopoulos C, Ballinger J, Bengel F, De Bondt P et al (2015) EANM procedural guidelines for radionuclide myocardial perfusion imaging with SPECT and SPECT/CT: 2015 revision. *Eur J Nucl Med Mol Imaging* 42(12):1929–1940
2. Hansen CL, Goldstein RA, Akinboboye OO, Berman DS, Botvinick EH, Churchwell KB et al (2007) Myocardial perfusion and function: single photon emission computed tomography. *J Nucl Cardiol* 14(6):e39–e60
3. Oddstig J, Hedeer F, Jögi J, Carlsson M, Hindorf C, Engblom H (2013) Reduced administered activity, reduced acquisition time, and preserved image quality for the new CZT camera. *J Nucl Cardiol* 20(1):38–44
4. Duvall WL, Sweeny JM, Croft LB, Ginsberg E, Guma KA, Henzlova MJ (2012) Reduced stress dose with rapid acquisition CZT SPECT MPI in a non-obese clinical population: comparison to coronary angiography. *J Nucl Cardiol* 19(1):19–27
5. Mouden M, Timmer JR, Ottervanger JP, Reiffers S, Oostdijk AH, Knollema S et al (2012) Impact of a new ultrafast CZT SPECT camera for myocardial perfusion imaging: fewer equivocal results and lower radiation dose. *Eur J Nucl Med Mol Imaging* 39(6):1048–1055
6. Hayes SW, De Lorenzo A, Hachamovitch R, Dhar SC, Hsu P, Cohen I et al (2003) Prognostic implications of combined prone and supine acquisitions in patients with equivocal or abnormal supine myocardial perfusion SPECT. *J Nucl Med* 44(10):1633–1640
7. Burrell S, MacDonald A (2006) Artifacts and pitfalls in myocardial perfusion imaging. *J Nucl Med Technol* 34(4):193–211 (quiz 2–4)
8. Berman DS, Kang X, Van Train KF, Lewin HC, Cohen I, Areeda J et al (1998) Comparative prognostic value of automatic quantitative analysis versus semiquantitative visual analysis of exercise myocardial perfusion single-photon emission computed tomography. *J Am Coll Cardiol* 32(7):1987–1995
9. Berman DS, Hachamovitch R, Kiat H, Cohen I, Cabico JA, Wang FP et al (1995) Incremental value of prognostic testing in patients with known or suspected ischemic heart disease: a basis for optimal utilization of exercise technetium-99m sestamibi myocardial perfusion single-photon emission computed tomography. *J Am Coll Cardiol* 26(3):639–647
10. Hachamovitch R, Berman DS, Shaw LJ, Kiat H, Cohen I, Cabico JA et al (1998) Incremental prognostic value of myocardial perfusion single photon emission computed tomography for the prediction of cardiac death: differential stratification for risk of cardiac death and myocardial infarction. *Circulation* 97(6):535–543
11. Lima R, Ronaldo L, De Lorenzo A, Andrea DL, Camargo G, Gabriel C et al (2014) Prognostic value of myocardium perfusion imaging with a new reconstruction algorithm. *J Nucl Cardiol* 21(1):149–157
12. Thygesen K, Alpert JS, White HD, Joint ESC/ACCF/AHA/WHF Task Force for the Redefinition of Myocardial Infarction (2007) Universal definition of myocardial infarction. *J Am Coll Cardiol* 50(22):2173–2195
13. Duvall WL, Croft LB, Ginsberg ES, Einstein AJ, Guma KA, George T et al (2011) Reduced isotope dose and imaging time with a high-efficiency CZT SPECT camera. *J Nucl Cardiol* 18(5):847–857
14. Oldan JD, Shaw LK, Hofmann P, Phelan M, Nelson J, Pagnanelli R et al (2016) Prognostic value of the cadmium-zinc-telluride camera: a comparison with a conventional (Anger) camera. *J Nucl Cardiol* 23(6):1280–1287
15. Hachamovitch R, Berman DS, Kiat H, Bairey CN, Cohen I, Cabico A et al (1996) Effective risk stratification using exercise myocardial perfusion SPECT in women: gender-related differences in prognostic nuclear testing. *J Am Coll Cardiol* 28(1):34–44
16. Navare SM, Mather JF, Shaw LJ, Fowler MS, Heller GV (2004) Comparison of risk stratification with pharmacologic and exercise stress myocardial perfusion imaging: a meta-analysis. *J Nucl Cardiol* 11(5):551–561



Comparison of the prognostic value of myocardial perfusion imaging using a CZT-SPECT camera with a conventional anger camera

Ronaldo Lima, MD, PhD,^{a,b} Thais Peclat, MD,^c Thalita Soares, BMBS,^c
Caio Ferreira, BMBS,^c Ana Carolina Souza, BMBS,^c and Gabriel Camargo, MD^a

^a Department of Cardiology, Universidade Federal do Rio de Janeiro, Rio de Janeiro, Brazil

^b Nuclear Medicine, Clínica de Diagnóstico por Imagem, Rio de Janeiro, Brazil

^c Universidade Federal do Rio de Janeiro, Rio de Janeiro, Brazil

Received May 21, 2016; accepted Jul 15, 2016

doi:10.1007/s12350-016-0618-9

Background. Recent studies have shown that myocardial perfusion imaging (MPI) in cadmium-zinc-telluride (CZT) cameras allow faster exams with less radiation dose but there are little data comparing its prognosis information with that of dedicated cardiac Na-I SPECT cameras

Objective. The objective of this study is to compare the prognostic value of MPI using an ultrafast protocol with low radiation dose in a CZT-SPECT and a traditional one.

Methods. Group 1 was submitted to a two-day MIBI protocol in a conventional camera, and group 2 was submitted to a 1-day MIBI protocol in CZT camera. MPI were classified as normal or abnormal, and perfusion scores were calculated. Propensity score matching methods were performed

Results. 3554 patients were followed during 33±8 months. Groups 1 and 2 had similar distribution of age, gender, body mass index, risk factors, previous revascularization, and use of pharmacological stress. Group 1 had more abnormal scans, higher scores than group 2. Annualized hard events rate was higher in group 1 with normal scans but frequency of revascularization was similar to normal group 2. Patients with abnormal scans had similar event rates in both groups

Conclusion. New protocol of MPI in CZT-SPECT showed similar prognostic results to those obtained in dedicated cardiac Na-I SPECT camera, with lower prevalence of hard events in patients with normal scan. (J Nucl Cardiol 2016)

Key Words: myocardial perfusion imaging • coronary artery disease • SPECT

Abbreviations		BMI	Body mass index
MPI	Myocardial perfusion imaging	PCI	Percutaneous coronary intervention
CAD	Coronary artery disease	CABG	Coronary artery bypass surgery
SPECT	Single-photon emission computed tomography		
CZT	Cadmium-zinc-telluride		

Electronic supplementary material The online version of this article (doi:10.1007/s12350-016-0618-9) contains supplementary material, which is available to authorized users.

The authors of this article have provided a PowerPoint file, available for download at SpringerLink, which summarises the contents of the paper and is free for re-use at meetings and presentations. Search for the article DOI on <http://SpringerLink.com>

Reprint requests: Ronaldo Lima, MD, PhD, Cardiology, Universidade Federal do Rio de Janeiro, Cardiology, Rio de Janeiro, Brazil; ronlima@hotmail.com

1071-3581/\$34.00

Copyright © 2016 American Society of Nuclear Cardiology.

See related editorial, doi:10.1007/s12350-016-0640-y.

INTRODUCTION

It is well known that myocardial perfusion imaging (MPI) with stress testing is an independent predictor of prognosis in patients with suspected or known coronary artery disease (CAD). The gated single-photon emission computed tomography (SPECT) appears to be the best predictor of cardiac event-free survival in this population.¹ Also, compared with other methods such as stress-ECG and coronary angiography, SPECT-based strategies seem to be more cost-effective.²

Over time, numerous technological advances have increased MPI's performance, with the most meaningful being the introduction of tomographic imaging and, later, of the multidetector gamma cameras. Recent developments have allowed for reductions in scan time and radiation dose used to its acquisition.³ Specifically, new multipinhole cameras with cadmium-zinc-telluride solid state detectors (CZT-SPECT) technology allow for faster image acquisition and lower radiation doses in comparison with traditional Sodium-Iodine Anger cameras. This allows for 1-day stress/rest MPI protocols, preserving diagnostic image quality and diagnostic accuracy.^{4,5} The CZT technology improves the energy and spatial resolutions, while using simultaneously acquired views improves the overall sensitivity, resulting in high-quality images.⁶

Previous examination of the prognostic value in specific groups, like the obese, demonstrated that CZT-SPECT provides adequate risk stratification.⁷ However, there are little data comparing the prognostic value between ultrafast protocol CZT-SPECT and dedicated cardiac Na-I SPECT cameras. That could impair the broad use of this technology. Our objective is to compare the prognostic value of MPI using these two camera protocols.

METHODS

Population and Study Design

We analyzed two different groups of patients clinically referred to a SPECT-MPI in an outpatient clinic between 2008 and 2012. Patients in group 1 scanned in Na-I SPECT cameras from 2008 to 2010, and in group 2 were scanned using CZT-SPECT from 2011 to 2012.

Ninety-nine patients who underwent revascularization in the first 60 days after nuclear testing were excluded, and history of significant cardiac valve disease or severe nonischemic cardiomyopathy (33 patients) or any condition which might adversely affect short-term prognosis were also considered exclusion criteria (Figure 1). Three patients were

excluded because the images acquired in gamma camera CZT were inadequate for interpretation (BMI > 45). The research was approved by the institutional review board, and all subjects signed informed consent.

Prior to scanning, a team of cardiologists collected information on the presence of categorical cardiac risk factors in each individual including hypertension, diabetes, hypercholesterolemia, smoking, and family history of CAD using a standard questionnaire.

Cardiac symptoms were based on Diamond and Forrester criteria,⁸ divided as asymptomatic, nonanginal pain, atypical angina, typical angina, and shortness of breath.

From a total of 6128 patients meeting inclusion criteria, follow-up was complete in 5828 (95.1% of the total); we selected 3554 using propensity score matching based on sex, age, body mass index (BMI), symptoms, cardiac risk factors, history of coronary events, and type of stress used. A 1 to 1 nearest neighbor matching with no replacement was performed to produce two groups with 1777 individuals in each, divided according to the type of gamma camera used.

Cardiac Imaging and Stress Protocol

Patients were instructed to abstain from any products containing caffeine for 24 hours before the test. Beta-blockers and calcium-channel antagonists were terminated 48 hours before testing, and nitrates were withheld for at least 6 hours before testing. Stress testing was performed with a symptom-limited Bruce treadmill exercise protocol or pharmacologic protocol (dipyridamole or dobutamine). In general, stress using dipyridamole was the first choice, while dobutamine was

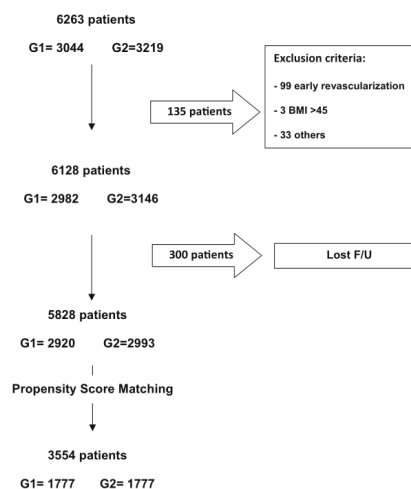


Figure 1. Flow diagram of the study.

reserved for patients with contraindications to vasodilator stress (mainly bronchospastic airway disease).

Patients in group 1 underwent 2-day Tc-99 m sestamibi (near-maximal exercise, 10-12 mCi) was injected intravenously, and exercise was continued at maximal workload for at least 1 minute) gated MPS with scan time of 6 minutes stress and rest studies (15-18 mCi). Mean radiation dose was 9.5 mSv. Stress-only imaging was not performed due to reimbursement issues. Three minutes prone images were acquired in all male patients but gating was not performed. All supine images were gated. The full protocols used have been previously described.⁹ MPI studies were classified as normal or abnormal, and perfusion scores (SSS, SRS, and SDS) were calculated. Images were acquired using a two-headed gamma camera equipped with 90°-angled detectors (Ventri, GE Healthcare, Waukesha, WI, USA) equipped with a low-energy, high-resolution collimator, and 30 stops in a 64 × 64 matrix. Image acquisition began 15-45 minutes after tracer injection. Scans were reconstructed with Evolution for Cardiac™ (GE healthcare), using 12 iterations. Poststress-gated short-axis images were processed using quantitative-gated SPECT software (QGS; Cedars-Sinai Medical Center, Los Angeles, California), and left ventricular ejection fraction (LVEF) was automatically calculated after inspection of myocardial contours.

Patients in group 2 underwent treadmill exercise or pharmacological stress using standard dipyridamole or dobutamine infusion protocols.¹⁰ Exercise testing was performed using a symptom-limited Bruce protocol. A 1-day 99m-Tc-MIBI, rest/stress protocol was used, starting with rest study (injection of 5 mCi) followed by stress (15 mCi) in a CZT camera. Mean radiation dose was 6 mSv. The MPI were also classified as normal or abnormal and perfusion scores (SSS, SRS, and SDS) were also calculated. Poststress prone acquisitions were performed in all patients. CZT-SPECT was performed using a camera with multipinhole collimator (Discovery 530, GE Healthcare, Milwaukee, USA). The system design allows acquisition without detector or collimator motion. Images were acquired in 6, 3, and 1 minute, respectively, for rest, supine stress and prone stress, as previously described.¹¹ A 10% symmetric energy window at 140 keV was used. Images were reconstructed on a dedicated Xeleris workstation (GE Healthcare) applying an iterative reconstruction algorithm with maximum-likelihood expectation maximization. Assessment of image quality and perfusion abnormalities was performed visually by two experienced nuclear cardiologists blinded to patient characteristics. Poststress left ventricular volumes and ejection fraction were calculated from the poststress-gated images using commercially available software (QGS, Cedars-Sinai Medical Center, Los Angeles, California, USA).

In both group, semiquantitative visual interpretation of MPI images was performed with short-axis and vertical long-axis tomograms divided into 17 segments.¹⁰ Each segment was scored by consensus of two expert observers (aware of clinical and stress data) using a 5-point scale (0 = normal; 1 = equivocal; 2 = moderate; 3 = severe reduction of tracer uptake; 4 = the absence of detectable radiotracer activity in a

segment). Then, perfusion scores were calculated to express the extent and severity of myocardial perfusion abnormalities. The summed stress score (SSS, a measure of the total poststress perfusion defect) and summed rest score (SRS, a measure of rest defect or myocardial fibrosis) were obtained by means of adding the scores for the 17 segments of the stress and rest images, respectively. The difference between the SSS and SRS was defined as the summed difference score (SDS, a measure of reversible defect or myocardial ischemia). For the purpose of evaluating the SSS and the SDS as predictors of events, we performed separate analyses with different cut points for each perfusion variable. We classified SSS as abnormal when it was >3 and SDS when it was >1.

Follow-Up

Follow-up was performed by telephone interview every 6 months after MPI. Events were defined as all-cause death and nonfatal myocardial infarction (classified as hard events) and late revascularization (>60 days after MPI), by percutaneous coronary intervention (PCI) or bypass surgery (CABG). Events were confirmed through review of hospital charts or physician's records. Nonfatal myocardial infarction was defined based on the criteria of typical chest pain, elevated cardiac enzyme levels, and typical alterations of the electrocardiogram.¹²

Statistical Analysis

All statistical calculations were performed using SPSS (Version 17). Categorical variables are presented as frequencies and continuous variables as mean ± SD. Variables were compared with Pearson Chi-squared test for categorical variables and by Student's two sample *t* test for continuous variables. Event-free survival curves were constructed using the Kaplan-Meier methods to account for censored survival times and were compared with the log-rank test.

RESULTS

Patients were divided into group 1 and 2, each with of 1777 subjects, and its overall baseline characteristics are summarized in Table 1. There were no statistically significant differences between groups in regard of gender, prevalence of hypertension, diabetes, smoking, hypercholesterolemia, previous revascularization, and use of pharmacological stress. The more frequent indications in asymptomatic patients were a previous treadmill test with intermediate-high risk Duke score, pre-op risk stratification and a previous calcium score >100. Patients with previous MI or revascularization were considered to have known CAD. The mean follow-up interval was 34 ± 9 months in group 1 and 33 ± 8 months in group 2.

Comparing the two groups, the classification as normal or abnormal scans and the perfusion scores (SSS,

Table 1. Baseline characteristics

	Total (6128)	Select (3554)	Group 1 (1777)	Group 2 (1777)	p value
Age (years)	63.0 ± 12.3	62.8 ± 12.0	62. ± 12.0	62.9 ± 12.0	1
Male	3370 (55.0%)	1920 (54.0%)	949 (53.4%)	971 (54.6%)	0.46
Weight (kg)	78.5 ± 17.7	78.1 ± 16.6	77.9 ± 16.3	78.2 ± 16.9	0.47
BMI	28.0 ± 6.1	27.8 ± 5.9	27.7 ± 6.0	27.9 ± 6.0	0.26
Asymptomatic	4221 (68.9%)	2377 (66.9%)	1171 (65.9%)	1206 (67.9%)	0.21
Diabetes	1396 (22.8%)	815 (22.9%)	390 (21.9%)	425 (23.9%)	0.16
Hypertension	3908 (63.8%)	2165 (60.9%)	1081 (60.8%)	1084 (61.0%)	0.92
Hypercholesterolemia	3166 (51.7%)	1764 (49.8%)	885 (49.6%)	879 (49.5%)	0.84
Beta-blockers	1782 (29.1%)	1074 (30.2%)	541 (30.4%)	533 (30.0%)	0.39
ACEI	3247 (38.6%)	1365 (38.4%)	400 (22.5%)	410 (23.1%)	0.3
Statins	3062 (50.0%)	1777 (50.0%)	886 (49.9%)	891 (50.1%)	0.78
Previous MI	767 (12.5%)	439 (12.4%)	225 (12.7%)	214 (12.0%)	0.31
Previous PCI	1195 (19.5%)	628 (17.7%)	314 (17.7%)	314 (17.7%)	1
Previous CABG	550 (9.0%)	302 (8.5%)	159 (9.0%)	143 (8.0%)	0.34
Pharmacological stress	2566 (41.9%)	1458 (41.0%)	752 (42.3%)	706 (39.7%)	0.13

p value comparison between Group 1 and 2; n (%) or mean ± standard deviation
ACEI angiotensin-converting enzyme inhibitor; BMI body mass index; CABG coronary artery bypass; MI myocardial infarction; PCI percutaneous coronary intervention

Table 2. Scans results, perfusion scores, and gated SPECT measurements

	Group 1 (1777)	Group 2 (1777)	p value
Abnormal Scans	487 (27.4%)	383 (21.6%)	<0.001
Reversible	237 (13.3%)	154 (8.7%)	
Fixed	126 (7.1%)	128 (7.2%)	
Mixed defect	124 (7.0%)	101 (5.7%)	
SSS	2 (0-4)	1 (0-3)	<0.01
SRS	1 (1-3)	0 (0-2)	<0.01
SDS	0 (0-1)	0 (0-0)	<0.01
LVEF stress	58.5 ± 11.9	59.3 ± 13.0	0.07
EDV stress	80.1 ± 33.9	82.1 ± 33.5	0.1
ESV stress	36.4 ± 28.3	36.1 ± 26.5	0.7

EDV end diastolic volume; ESV end systolic volume; LVEF left ventricle ejection fraction; SSS summed stress score; SRS summed rest score; SDS summed difference score
Perfusion scores are expressed as median and interquintile 25 and 75

SRS, and SDS) were statistically different. Group 1 had more abnormal scans (27.4% vs 21.6%; $p < 0.001$) and higher SSS, SRS, and SDS than group 2. Scan results, perfusion scores, left ventricle ejection fraction, and ventricular volumes of both groups are summarized in Table 2.

During follow-up, 98 deaths and 48 myocardial infarctions, 188 percutaneous coronary interventions, and 48 coronary artery bypass graft surgeries occurred. Assessing data from patients with normal scans, it was found that the annualized hard events rate was higher in patients of Group 1 (1.0%/year vs 0.5%/year; $p < 0.01$),

but the percentage of PCI and CABG were not different (0.9% vs 0.8%; 0.3% vs 0.1%, respectively; $p = \text{NS}$) comparing with Group 2. However, patients with abnormal scans had no significant difference between the two groups in regard of both annualized hard events (3.3%/year and 3.2%/year; $p = \text{NS}$) and percentage of revascularization (6.6% vs 6.3%, $p = \text{NS}$). Event rates comparison between two groups are demonstrated in Table 3. Kaplan-Meier cumulative survival comparing group 1 and 2 with normal or abnormal scan are shown in Figure 2 (hard events) and Figure 3 (late revascularization).

Table 3. Annualized event rate (%/year)

	Group 1		Group 2	
	Normal scan (N = 1290)	Abnormal scan (N = 487)	Normal scan (N = 1394)	Abnormal scan (N = 383)
Hard events	1.0*† (41)	3.3 (54)	0.5* (18)	3.2 (33)
Late Revasc	1.2*† (46)	4.2 (92)	0.7* (33)	3.3 (65)
Death	0.7*† (26)	2.3 (33)	0.5* (16)	2.4 (23)
MI	0.4*† (15)	1.5 (21)	0.06* (2)	1.0 (10)
PCI	0.9* (36)	5.0 (72)	0.8* (30)	5.1 (50)
CABG	0.3* (10)	1.6 (20)	0.1* (3)	1.2 (15)

*Significant difference between normal and abnormal scan

†Significant difference between Group 1 and Group 2; (number of events)

CABG coronary artery bypass graft; MI myocardial infarction; PCI percutaneous coronary intervention

DISCUSSION

MPI is an established method for diagnostic and prognostic evaluation of patients with CAD.¹ However, two considerable limitations of this method are the prolonged time required to scan acquisition and the radiation dose.¹³ New high-speed SPECT cameras using cadmium-zinc-telluride detectors are a new technology of gamma camera that allows shorter acquisition time and lower tracer doses.¹⁴ Nevertheless, the prognostic value of this ultrafast, low-dose radiation, protocol is not yet established and has not been compared with the protocol in dedicated cardiac Na-I SPECT cameras.^{15,17}

In an attempt to do this comparison, we studied two different groups with 1777 patients. They were standard to each other through a propensity score matching with the purpose of showing the association, in both groups, between scan results and the hard events rate. As can be seen in Table 1, the strict matching parameter we used produced two groups with very similar exposition to factors that could influence results.

Statistically significant differences in the distribution of perfusion scores (SSS, SRS, and SDS) and the classification as normal and abnormal scans were noted between the CZT camera and the conventional camera. The CZT camera having, on average, 6% less abnormal scans and lower SSS, SDS, and SRS as previously demonstrated by Oldan et al.¹⁶ Results showed that the rate of events and myocardial revascularization was not higher in group 1. Someone might argue that the more frequently abnormal tests in Group 1 could mean greater accuracy of traditional equipments. In this case, a larger number of false negative tests should have occurred in Group 2, which did not happen. In fact patients with normal examination evaluated in CZT cameras showed a lower percentage of events.

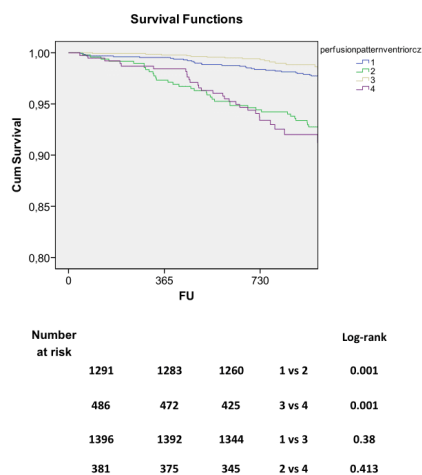


Figure 2. Kaplan-Meier curves for hard events. (1) Blue: Ventr normal scans; (2) Green: Ventr-abnormal scans; (3) Yellow: CZT normal scans; and (4) Purple: CZT abnormal scans.

In the follow-up data, our study has found that among patients with normal scans, the annualized hard events rate was higher in patients from traditional Na-I camera. The difference among hard event rate between both cameras may be an objective representation of the already known higher sensitivity for these new cameras, reflecting in a higher negative predicted value. In the follow-up of patients with abnormal scans, the study has

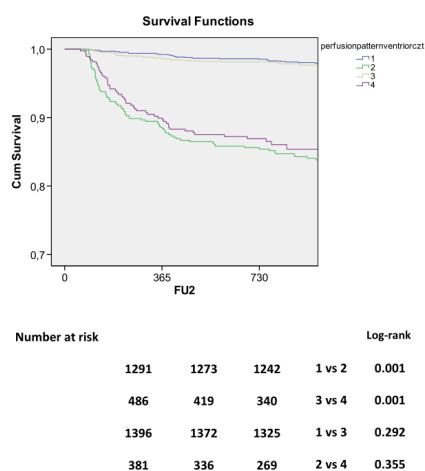


Figure 3. Kaplan-Meier curves for late revascularization. (1) Blue: Ventri normal scans; (2) Green: Ventri-abnormal scans; (3) Yellow: CZT normal scans; and (4) Purple: CZT abnormal scans.

shown no significant difference between the two groups in regard of both annualized hard events and percentage of revascularization. These data support that in patients with a higher probability of disease; both cameras were totally able to stratify the risk of events and thereby definitely established the MPI good prognostic value for patients with CAD.

There has been controversy regarding the diagnostic value of SPECT-MPI using CZT cameras in obese patients,⁷ therefore the weight and BMI were included in the propensity score. As described in Population section, three patients were excluded because the images acquired in gamma camera CZT were inadequate for interpretation but more than 300 patients with at least 220 pounds were included in group 2. De Lorenzo et al demonstrated that in obese patients CZT-SPECT camera provides prognostic discrimination with high image quality and our data suggest. This is consistent with the results of the present study.

Our study was a retrospective analysis of outpatients who underwent CZT-SPECT or traditional Anger camera for clinical indications which carries the obvious and inherent bias of this type of study design. This is also a single-institution study and thus may not be applicable to others institutions and others types of camera designs, both CZT and conventional. Beyond that, reviewers were not blinded to clinical data. While

this is necessary to clinical interpretation of scan results, it can bias the interpretation for research purposes. However, we can assume that any bias introduced by use of clinical information should affect both cameras in the same degree. Finally, it is important to stress that while the propensity score matching was successful in producing groups with similar baseline characteristics that could bias the results, there could be other potential unknown sources of bias that may not have been balanced in our two groups using this approach.

Analyzing the few data produced by similar studies,¹⁵⁻¹⁷ we concluded that our study also showed a pattern of maintenance of the prognostic value of CZT comparing with traditional cameras. However, we had the opportunity to use a larger population that was matched in baseline characteristics and exposed to two totally different protocols. We used a standard protocol as mentioned before to dedicated Na-I cameras and a faster, lower-dose protocol in CZT-SPECT, something pioneer to this type of study.

NEW KNOWLEDGE GAINED

The CZT camera has similar utility for prognostication to conventional Anger cameras even when they are using smaller radiation doses and shorter acquisition time.

CONCLUSION

In our study, a new protocol of MPI in CZT-SPECT camera showed similar prognostic results to those obtained in dedicated cardiac Na-I SPECT camera, with lower prevalence of hard events in patients with normal scan. According to these data, we can assume that the new ultrafast protocol, using considerable lower dose of radiation, has a reliable prognostic value and is noninferior to traditional cameras.

Acknowledgments

The authors had no financial support for this research. The authors would like to thanks Dr. Ilan Gottlieb for his review and valuable suggestions.

Compliance with Ethical Standards

Disclosure The authors declare that they have no conflict of interest.

Ethical standards All procedures performed in studies involving human participants were in accordance with the ethical standards of the institutional and/or national research

committee and with the 1964 Helsinki declaration and its later amendments of comparable ethical standards.

Informed consent *Informed consent was obtained from all individual participants included in the study.*

References

- Gimelli A, Rossi G, Landi P, Marzullo P, Iervasi G, L'abbate A, et al. Stress/rest myocardial perfusion abnormalities by gated SPECT: Still the best predictor of cardiac events in stable ischemic heart disease. *J Nucl Med.* 2009;50(4):546–53.
- Underwood SR, Godman B, Salyani S, Ogle JR, Ell PJ. Economics of myocardial perfusion imaging in Europe—the EMPIRE Study. *Eur Heart J.* 1999;20(2):157–66.
- De Puey EG. Advances in SPECT camera software and hardware: Currently available and new on the horizon. *J Nucl Cardiol.* 2012;19(3):551–81.
- Duvall WL, Croft LB, Ginsberg ES, Einstein AJ, Guma KA, George T, et al. Reduced isotope dose and imaging time with a high-efficiency CZT SPECT camera. *J Nucl Cardiol.* 2011;18(5):847–57.
- Herzog BA, Buechel RR, Katz R, Brueckner M, Husmann L, Burger IA, et al. Nuclear myocardial perfusion imaging with a cadmium-zinc-telluride detector technique: optimized protocol for scan time reduction. *J Nucl Med.* 2010;51(1):46–51.
- Slomka PJ, Patton JA, Berman DS, Germano G. Advances in technical aspects of myocardial perfusion SPECT imaging. *J Nucl Cardiol.* 2009;16(2):255–76.
- De Lorenzo A, Peclat T, Amaral AC, Lima RSL. Prognostic evaluation in obese patients using a dedicated multipinhole cadmium-zinc telluride SPECT camera. *Int J Cardiovasc Imaging.* 2015;2015:1–7.
- Diamond GA, Forrester JS, Hirsch M, Staniloff HM, Vas R, Berman DS, et al. Application of conditional probability analysis to the clinical diagnosis of coronary artery disease. *J Clin Investig.* 1980;65(5):1210–21.
- Lima R, De Lorenzo A, Camargo G, Oliveira G, Reis T, Peclat T, et al. Prognostic value of myocardium perfusion imaging with a new reconstruction algorithm. *J Nucl Cardiol.* 2014;21(1):149–57.
- Henzlova MJ, Cerqueira MD, Hansen CL, Taillefer R, Yao S-S. ASNC imaging guidelines for nuclear cardiology procedures: stress protocols and tracers. *J Nucl Cardiol.* 2009. doi: [10.1007/s12350-009-9062-4](https://doi.org/10.1007/s12350-009-9062-4).
- Lima R, Peclat T, Amaral AC, Nakamoto A, Lavagnoli D, De Lorenzo A. Preliminary data on the prognostic value of a new protocol of ultra-fast myocardial scintigraphy with less radiation in CZT gamma camera. *Arq Bras Cardiol: Im Cardio.* 2016;29(1):11–6.
- Thygesen K, Alpert JS, White HD. Universal definitions of myocardial infarction. *J Am Coll Cardiol.* 2007;50:2173–95.
- Douglas PS, Hendel RC, Cummings JE, Dent JM, Hodgson JM, Hoffmann U, et al. ACCF/ACR/AHA/ASE/ASNC/HRS/NASCI/RSNA/SAIP/SCAI/SCCT/SCMR 2008 Health Policy Statement on Structured Reporting in Cardiovascular Imaging. *J Am Coll Cardiol.* 2009;53:76–90.
- Sharir T, Pinskiy M, Pardes A, Rochman A, Prokhorov V, Kovalski G, et al. Comparison of the diagnostic accuracies of very low stress-dose with standard-dose myocardial perfusion imaging: Automated quantification of one-day, stress-first SPECT using a CZT camera. *J Nucl Card.* 2016;23(1):11–20.
- Gimelli A, Bottai M, Giorgetti A, Genovesi D, Kusch A, Ripoli A, et al. Comparison between ultrafast and standard single-photon emission CT in patients with coronary artery disease: a pilot study. *Circ Cardiovasc Imaging.* 2011;4(1):51–8.
- Oldan JD, Shaw LK, Hofmann P, Phelan M, Nelson J, Pagnanelli R, et al. Prognostic value of the cadmium-zinc-telluride camera: A comparison with a conventional (Anger) camera. *J Nucl Cardiol.* 2015. doi:[10.1007/s12350-015-0224-2](https://doi.org/10.1007/s12350-015-0224-2).
- Yokota S, Mouden M, Ottervanger JP, Engbers E, Knollema S, Timmer JR, et al. Prognostic value of normal stress-only myocardial perfusion imaging: a comparison between conventional and CZT-based SPECT. *Eur J Nucl Med Mol Imaging.* 2016;43(2):296–301.



The additional prognostic value of myocardial perfusion SPECT in patients with known coronary artery disease with high exercise capacity

Thais R. Peclat, MD,^a Ana Carolina do A. H. de Souza, MD,^a Victor F. Souza, MD,^a Aline M. K. Nakamoto, MD,^a Felipe M. Neves, MD,^a Izabella C. R. Silva,^a and Ronaldo S. L. Lima, MD^{a,b,c}

^a Cardiology, Clementino Fraga Filho University Hospital, Federal University of Rio de Janeiro, Rio de Janeiro, Brazil

^b Fonte Imagem, Rio de Janeiro, Brazil

^c Clínica de Diagnóstico por Imagem, Rio de Janeiro, Brazil

Received Sep 12, 2019; Revised Nov 2, 2019; accepted Nov 4, 2019

doi:10.1007/s12350-019-01960-0

Background. The prognostic value of myocardial perfusion imaging (MPI) in patients with known coronary artery disease (CAD) and high exercise capacity is still unknown. We sought to determine the MPI additional prognostic value over electrocardiography (ECG) stress testing alone in patients with known CAD who achieved ≥ 10 metabolic equivalents (METs).

Methods and Results. We evaluated 926 patients with known CAD referred for MPI with exercise stress. Patients were followed for a mean of 32.4 ± 9.7 months for the occurrence of all-cause death or nonfatal myocardial infarction (MI). Those achieving ≥ 10 METs were younger, predominantly male, and had lower prevalence of cardiovascular risk factors. Patients reaching ≥ 10 METs had a lower annualized rate of hard events compared to their counterparts achieving < 10 METs (1.13%/year vs 3.95%/year, $P < .001$). Patients who achieved ≥ 10 METs with abnormal scans had a higher rate of hard events compared to those with normal scans (3.37%/year vs 0.57%/year, $P = .023$). Cardiac workload < 10 METs and an abnormal MPI scan were independent predictors of hard events.

Conclusions. MPI is able to stratify patients with known CAD achieving ≥ 10 METs for the occurrence of all-cause death and nonfatal MI, with incremental prognostic value over ECG stress test alone. (J Nucl Cardiol 2019)

Key Words: CAD • MPI • SPECT • ECG stress • METs • prognostic • outcomes • exercise capacity

Electronic supplementary material The online version of this article (<https://doi.org/10.1007/s12350-019-01960-0>) contains supplementary material, which is available to authorized users.

The authors of this article have provided a PowerPoint file, available for download at SpringerLink, which summarizes the contents of the paper and is free for reuse at meetings and presentations. Search for the article DOI on SpringerLink.com.

The authors have also provided an audio summary of the article, which is available to download as ESM, or to listen to via the JNC/ASNC Podcast.

Reprint requests: Thais R. Peclat, MD, Cardiology, Clementino Fraga Filho University Hospital, Federal University of Rio de Janeiro, Rio de Janeiro, Brazil; thais_peclat@hotmail.com

J Nucl Cardiol 2019

1071-3581/\$34.00

Copyright © 2019 American Society of Nuclear Cardiology.

Abbreviations

MPI	Myocardial perfusion imaging
CAD	Coronary artery disease
METs	Metabolic equivalents
SPECT	Single photon emission computed tomography
MI	Myocardial infarction
CABG	Coronary artery bypass graft
PCI	Percutaneous coronary intervention
SSS	Summed stress score
SDS	Summed difference score
SRS	Summed rest score

INTRODUCTION

Coronary artery disease (CAD) remains as the leading cause of death in adults in the USA, accounting for about one-third of all deaths in subjects over age 35.¹ In patients with known or suspected CAD, accurate risk stratification and management guidance is of great value to improve outcomes.

Exercise electrocardiography (ECG) stress test and myocardial perfusion imaging with single photon emission computed tomography (MPI SPECT) are both robust, widely used tools for risk stratification in stable CAD.^{2,3} It is known that MPI has higher sensitivity over exercise ECG stress test for detection of ischemia in patients with an intermediate pretest likelihood of CAD.⁴ Moreover, MPI may provide additional clinical information on ventricular function and regional perfusion.

Exercise capacity is an established predictor of mortality⁵⁻¹⁰ and along the past two decades several authors have brought to discussion whether this parameter would be sufficient to support clinical decision. Patients achieving ≥ 10 metabolic equivalents (METs) were shown to have excellent prognosis with low rates of cardiovascular events and low prevalence of $\geq 10\%$ LV ischemia regardless of peak exercise heart rate. That led to questioning on the usefulness of MPI-derived information^{11,12} and later, on the use of exercise capacity as criteria to skip imaging protocols. In that context, provisional protocols were created to better address the groups of patients who could have been selected for this approach, preserving them from unnecessary radiation exposure.^{13,14} However, these provisional protocols typically excluded patients with known CAD.¹⁴

Patients with known CAD are an important segment of the population commonly referred to MPI due to its well-established prognostic value, worthy to be used in

the management of those patients. An association between exercise capacity and overall mortality in patients with known cardiovascular disease has been previously demonstrated.¹⁵ However, no further investigation was done to better understand how workload relates to MPI results regarding the ability to predict outcomes in this particular group.

The aim of this study is to determine the additional MPI prognostic value over ECG stress testing alone in patients with known CAD who achieved high exercise capacity (≥ 10 METs).

METHODS**Study Cohort**

We evaluated 4,187 consecutive patients with known or suspected CAD referred for clinically indicated MPI with exercise stress in an outpatient clinic in Rio de Janeiro, Brazil, between March 2008 and October 2012. The following were considered as exclusion criteria: suspected CAD, early revascularization (coronary angioplasty or coronary artery bypass grafting surgery occurring < 60 days after MPI), and a history of significant cardiac valve disease, severe nonischemic cardiomyopathy, or any condition which might affect short-term prognosis.

Patients were classified as having known CAD based on reported medical history of myocardial infarction (MI), coronary artery bypass graft (CABG), or percutaneous coronary intervention (PCI). From 948 patients meeting all criteria, follow-up was completed in 926 (97.6% of the total). Study cohort flowchart is shown on Figure 1.

Prior to the scan, patients' medical history and physical examination data were collected in a standard questionnaire by a team of experienced cardiologists. Cardiac risk factors including hypertension, diabetes, hypercholesterolemia, smoking, obesity, and family history of CAD were collected. Cardiac symptoms were based on Diamond and Forrester criteria¹⁶ and classified as asymptomatic, noncardiac pain, atypical angina, typical angina, and shortness of breath.

All study procedures were in accordance with the Ethical Standards of the Institutional Research Committee. Informed consent was obtained from all individual participants included in the study.

Study Protocol

Exercise testing Stress-ECG test was performed based on a symptom-limited Bruce treadmill protocol. Exercise workload was defined by the total METs achieved. Ischemic ST segment depression was defined

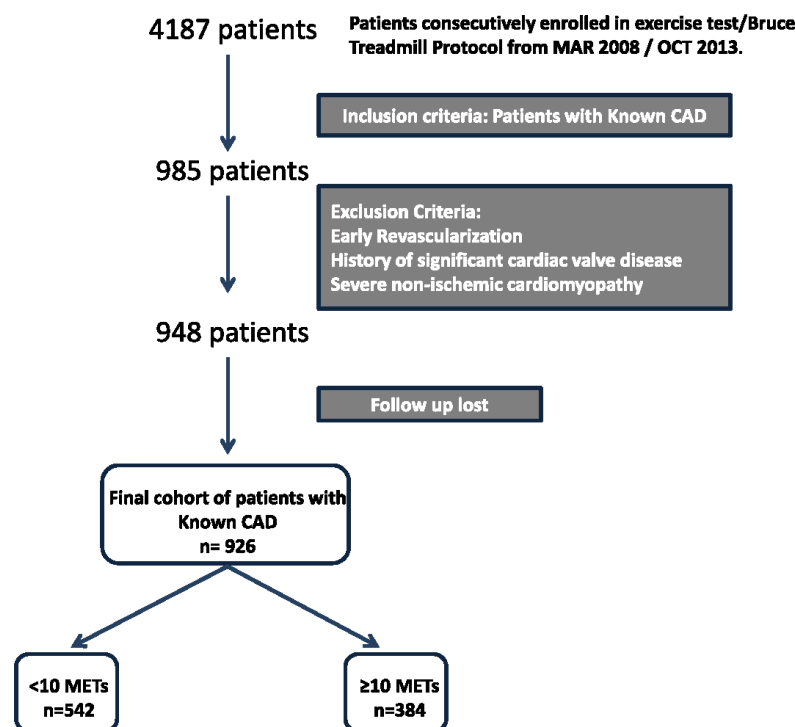


Figure 1. Flowchart of the study cohort.

as a horizontal or down-sloping depression of the ST segment by ≥ 1 mm present ≥ 80 ms after the J-point for three consecutive beats.

SPECT imaging SPECT imaging protocols have been previously described and validated,^{17–19} and will be summarized here. Patients underwent either a 2-day or 1-day Tc-99m-sestamibi-gated MPI protocol based on the scan date, since the camera used for most patients in our laboratory changed during the observation period. For the 2-day protocol a dose of 10–12 mCi ^{99m}Tc-sestamibi was injected with a scan time of 6 minutes. For the rest phase, images were acquired after 15 to 40 minutes. In the stress phase, ^{99m}Tc-sestamibi was injected near maximal exercise, which was continued at maximal workload for at least 1 minute and image acquisition was performed after 15 to 30 minutes. MPI images were acquired through the gated SPECT technique using a two-headed gamma camera (Venti, GE Healthcare, Waukesha, WI, USA).

The 1-day ^{99m}Tc-sestamibi rest/stress protocol was also used, starting with rest study (injection of 5 mCi) followed by stress (15 mCi), in a CZT camera. CZT-SPECT was performed using a camera with multipinhole collimator (Discovery 530, GE Healthcare, Milwaukee, USA). Images were acquired in 6, 3, and 1 minute, respectively, for rest, supine stress, and prone stress.

Imaging Interpretation

All images were jointly interpreted by two experienced cardiologists. Image processing was performed with the software Evolution for Cardiac[®] using 12 iterations. Images were reconstructed without scatter or attenuation correction. Poststress-gated short axis, and vertical and horizontal long-axis tomograms as well as polar maps were generated and analyzed.

Semi quantitative 17-segment visual interpretation of the gated myocardial perfusion images was

performed.^{20,21} Each segment was scored by consensus using a standard five-point scoring system²² (0 = normal, 1 = equivocal, 2 = moderate, 3 = severe reduction of uptake, and 4 = absence of detectable tracer uptake) and each reader chose a score based on both quantitative perfusion data and qualitative visual assessment. Summed stress scores (SSS) were obtained by adding the scores of the 17 segments of the stress images. Summed rest scores (SRS) were obtained by adding scores of the 17 segments of the rest images and a summed difference score (SDS) was calculated by segmental subtraction (SSS – SRS).

For evaluating the correlation of SSS and the SDS with outcomes, we performed separate analyses with different cut points for each perfusion variable. With the purpose of evaluating the prognostic value and the stratification power based on the extent of defect and ischemia, we segmented our study population based on SSS and SDS values, as it is a widely established type of classification^{17,23} to achieve the result.

We converted SSS into percentage of total myocardial defect extension by calculating the ratio between SSS and its maximum possible score (68). An abnormal scan was considered as having an SSS ≥ 4 or percentage of total defect $\geq 5\%$.

Left ventricular ejection fraction (LVEF) and end-systolic and end-diastolic volumes (ESV and EDV, respectively) were automatically calculated (Cedars-Sinai Medical Center, Los Angeles, California).

Follow-Up

Follow-up was performed by telephone interview every 6 months after MPI. All-cause death and nonfatal MI were registered. Events were confirmed through review of hospital charts, physician's records, and national death certification. Nonfatal MI was defined based on the criteria of typical chest pain, elevated cardiac enzyme levels, and typical alterations of the electrocardiogram.²⁴ All-cause death and nonfatal MI were classified as hard events and time to first event was considered.

Statistical Analysis

Categorical variables are presented as frequencies and were calculated using the Pearson χ^2 or Fisher's exact test. Continuous variables are expressed as mean \pm SD or median and interquartile range (IQR) and were compared using Student *T* test or Mann-Whitney test, accordingly. Poisson regression was performed to calculate annualized rate of hard events. Kaplan-Meier curves were generated to visually assess survival in different clinical groups. For pairwise

comparisons between these groups, the log-rank test was used. A Cox regression model was used for testing predictors of hard events. Variables with a *P* value < 0.05 in the univariable analysis or clinical significance were considered in the model. Proportional hazard assumption was tested by using Martingale residuals and we tested for an interaction between exercise capacity and MPI results. Incremental prognostic value of MPI was evaluated by sequential multivariable models, built by the addition of exercise capacity and MPI results to demographic and clinical characteristics. Final model fit was assessed with the goodness-of-fit χ^2 test. A *P*-value $< .05$ was considered statistically significant. All analyses were performed with IBM SPSS statistics version 22.0 Armonk, NY: IBM Corp.

RESULTS

Cohort Baseline Characteristics

A total of 926 patients were followed for a mean 32.4 ± 9.7 months. The clinical characteristics of this study cohort are summarized in Table 1. Patients were divided into two groups: those who achieved ≥ 10 METs (41.5%), named Group 1; and < 10 METs (58.5%), named Group 2. Patients achieving higher workloads were younger, more often male, and had lower rates of hypertension, diabetes mellitus, and obesity. There was no significant difference between groups concerning the presence of angina.

Stress-ECG Test and SPECT Findings

Table 2 shows findings on the stress-ECG test and SPECT imaging stratified by groups of workload achievement. Maximum heart rate during the test was higher in the group of patients who achieved ≥ 10 METs (148 vs 137, *P* $< .001$), as well the prevalence of patients achieving $\geq 85\%$ of their maximum age-predicted heart rate (MAPHR, 82.8% vs 74.1%, *P* = .002). The prevalence of chest pain during the ECG stress was lower in Group 1 for both typical (2.3% vs 7.4%, *P* = .003) and atypical angina (1.8% vs 2.4%, *P* = .003) compared to Group 2. There was no significant difference in the prevalence of exercise ST depression between groups.

When comparing exercise capacity to SPECT imaging results, there was no significant difference between Groups 1 and 2, respectively, on mean SSS (2.69 vs 2.97, *P* = .824), SDS (0.69 vs 0.87, *P* = .424), or percentage of total defect (3.9 vs 4.3, *P* = .824). The prevalence of patients with significant left ventricular

Table 1. Baseline characteristics relative to cardiac workload

Baseline characteristics	Group 1 ≥ 10 METs 384 (41.5%)	Group 2 < 10 METs 542 (58.5%)	Entire cohort n = 926	P value*
Age	59.6 (9)	66.7 (9.2)		< .001
Male	363 (94.5%)	379 (69.9%)	742 (80.1%)	< .001
Symptoms				
Asymptomatic	286 (74.5%)	396 (73.1%)	682 (73.6%)	.63
Typical angina	16 (4.2%)	24 (4.4%)	40 (4.3%)	.847
Atypical angina	64 (16.7%)	93 (17.2%)	157 (16.9%)	.844
Shortness of breath	5 (1.3%)	12 (2.2%)	17 (1.8%)	.308
Non-cardiac chest pain	13 (3.3%)	17 (3.1%)	30 (3.4%)	.331
Hypertension	216 (56.3%)	345 (63.7%)	561 (60.5%)	.023
Diabetes mellitus	67 (17.4%)	162 (29.9%)	229 (24.7%)	< .001
Hyperlipidemia	220 (57.3%)	327 (60.3%)	547 (59%)	.354
BMI ≥ 30	65 (17.6%)	123 (24%)	188 (20.3%)	.023
History of tobacco use	140 (36.4%)	202 (37.3%)	342 (36.9%)	.968
Previous MI	158 (41.1%)	240 (44.3%)	398 (42.9%)	.342
Previous CABG	174 (32.1%)	107 (27.9%)	281 (30.3%)	.095
Previous PCI	356 (65.7%)	253 (65.9%)	609 (65.7%)	.503
Family history of CAD	177 (46.1%)	225 (41.5%)	402 (43.4%)	.166

BMI, body mass index; MI, myocardial infarction; CABG, coronary artery bypass graft; PCI, percutaneous coronary intervention; CAD, coronary artery disease

*Values < .05 are considered statistically significant

Table 2. Exercise test and SPECT parameters relative to cardiac workload

Tests parameters	Group 1 ≥ 10 METs n = 384	Group 2 < 10 METs n = 542	P value*
Stress-ECG test			
Exercise ST depression [n (%)]	35 (9.1)	47 (8.7)	.815
Maximum HR (bpm) (median (25th, 75th))	148 (138, 162)	137 (126, 149)	< .001
> 85% MAPHR [n (%)]	303 (82.8)	380 (74.1)	.002
Chest pain during stress [n (%)]	16 (4.1)	53 (9.7)	.003
SPECT imaging			
Abnormal scans [n (%)]	74 (19.3)	119 (22)	.322
Mean of SSS (± SD)	2.69 (4.5)	2.97 (5)	.824
Mean of SDS (± SD)	0.69 (1.8)	0.87 (2.2)	.424
Mean % of LV defect (± SD)	3.9 (0.33)	4.3 (0.31)	.824
Percentage of LV defect n (%)			
< 5%	310 (80.7)	423 (78)	
5-7%	18 (4.7)	29 (5.4)	
8-9%	10 (2.6)	12 (2.2)	.678
> 10%	46 (12)	78 (14.4)	
EF < 40% [n (%)]	24 (6.3)	63 (11.7)	.006

HR, heart rate; MAPHR, maximum age-predicted heart rate; SSS, summed stress score; SDS, summed difference score; LV, left ventricle; EF, ejection fraction

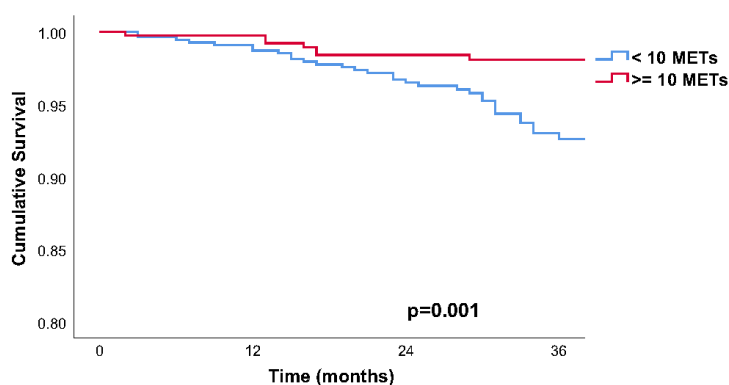
*Values < .05 are considered statistically significant

Table 3. Prevalence of outcomes relative to cardiac workload

Event	Group 1 ≥ 10 METs 384 (41.5%)	Group 2 < 10 METs 542 (58.5%)	Entire cohort n = 926	P value*
Hard events [n (%)]	10 (2.6)	48 (8.9)	58 (6.3)	< .001
All-cause mortality [n (%)]	6 (1.6)	36 (6.6)	42 (4.5)	< .001
Nonfatal MI [n (%)]	4 (1)	16 (3)	20 (2.1)	.04

MI, myocardial infarction

*Values < .05 are considered statistically significant

**Number at risk**

Time(months)	0	12	24	36
< 10 METs	542	524	436	233
≥10 METs	384	376	311	166

Figure 2. Survival that is free of hard events stratified by cardiac workload. *Blue line* patients reaching < 10 METs; *red line* patients reaching ≥ 10 METs.

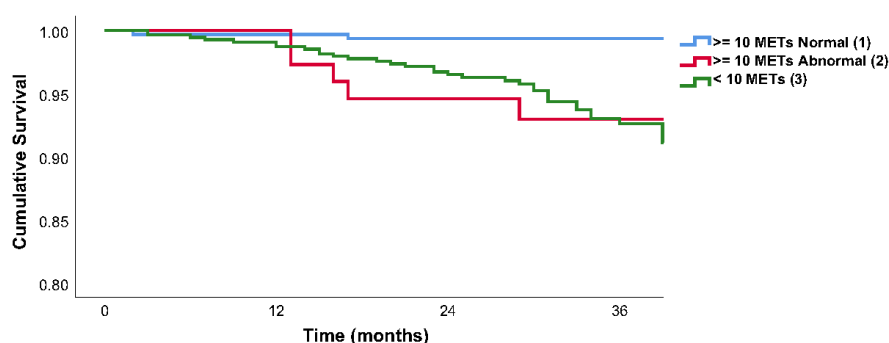
dysfunction (EF < 40%) was lower in those reaching higher cardiac workloads (6.3% vs 11.7% $P = .006$).

Outcomes

A total of 42 deaths (4.5%) and 20 nonfatal MIs (2.1%) (58 hard events) occurred during the follow-up period, as shown on Table 3. The group of patients who achieved ≥ 10 METs had a lower annualized rate of hard events when compared to Group 2 (1.13%/year vs 3.95%/year, $P < .001$). The difference in the cumulative

survival that is free of hard events according to cardiac workload achievement is shown in the Kaplan–Meier survival curve ($P = .001$, Figure 2).

In order to evaluate MPI prognostic contribution for patients with high exercise capacity, we analyzed survival only in patients achieving ≥ 10 METs, stratified for scan results, SSS, and SDS groups. Kaplan–Meier curves show the comparison of cumulative survival among patients achieving < 10 METs, ≥ 10 METs with abnormal scans, and ≥ 10 METs with normal scans, showing increased survival rate in the



	Number at risk				Pairwise comparisons	p value
Time(months)	0	12	24	36	1 vs 2	0.023
≥ 10 METs Normal	310	302	257	137	1 vs 3	<0.001
≥ 10 METs Abnormal	74	74	62	39	2 vs 3	0.394
< 10 METs	542	524	436	233		

Figure 3. Survival that is free of hard events stratified by patients achieving < 10 METs, ≥ 10 METs with abnormal scans, and ≥ 10 METs with normal scans. *Green line* patients reaching < 10 METs; *red line* patients reaching ≥ 10 METs with abnormal scans; *blue line* patients reaching ≥ 10 METs with normal scans. For the pairwise comparisons, 1: ≥ 10 METs normal, 2: ≥ 10 METs abnormal, and 3: < 10 METs.

latter (Figure 3). Consistently, patients who reached ≥ 10 METs with a normal scan had a significant lower annualized rate of hard events compared to those who reached ≥ 10 METs with abnormal scans and those who reached < 10 METs (0.57%/year, 3.37%/year, and 3.95%/year, respectively, $P = .001$, Figure 4). There was also a stepwise increment in the annualized rate of events according to the increase in total defect severity, based on SSS groups. There was no difference in the prevalence of these events when stratifying patients with ≥ 10 METs according to the presence of ischemia (Figure 5).

Finally, in the Cox proportional hazards model, cardiac workload achievement < 10 METs (2.72 [1.28-5.77], $P = .009$) and an abnormal MPI result (1.9 [1.15-3.39], $P = .01$) were independently associated with hard events. The variables considered in the univariable and multivariable models are shown in Table 4. In order to assess the incremental prognostic value of MPI results, we constructed multivariable models by sequentially adding exercise capacity and MPI results to demographic and clinical characteristics. Figure 6 shows improvement in the model statistics when these two variables were added. The final model global is

$\chi^2 = 22.5$, $P = .001$. No interaction between exercise capacity and MPI results was observed.

DISCUSSION

Clinical application of exercise testing as a gatekeeper for nuclear imaging has been a matter of debate along the last decade. MPI cost-effectiveness, procedure costs, and related benefits are mounting challenges in an era of advanced cardiac imaging technologies.³ In this context, it is crucial to reassess the risk stratification ability of each method in specific populations.

It is established that patients achieving ≥ 10 METs have low rates of cardiovascular events and low prevalence of $\geq 10\%$ LV ischemia on MPI regardless of peak exercise heart rate.^{11,12} Duvall et al attempted to create a provisional injection protocol by applying the ≥ 10 METs cutoff as criterion to abstain from radiotracer injection. However, groups such as older adults and patients with known CAD were excluded.¹⁴ More recently, Smith et al described that exercise capacity also influences outcomes in patients who are ≥ 65 years old and is associated with a low occurrence of significant ischemia in MPI.¹³ Nonetheless, it is still

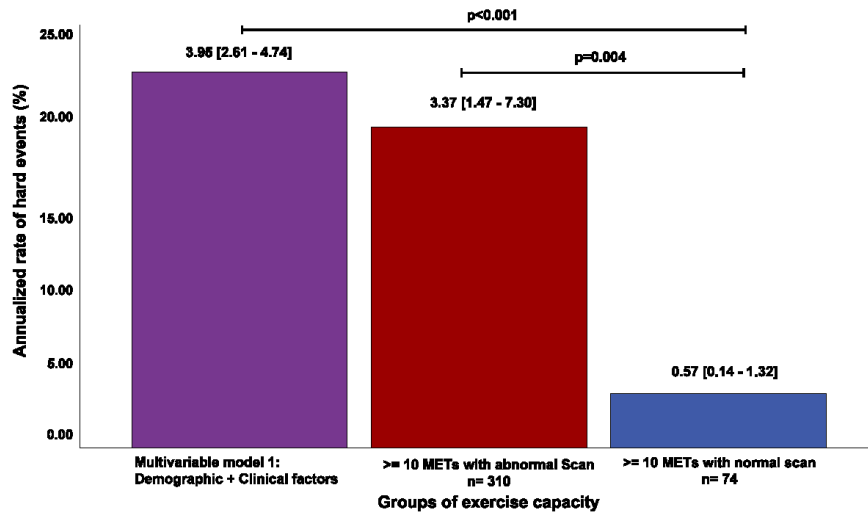
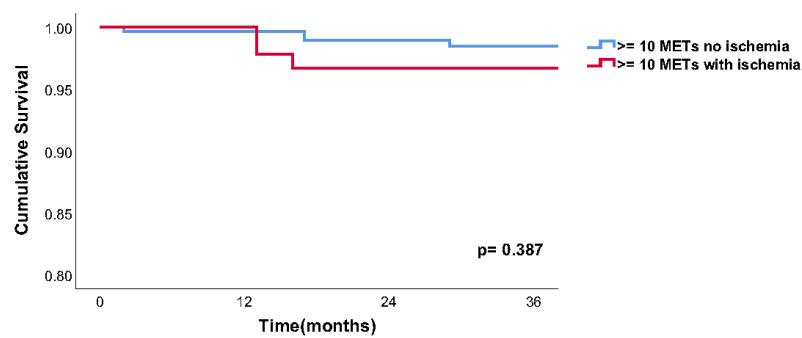


Figure 4. Annualized rate of hard events (%/year [95% CI]) per group of cardiac workload and scan results in % person-years.



Number at risk				
Time(months)	0	12	24	36
≥10 METs no ischemia	292	285	240	132
≥10 METs with ischemia	92	91	79	45

Figure 5. Survival that is free of hard events in patients achieving ≥ 10 METs according to presence of ischemia in MPI. Blue line patients achieving ≥ 10 METs with no ischemia; red line patients achieving ≥ 10 METs with ischemia.

not clear if patients with known CAD would show similar results.

In this study, we addressed the association of high exercise capacity (≥ 10 METs) with mortality and

cardiovascular events in a population comprised of patients with known CAD referred for exercise ECG-stress MPI. Of most importance, we tried to determine the additional contribution of MPI prognostic value in

Table 4. Univariable and multivariate indicators of hard events

Predictors	Univariable		Multivariable	
	Hazard ratio (95% CI)	P value*	Hazard ratio (95% CI)	P value*
Age	1.03 (1.00-1.07)	.014	1.02 (0.98-1.05)	.254
Male gender	1.16 (0.54-2.47)	.697	0.64 (0.30-1.4)	.268
Diabetes mellitus	1.66 (0.96-2.87)	.068	0.64 (0.36-1.14)	.133
< 10 METs	3.1 (1.55-6.16)	.001	2.72 (1.28-5.77)	.009
Abnormal scan	1.74 (1.03-2.95)	.037	1.98 (1.15-3.39)	.013
LVEF	0.99 (0.98-1.01)	.818	1 (0.99-1)	.876
< 10 METs * abnormal scan	-	-	0.51 (0.11-2.29)	.386
Hypertension	0.85 (0.5-1.46)	.57		
Dyslipidemia	1.01 (0.59-1.74)	.958		
Previous MI	0.89 (0.52-1.53)	.688		
Family history of CAD	0.83 (0.48-1.42)	.5		
ST segment depression	0.32 (0.07-1.31)	.114		
SSS	0.98 (0.93-1.03)	.588		
SDS	1.00 (0.99-1.01)	.096		

No significant interaction was observed between exercise capacity and MPI results in the multivariable analysis
 CI, confidence interval; METs, metabolic equivalents; LVEF, left ventricle ejection fraction; MI, myocardial infarction; CAD, coronary artery disease; SSS, summed stress score; SDS, summed difference score
 *Values < .05 are considered statistically significant

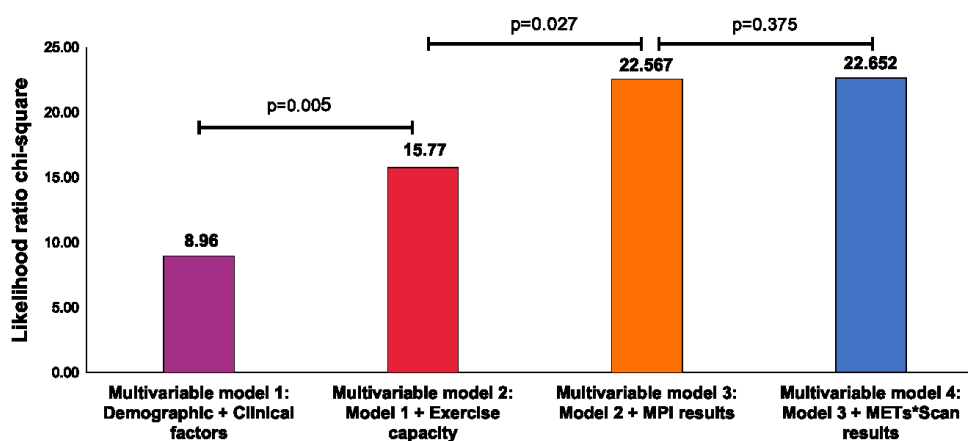


Figure 6. Multivariable-adjusted models showing incremental prognostic value of exercise capacity and MPI results in patients with known CAD.

that specific population. We showed that patients attaining higher workloads were younger, predominantly male, and had significant lower rates of cardiac risk factors. Approximately 70% of the population was asymptomatic before the test, with no significant

difference on the prevalence of pretest symptoms among Groups 1 and 2 in this study. This fact is suggestive of CAD follow-up as the main reason for scan referral. There was no significant difference in the prevalence of ST depression between Groups 1 and 2. Also, there was

no difference in the prevalence of abnormal scans or extent of ischemia in patients with ST depression compared to those without ST depression.

Survival analyses showed that patients with known CAD achieving ≥ 10 METs had a significantly better prognosis compared to those attaining < 10 METs for all-cause mortality and nonfatal MI, with a lower annualized rate of hard events. This finding is similar to what has been previously described.¹¹ To further understand how scan results predicted hard events in the study population, we performed survival analyses only in patients attaining ≥ 10 METs and found out that those with abnormal scans had a significant higher rate of events. Furthermore, the increase in the annualized rate of hard event is proportional to the extent of defect, as determined by SSS values. The results suggest that although a higher exercise capacity is associated with a lower prevalence of all-cause mortality and nonfatal MI, MPI can still provide valuable prognostic information. These findings were corroborated by Cox regression analyses which showed that both exercise capacity and scan results were independently associated with hard events.

Regarding ischemic burden, we did not find significant difference in the survival that is free of hard event in this cohort with established CAD achieving ≥ 10 METs. Although it is worth mentioning that the survival analysis stratified by SDS groups was potentially limited by the number of events in this subgroup (10 events), we also believe that our study cohort's peculiarities may explain the lack of prognostic value of SDS. In a previous study, Gimelli et al.²⁵ aimed to evaluate the incremental prognostic value of MPI over other imaging methods. The group described that when focusing only in a population of ascertained known CAD, without early revascularized patients and a small number of events, SDS was also not a predictor of cardiac events.

Based on what was mentioned above and the fact that under the same constraints the percentage of total defect kept its prognostic value, we believe that for our cohort, the greater contribution of MPI is determined not by quantification of new ischemia, but by the sum of ischemia and previous myocardial scar. Nevertheless, we agree that new studies focusing exclusively on the MPI prognostic value for similar cohorts are necessary to further support this assumption. Thus, our study's results may contribute to better determine the appropriate referral criteria to MPI in patients with known CAD who achieved high exercise capacity in the stress-ECG test.

Limitations

Our study has some limitations, including its retrospective, observational, and single-institution

nature. It is worth noticing that despite having a large sample size, the prevalence of events in the group with higher exercise capacity is low and it might have limited further subgroup analyses.

Additionally, the cardiologists who interpreted the scans were not blinded to clinical data, as the protocol was part of the clinical routine. Hence, it could have been a source of bias.

NEW KNOWLEDGE GAINED

MPI is able to stratify patients with known CAD and high exercise capacity for the occurrence of all-cause death and nonfatal MI, with an incremental prognostic value over ECG stress test alone.

CONCLUSION

MPI was able to stratify the risk for the occurrence of all-cause death and nonfatal MI in patients with known CAD achieving ≥ 10 METs, with an incremental prognostic value compared to ECG stress test alone. These results support the performance of perfusion imaging in this subset of patients, as opposed to what had been proposed with provisional protocols that aimed to reduce patients' exposure to radiation.

Disclosure

The authors Thais R. Peclat, Ana Carolina do A. H. de Souza, Victor F. Souza, Aline M. K. Nakamoto, Felipe M. Neves, Izabella C. R. Silva, and Ronaldo S. L. Lima have nothing to disclose.

References

1. Sanchis-Gomar F, Perez-Quilis C, Leischik R, Lucia A. Epidemiology of coronary heart disease and acute coronary syndrome. *Ann Transl Med* 2016;4:256.
2. Hansen CL, Goldstein RA, Akinboboye OO, Berman DS, Botvinick EH, Churchwell KB, et al. Myocardial perfusion and function: Single photon emission computed tomography. *J Nucl Cardiol* 2007;14:e39-60.
3. Bourque JM, Beller GA. Value of exercise ECG for risk stratification in suspected or known CAD in the era of advanced imaging technologies. *JACC Cardiovasc Imaging* 2015;8:1309-21.
4. Klocke FJ, Baird MG, Lorell BH, Bateman TM, Messer JV, Berman DS, et al. ACC/AHA/ASNC guidelines for the clinical use of cardiac radionuclide imaging—Executive summary: A report of the American College of Cardiology/American Heart Association Task Force on Practice Guidelines (ACC/AHA/ASNC Committee to Revise the 1995 Guidelines for the Clinical Use of Cardiac Radionuclide Imaging). *J Am Coll Cardiol* 2003;42:1318-33.
5. Peterson PN, Magid DJ, Ross C, Ho PM, Rumsfeld JS, Lauer MS, et al. Association of exercise capacity on treadmill with future cardiac events in patients referred for exercise testing. *Arch Intern Med* 2008;168:174-9.

6. Morise AP, Jalisi F. Evaluation of pretest and exercise test scores to assess all-cause mortality in unselected patients presenting for exercise testing with symptoms of suspected coronary artery disease. *J Am Coll Cardiol* 2003;42:842-50.
7. Goraya TY, Jacobsen SJ, Pellikka PA, Miller TD, Khan A, Weston SA, et al. Prognostic value of treadmill exercise testing in elderly persons. *Ann Intern Med* 2000;132:862-70.
8. Kodama S, Saito K, Tanaka S, Maki M, Yachi Y, Asumi M, et al. Cardiorespiratory fitness as a quantitative predictor of all-cause mortality and cardiovascular events in healthy men and women: A meta-analysis. *JAMA* 2009;301:2024-35.
9. Lee DS, Verocai F, Husain M, Al Khdair D, Wang X, Freeman M, et al. Cardiovascular outcomes are predicted by exercise-stress myocardial perfusion imaging: Impact on death, myocardial infarction, and coronary revascularization procedures. *Am Heart J* 2011;161:900-7.
10. Faselis C, Doumas M, Pittaras A, Narayan P, Myers J, Tsimploulis A, et al. Exercise capacity and all-cause mortality in male veterans with hypertension aged ≥ 70 years. *Hypertension* 2014;64:30-5.
11. Bourque JM, Holland BH, Watson DD, Beller GA. Achieving an exercise workload of $> \text{ or } = 10$ metabolic equivalents predicts a very low risk of inducible ischemia: Does myocardial perfusion imaging have a role? *J Am Coll Cardiol* 2009;54:538-45.
12. Bourque JM, Charlton GT, Holland BH, Belyea CM, Watson DD, Beller GA. Prognosis in patients achieving ≥ 10 METS on exercise stress testing: Was SPECT imaging useful? *J Nucl Cardiol* 2011;18:230-7.
13. Smith L, Myc L, Watson D, Beller GA, Bourque JM. A high exercise workload of ≥ 10 METS predicts a low risk of significant ischemia and cardiac events in older adults. *J Nucl Cardiol* 2018. <https://doi.org/10.1007/s12350-018-1376-7>.
14. Duvall WL, Levine EJ, Moonthungal S, Fardanesh M, Croft LB, Henzlova MJ. A hypothetical protocol for the provisional use of perfusion imaging with exercise stress testing. *J Nucl Cardiol* 2013;20:739-47.
15. Hung RK, Al-Mallah MH, McEvoy JW, Whelton SP, Blumenthal RS, Nasir K, et al. Prognostic value of exercise capacity in patients with coronary artery disease: The FIT (Henry Ford Exercise Testing) project. *Mayo Clin Proc* 2014;89:1644-54.
16. Diamond GA, Forrester JS, Hirsch M, Staniloff HM, Vas R, Berman DS, et al. Application of conditional probability analysis to the clinical diagnosis of coronary artery disease. *J Clin Investig* 1980;65:1210-21.
17. Lima R, Ronaldo L, De Lorenzo A, Andrea DL, Camargo G, Gabriel C, et al. Prognostic value of myocardium perfusion imaging with a new reconstruction algorithm. *J Nucl Cardiol* 2014;21:149-57.
18. Lima RSL, Peclat TR, Souza ACAH, Nakamoto AMK, Neves FM, Souza VF, et al. Prognostic value of a faster, low-radiation myocardial perfusion SPECT protocol in a CZT camera. *Int J Cardiovasc Imaging* 2017;33:2049-56.
19. Lima R, Peclat T, Soares T, Ferreira C, Souza AC, Camargo G. Comparison of the prognostic value of myocardial perfusion imaging using a CZT-SPECT camera with a conventional angler camera. *J Nucl Cardiol* 2017;24:245-51.
20. Berman DS, Kang X, Van Train KF, Lewin HC, Cohen I, Arceeda J, et al. Comparative prognostic value of automatic quantitative analysis versus semiquantitative visual analysis of exercise myocardial perfusion single-photon emission computed tomography. *J Am Coll Cardiol* 1998;32:1987-95.
21. Henzlova MJ, Duvall WL, Einstein AJ, Travin MI, Verberne HJ. ASNC imaging guidelines for SPECT nuclear cardiology procedures: Stress, protocols, and tracers. *J Nucl Cardiol* 2016;23:606-39.
22. Berman DS, Hachamovitch R, Kiat H, Cohen I, Cabico JA, Wang FP, et al. Incremental value of prognostic testing in patients with known or suspected ischemic heart disease: A basis for optimal utilization of exercise technetium-99m sestamibi myocardial perfusion single-photon emission computed tomography. *J Am Coll Cardiol* 1995;26:639-47.
23. Hachamovitch R, Berman DS, Shaw LJ, Kiat H, Cohen I, Cabico JA, et al. Incremental prognostic value of myocardial perfusion single photon emission computed tomography for the prediction of cardiac death: Differential stratification for risk of cardiac death and myocardial infarction. *Circulation* 1998;97:535-43.
24. Thygesen K, Alpert JS, White HD. Infarction JEAATWffRoM. Universal definition of myocardial infarction. *J Am Coll Cardiol* 2007;50:2173-95.
25. Gimelli A, Rossi G, Landi P, Marzullo P, Iervasi G, L'abbate A, et al. Stress/test myocardial perfusion abnormalities by gated SPECT: Still the best predictor of cardiac events in stable ischemic heart disease. *J Nucl Med* 2009;50:546-53.

Publisher's Note Springer Nature remains neutral with regard to jurisdictional claims in published maps and institutional affiliations.